# The Cure Chemistry of Brominated Butyl Rubber:

# A Model Compound Approach

By

Darren James Thom

A thesis submitted to the Department of Chemical Engineering
in conformity with the requirements for the degree of
Master of Science (Engineering)

Queen's University
Kingston, Ontario, Canada
December, 1999

To my family: Bob, Deanna, Christy and Anna

# Abstract

Poly(isobutene-*co*-isoprene), known as butyl rubber, is valued for its gas impermeability and mechanical damping properties. Bromination of the isoprene units affords a highly cure reactive elastomer with unique vulcanization chemistry.

The low level of residual unsaturation in bromobutyl rubber (BIIR), coupled with the insolubility of crosslinked networks, complicates the structural determination of its vulcanizates. In this regard, model compound reactions have proven to be an effective means of studying the accelerated sulphur cure chemistry of natural rubber and polybutadiene, as well as the ZnO cure chemistry of BIIR. These models, which contain the reactive functionality of an elastomer, can be isolated and characterized using solution chromatographic and spectroscopic techniques.

Brominated products of 2,2,4,8,8-pentamethyl-4-nonene (exomethylene and bromomethyl isomers) were used in the present study to represent the reactive functionality of BIIR. The objective of this work was to identify the principal model crosslinks formed for several curative formulations using mass spectroscopy and nuclear magnetic resonance.

In the presence of a neutral acid scavenger, the behavior of the brominated model compound (BrMC) at vulcanization temperatures was consistent with BIIR. Therefore, reactions of the BrMC were carried out with the curing agent 2,2'-dithiobisbenzothiazole (MBTS), sulphur, and S+MBTS.

Reaction of the BrMC with MBTS produced a thiomethyl adduct that is not believed to be a crosslink precursor. This could explain the uncharacteristic decrease in crosslink density when MBTS is incorporated into BIIR curative formulations.

Reaction of the BrMC with sulphur generated bromomethyl analogue sulphide dimers of various rank. Decomposition of these dimers afforded a thiophene, which was identified as a potential reversion product in sulphur cured BIIR vulcanizates.

A high exomethylene to bromomethyl isomer ratio consistent with BIIR was used in the model reactions with S+MBTS. The isomer ratio influenced the product distribution in that both exomethylene and bromomethyl analogue sulphide dimers and MBT adducts were generated.

# Acknowledgments

I wish to express my sincere appreciation to Dr. J. S Parent and Dr. R. A. Whitney for presenting me with the opportunity to work on this research project. Their consistent dedication, support, and guidance have been invaluable throughout the course of this work. Special thanks to Dr. Parent for his advice and attentiveness that have helped develop my research and engineering skills. Thanks also to Dr. Whitney for his understanding and encouragement, as well as the many informative discussions about organic chemistry during my time at Queen's. I would also like to express appreciation to Dr. W. Hopkins of Bayer Inc. for his dedication and input to this project.

Sincere thanks to the members of the Parent and Whitney labs past and present, whose friendships and assistance supported me throughout this work: Darren Clark, Jeff Robillard, Chris Kirk, Katharine Gerrimita, Tamsin Scott, Tyler Westcott, Marko Mrkoci, Mark Spencer and Mark Scott.

I would like to thank Ms. Sue Blake and Dr. Francoise Sauriol for their assistance in running the NMR spectrometer. Thanks also to Mr. Tom Hunter for conducting my MS experiments. The participation of Mr. Bob Campbell in many "breakthroughs" and insightful conversations was greatly appreciated.

Financial support from Queen's University and Bayer Inc. is gratefully acknowledged.

I would like to particularly thank those friends at Bethel who have had a positive impact on my time here. I am especially grateful to Rebecca Wiens, Scott Woodland, Chris Kirk and Leighton Block for their understanding and support through smooth and

difficult times. Thanks also to my housemates Darren, Jeff, Mike and James who have made the '250' a great place to live.

Most importantly, I would like to thank my family for their patience, understanding and support during my entire time at Queen's.

# Table of Contents

**3.0 Experimental**

# List of Tables

# List of Figures

# List of Abbreviations

| | |
|---|---|
| IIR | Butyl rubber |
| BIIR | Bromobutyl rubber |
| CIIR | Chlorobutyl rubber |
| NR | Natural rubber (cis-polyisoprene) |
| PBD | Polybutadiene |
| phr | Parts per hundred rubber |
| BrMC | Brominated 2,2,4,8,8-pentamethyl-4-nonene |
| exo | Exomethylene isomer of the BrMC |
| BrMe | Bromomethyl isomer of the BrMC |
| exo-CDB | Exomethylene conjugated diene |
| endo-CDB | Endomethylene conjugated diene |
| MBTS | 2,2'-Dithiobisbenzothiazole |
| MBT | Mercaptobenzothiazole |
| HPLC | High performance liquid chromatography |
| TLC | Thin layer chromatography |
| NMR | Nuclear magnetic resonance |
| MS | Mass Spectroscopy |

# List of Structures

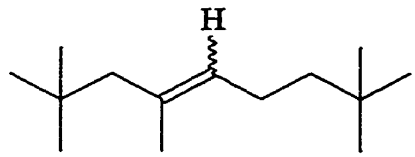


2,2,4,8,8-Pentamethyl-4-nonene **1**
(mixture of E and Z isomers)

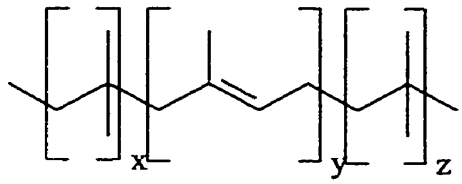


Butyl Rubber **2**

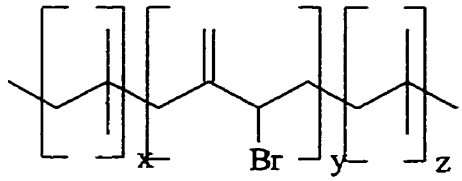


Bromobutyl Rubber: Exomethylene Isomer **3**

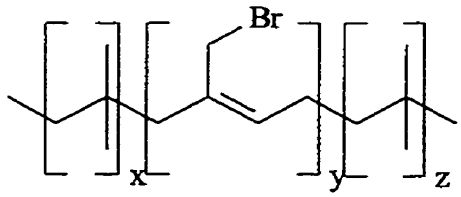


Bromobutyl Rubber: Bromomethyl Isomer **4**

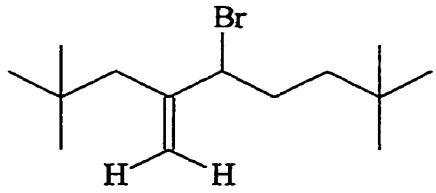


BrMC: Exomethylene isomer (exo) **5**

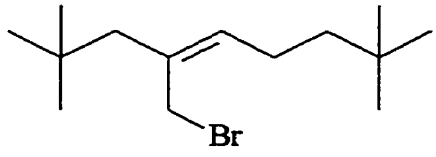


BrMC: Bromomethyl isomer (BrMe) **6**

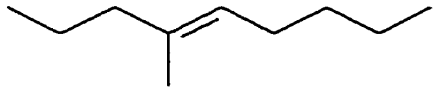

4-Methyl-4-nonene **7**

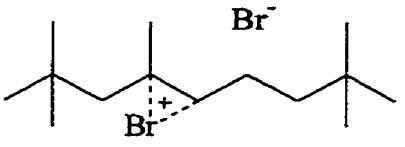


Bromium ion **8**

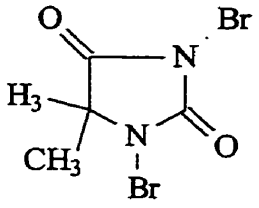


1,3-Dibromo-5,5-dimethylhydantoin **9**

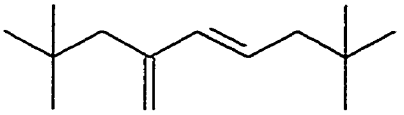

Exomethylene Conjugated Diene (exo-CDB) **10**

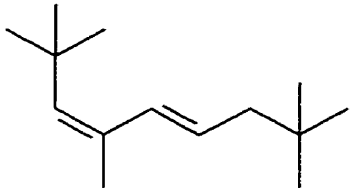

Endomethylene Conjugated Diene (endo-CDB) **11**

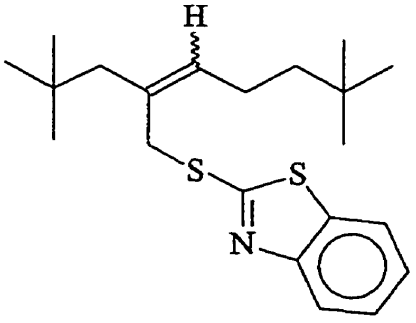


MBT graft product **12**
(mixture of E and Z isomers)

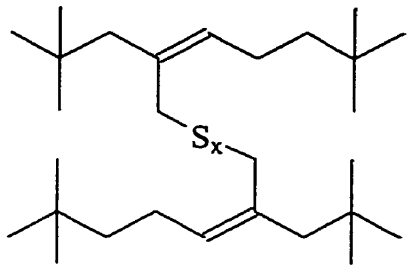


Thiomethyl sulphidic dimer **13**

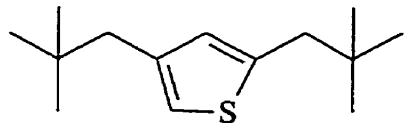


Thiophene **14**

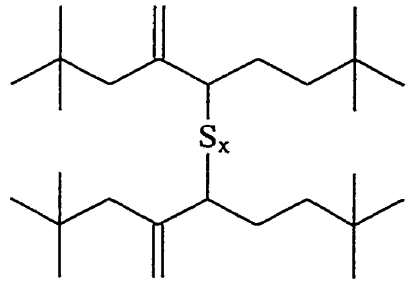


Exomethylene sulphidic dimer **15**

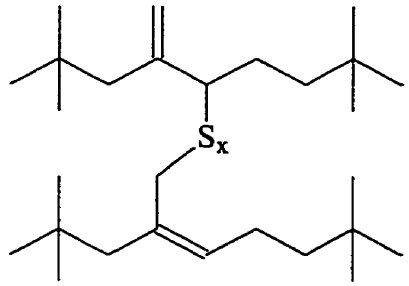


Hybrid sulphidic dimer **16**

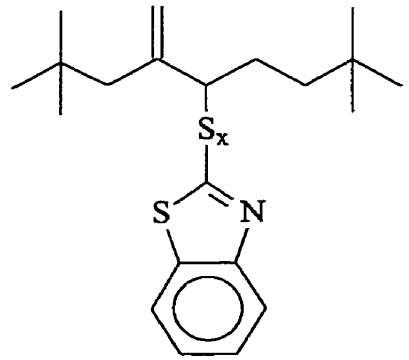


Exomethylene MBT adduct **17**

# 1.0 Introduction

Butyl rubber (IIR) is a copolymer of isobutylene (98-99%) and isoprene (1-2%) that was first discovered in 1937 and commercialized in the early 1940s.[1,2,3] The first of the limited functionality polymers, it combined the capability of forming crosslinked networks with the excellent chemical resistance of a saturated polymer. The exceptional air impermeability of butyl rubber has made it the elastomer of choice for the inner tubes and liners of tires. While this market consumes the majority of its annual worldwide production, butyl rubber is also used in mechanical damping applications due to its high loss modulus, extended fatigue life and oxidative stability.[2]

The low strength of green rubber limits its usefulness as an engineering material. However, vulcanization creates a three dimensional molecular network that demonstrates increased retractive force under an applied stress and reduced permanent deformation. Figure 1.1 illustrates three critical characteristics of a vulcanization process, including scorch resistance (delay time), cure rate, and extent of cure. A delay in the onset of crosslinking is required for processing, since vulcanizates do not flow. Of importance to manufacturing, the cure rate ($d\tau/dt$, $\tau$ = torque) can be determined from the second region of the cure curve. The extent of cure is the crosslink density when the vulcanization process is complete, and is proportional to the retractive force of a vulcanizate. In the overcure region, the crosslink density either reaches a plateau, increases slowly (marching modulus) or decreases due to nonoxidative thermal aging (reversion).

Butyl rubber cures slowly relative to diene based elastomers because of a low level of unsaturation and steric restrictions on the orientation of the isoprene units. Therefore, an IIR inner-liner cannot be vulcanized alongside tire sidewalls and tread

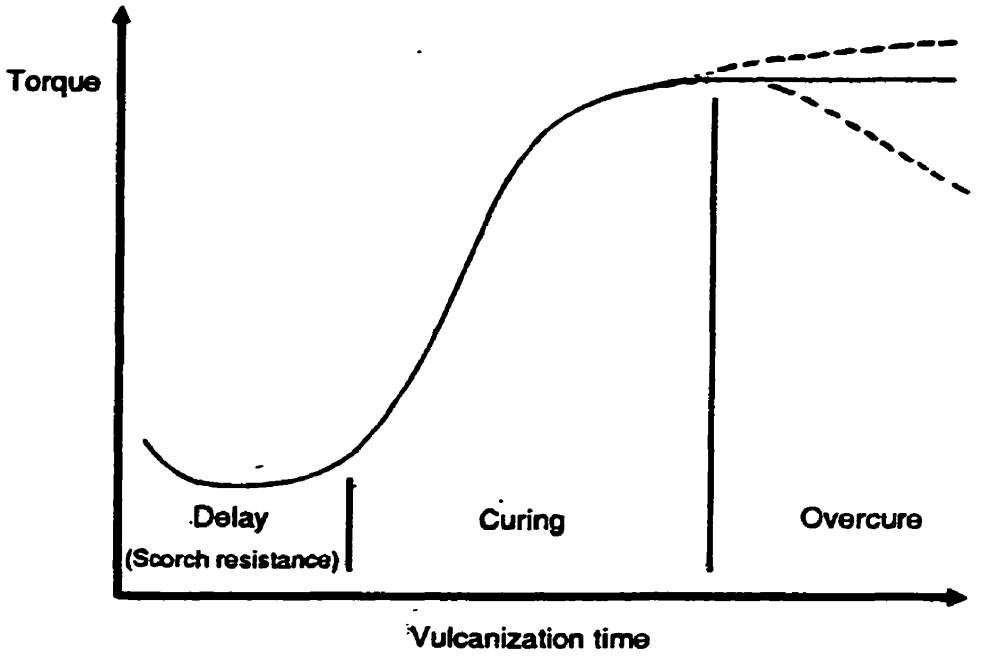


Figure 1.1: Rheometry cure curve[4]

components made from unsaturated elastomers such as polybutadiene.[1,3] Halogenation of IIR produces a highly reactive elastomer that cures as rapidly as unsaturated materials while generating the required vulcanizate properties.[1,5] Although bromobutyl rubber (BIIR) demonstrates greater cure reactivity, the chlorinated analogue is also of commercial significance.[3]

The practical applications of BIIR have preceded our understanding of its unique cure chemistry.[6] The increased reactivity of halobutyl rubber (XIIR) is afforded by the introduction of an allylic C-X bond (X = Cl, Br) that makes the vulcanization chemistry fundamentally different from that of other elastomers that rely on the reactivity of allylic C-H bonds. This difference gives rise to unique cure chemistry, including the ability of BIIR to be cured with ZnO alone, the rapid and efficient vulcanization of BIIR with

sulphur alone, and the ineffectiveness of standard organic accelerators.[1,5] The unique character of BIIR vulcanization behaviour is further described in Section 2.

The low level of functionality in BIIR, and the insolubility of the crosslinked network make it difficult to structurally characterize BIIR vulcanizates.[2] Therefore, studies of a model compound that is amenable to chromatographic separation and spectroscopic characterization by nuclear magnetic resonance (NMR) and mass spectroscopy (MS) are necessary to further our knowledge. The present study uses the brominated products of 2,2,4,8,8-pentamethyl-4-nonene (**1**) to identify the principal crosslink structures found for several curative formulations. It is expected that information gained from the model study regarding crosslink structure, sulphidic rank and mechanistic differences between curatives can be applied to bromobutyl rubber vulcanizates, thereby leading to improved curative formulations.

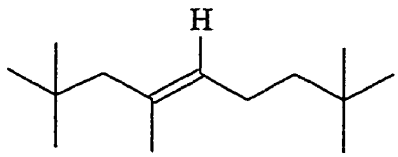


(4E)-2,2,4,8,8-Pentamethyl-4-nonene **1**

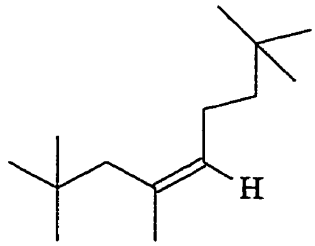


(4Z)-2,2,4,8,8-Pentamethyl-4-nonene **1**

# 2.0 Background and Literature Review

## 2.1 Vulcanization of Elastomers

Uncured elastomers are viscoelastic materials that flow under an applied stress and are therefore of little use in engineering applications. However, vulcanization transforms these materials into elastic networks through the formation of covalent crosslinks among polymer chains (Figure 2.1). The crosslinks generated by typical curative formulations containing elemental sulphur, metal oxides, and organic accelerators are sulphur chains. The resulting network restriction on polymer chain mobility gives vulcanizates a conformational "memory" that enables them to forcibly retract to their original conformation after a deforming stress is removed. Changes in the physical properties of an elastomer upon vulcanization are summarized in Table 2.1.

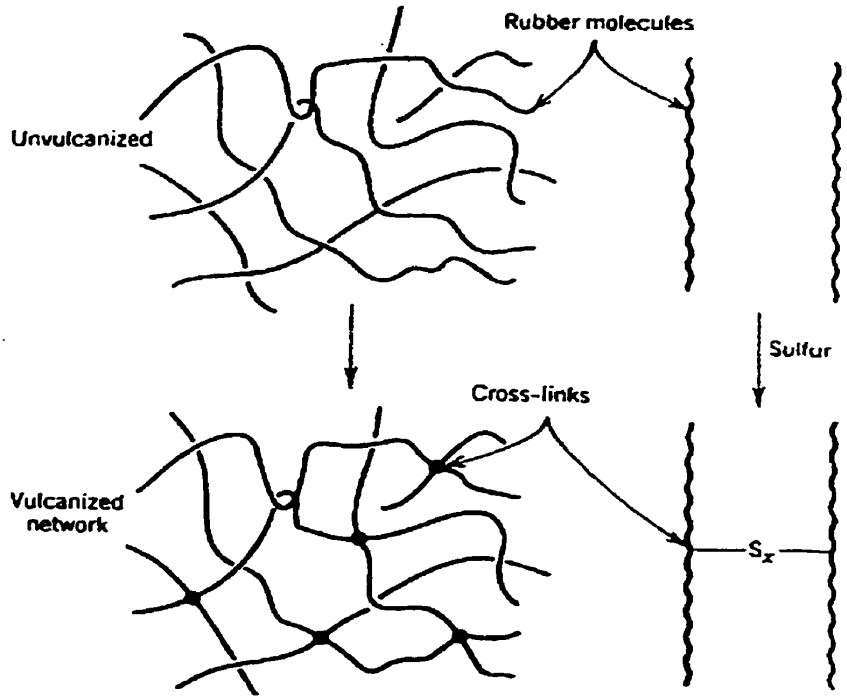


Figure 2.1: Network formation by sulphur vulcanization[4]

Table 2.1 Influence of Degree of Crosslinking on Physical Properties of Vulcanizates[7]

| Property | Change with increase in degree of crosslinking |
|---|---|
| *Properties dependent only on degree of crosslinking* | |
| stiffness (modulus) | increase |
| hardness | increase |
| *Properties partly dependent on degree of crosslinking* | |
| elongation at break | decrease |
| heat build-up | decrease |
| solvent swelling | decrease |
| creep, stress relaxation | decrease |
| set | decrease |
| resilience | increase |
| abrasion resistance | increase |
| fatigue cracking | increase |
| low-temperature crystallization | decrease in rate |
| tensile strength | increase, then decrease |

Although pure sulphur can be used to vulcanize elastomers, the cure rate and extent of cure are very poor for all materials except BIIR. Natural rubber (NR) vulcanizates cured by sulphur-only formulations typically have a low extent of cure and crosslinks of higher rank (number of sulphur atoms in a crosslink chain).[7] Unlike mono-sulphidic crosslinks that are stable, poly-sulphidic crosslinks are susceptible to reversion, and are prone to premature aging.[7,8]

The addition of organic accelerators (Ac) to sulphur cure recipes for *cis*-polyisoprene (natural rubber) increases vulcanizate crosslink densities and improves cure rates. With the wide range of delayed-action accelerators currently available, the cure rate and scorch time can be tailored for a particular application. The accelerated sulphur cure chemistry of diene-based elastomers, shown in Figure 2.2, is better understood than that of the sulphur-only cure since sulphuration is directed exclusively to the allylic sites and fewer rearrangement and reversion reactions occur.[7,9,10] The rubber-$S_x$-Ac and

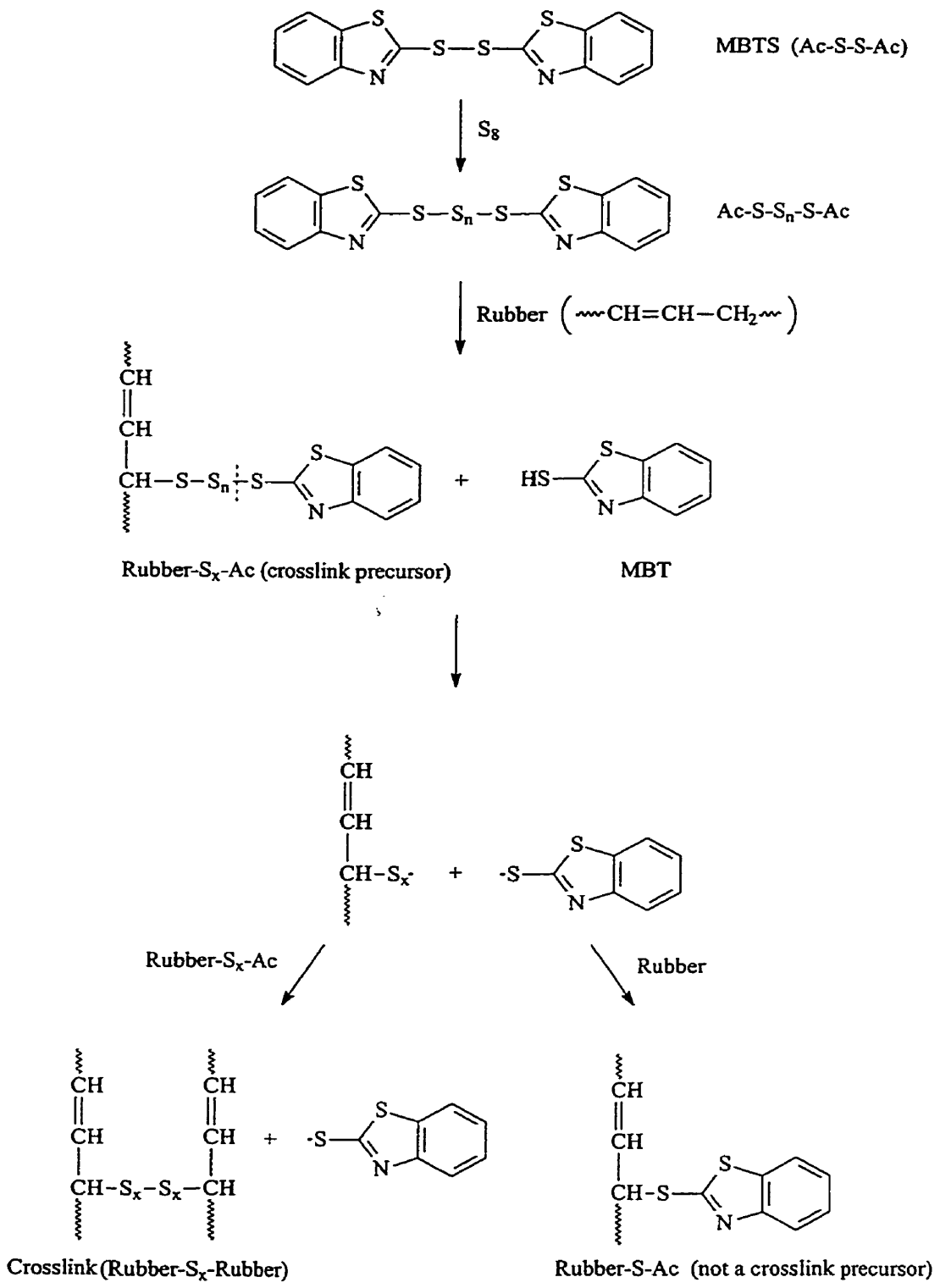


Figure 2.2: Accepted mechanism for the accelerated sulphur cure of unsaturated elastomers[11]

Ac-$S_x$-Ac groups are thought to be crosslink precursors since their concentrations reach a maximum at the onset of crosslinking. An increase in the ratio of accelerator to sulphur reduces the average sulphidic rank and increases the number of rubber-$S_x$-Ac groups, leading to vulcanizates with greater crosslink density and improved thermal stability.[12] Conversely, a decrease in the accelerator to sulphur ratio produces crosslinks of higher rank as well as six-membered sulphur rings appended along the polymer chain.

The incorporation of zinc oxide into accelerated sulphur cure formulations can lead to further increases in cure rate and the final state of cure of vulcanizates.[11, 13,14] Zinc oxide preserves the sulphur crosslink network by catalyzing the reduction in rank of poly-sulphides to more thermally stable mono-sulphides, resulting in an apparent increase in crosslink density.[7] It is also believed that ZnO activates the accelerator by forming Zn-accelerator complexes that catalyze the reaction of the rubber-$S_x$-Ac crosslink precursors and the initial sulphuration of the rubber.[7, 14, 15]

## 2.2 Structure of Brominated Butyl Rubber

Butyl rubber (**2**) is a random copolymer of isobutylene with 0.5 to 2.5 mol percent isoprene incorporated to facilitate vulcanization. Isoprene is incorporated by trans-1,4-addition, and the configuration of both isobutylene and isoprene is head to tail.[2]

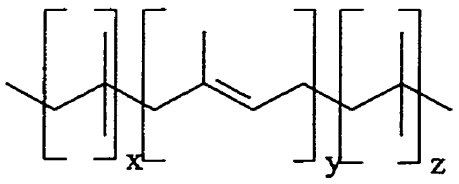


**2**

Bromination of IIR to form bromobutyl rubber is carried out in a hydrocarbon solution at 40-65°C using a 1:1 mole ratio of $Br_2$ to C=C. Unlike typical alkenes that

react with bromine to produce an addition product, the reaction of bromine and IIR leads predominantly to substituted allylic halide structures, and in particular to the exomethylene isomer (**3**) (Figure 2.3).[5,16] Under cure conditions, the low C-Br bond strength of the exomethylene isomer facilitates thermal isomerization to the bromomethyl isomer (**4**). Elimination of HBr is known to generate conjugated diene structures that are believed to be unreactive in the presence of conventional curatives.[1] The bromination of IIR as well as subsequent rearrangement and elimination reactions are shown in Figure 2.3.

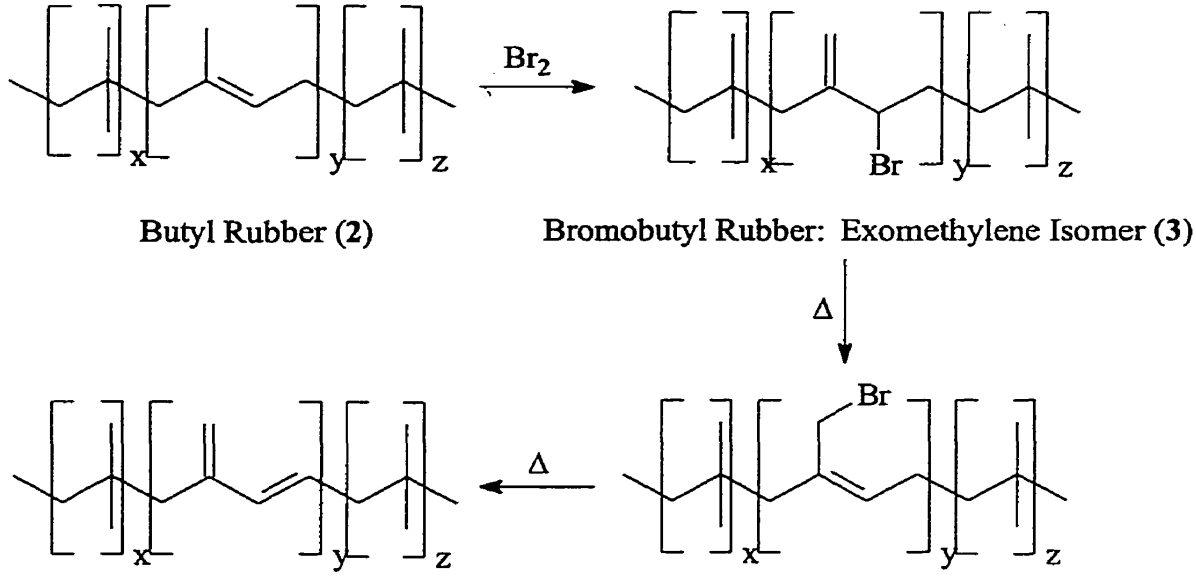


Butyl Rubber (**2**) Bromobutyl Rubber: Exomethylene Isomer (**3**)

Conjugated Diene Butyl Bromobutyl Rubber: Bromomethyl Isomer (**4**)

Figure 2.3: Bromination of IIR followed by thermal isomerization and elimination

## 2.3 Vulcanization of Bromobutyl Rubber

Bromobutyl rubber is usually vulcanized at temperatures in the range of 150°C for approximately 20 minutes. Although the crosslinking chemistry of natural rubber (which contains the reactive functionality found in butyl rubber) has been studied extensively, comparatively little is known about the reactive allylic bromides in BIIR. Bromine is a good leaving group in substitution reactions, making the allylic functionality highly reactive to nucleophilic attack. This enables BIIR to be efficiently cured with sulphur alone and to crosslink in the presence of ZnO alone.[1,5] While the primary sulphur and ZnO cures are of no practical importance because of the comparatively poor performance of their vulcanizates in engineering applications, they are studied to obtain a fundamental knowledge of the cure chemistry.

Bromobutyl rubber is usually cured by S+ZnO+MBTS formulations similar to the bromobutyl inner liner recipe shown in Table 2.2. Reinforcing fillers such as carbon black are added to improve strength, while paraffinic oils aid in processing and stearic acid solubilizes ZnO in the rubber phase.

Table 2.2 Typical formulation for a 100% bromobutyl inner liner[5]

| Component | Parts Per Hundred Rubber (phr) |
|---|---|
| Bromobutyl | 100.0 |
| Carbon Black | 62.00 |
| Paraffinic oil | 14.00 |
| Stearic acid | 1.00 |
| Zinc oxide (ZnO) | 5.00 |
| Sulphur | 0.50 |
| MBTS | 1.25 |

### 2.3.1 Sulphur Cure of Bromobutyl Rubber

Unlike IIR, bromobutyl rubber can be cured rapidly and efficiently by sulphur alone. This is demonstrated by the high state of cure obtained using only 0.5 phr sulphur (parts per hundred rubber) illustrated in Figure 2.4.[5] The higher states of cure obtained

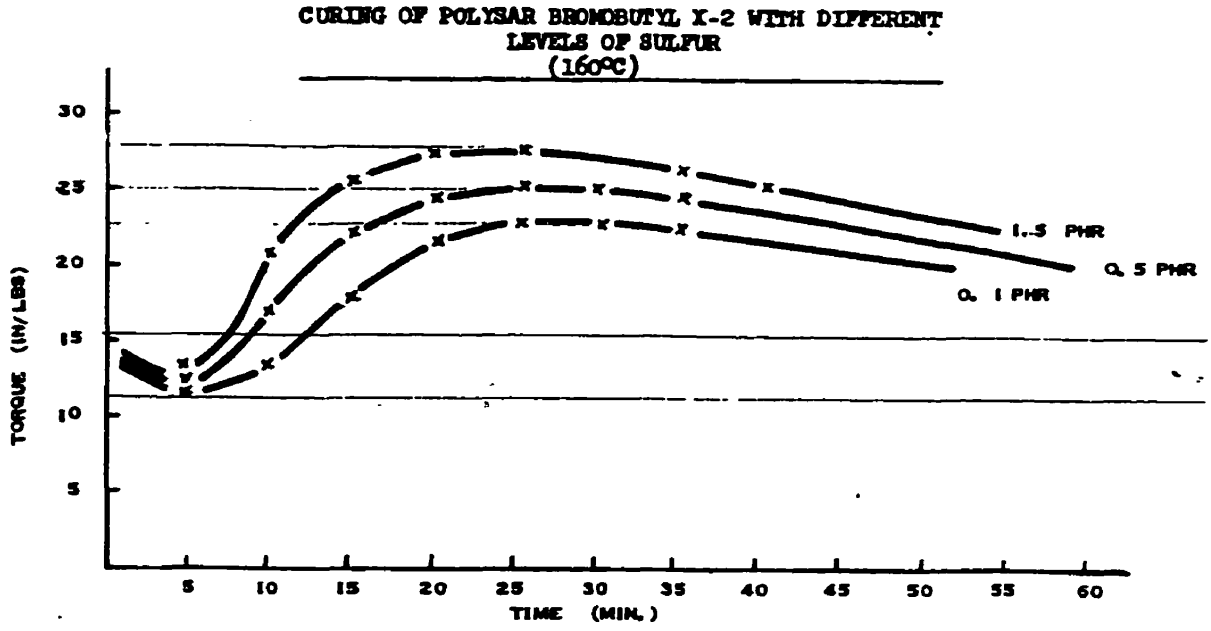


Figure 2.4: Rheometry curves of the sulphur vulcanization of BIIR[5]

with increasing sulphur levels are accompanied by a corresponding increase in the average sulphur rank of the crosslinks. At longer cure times, many crosslinks undergo nonoxidative thermal aging and revert to their pre-vulcanization state. The incorporation of a base reduces reversion and dramatically increases the final state of cure by inhibiting the acid catalyzed cleavage of poly-sulphidic crosslinks by HBr.[5]

Although many physical features of sulphur cured BIIR vulcanizates are known, the reaction mechanisms and crosslink structures have not been unambiguously determined. In the presence of BIIR, natural rubber can also be efficiently cured by

sulphur alone. This suggests the formation of an intermediate migratory curative that can move from the BIIR phase into the NR phase.[5] Reactions between sulphur and reactive alkyl chlorides have shown that sulphur can abstract chlorine to form sulphur chloride, which can cure natural rubber. Based on these results, a mechanism relying on the formation of $S_2Br_2$ has been proposed for the S+BIIR cure.[5] However, the instability of sulphur dibromide was not considered.

### 2.3.2 Zinc Oxide Cure of Bromobutyl Rubber

Only halobutyl and chlorobutadiene rubbers may be cured by ZnO alone, a characteristic imparted by reactivity of an allylic halide. Although the C-C crosslinks generated by this reaction pathway are thermally stable, ZnO+BIIR vulcanizates exhibit poor wear resistance and dynamic properties.[1] Figure 2.5 contrasts the stability of ZnO+BIIR networks with sulphur containing vulcanizates that experience significant reversion at longer cure times.

Much of what is known about the ZnO cure of bromobutyl comes from the model compound studies detailed in Section 2.4.3. Under cure conditions, elimination of HBr to form conjugated diene butyl has been observed in BIIR and in the brominated model compound (**5,6**).[17] Vukov has proposed that HBr eliminated by **3** reacts with ZnO to form $ZnBr_2$, a Lewis acid initiator for the cationic crosslinking mechanism illustrated in Figure 2.9.[6, 17] This theory also accounts for ZnO vulcanization of chlorobutyl rubber in which the removal of HCl to form $ZnCl_2$ has been identified as an essential step.[18] Dramatic differences in the reaction rates of BIIR and CIIR suggest that the halogen must influence the attack of the allylic halide on the allylic carbocation.

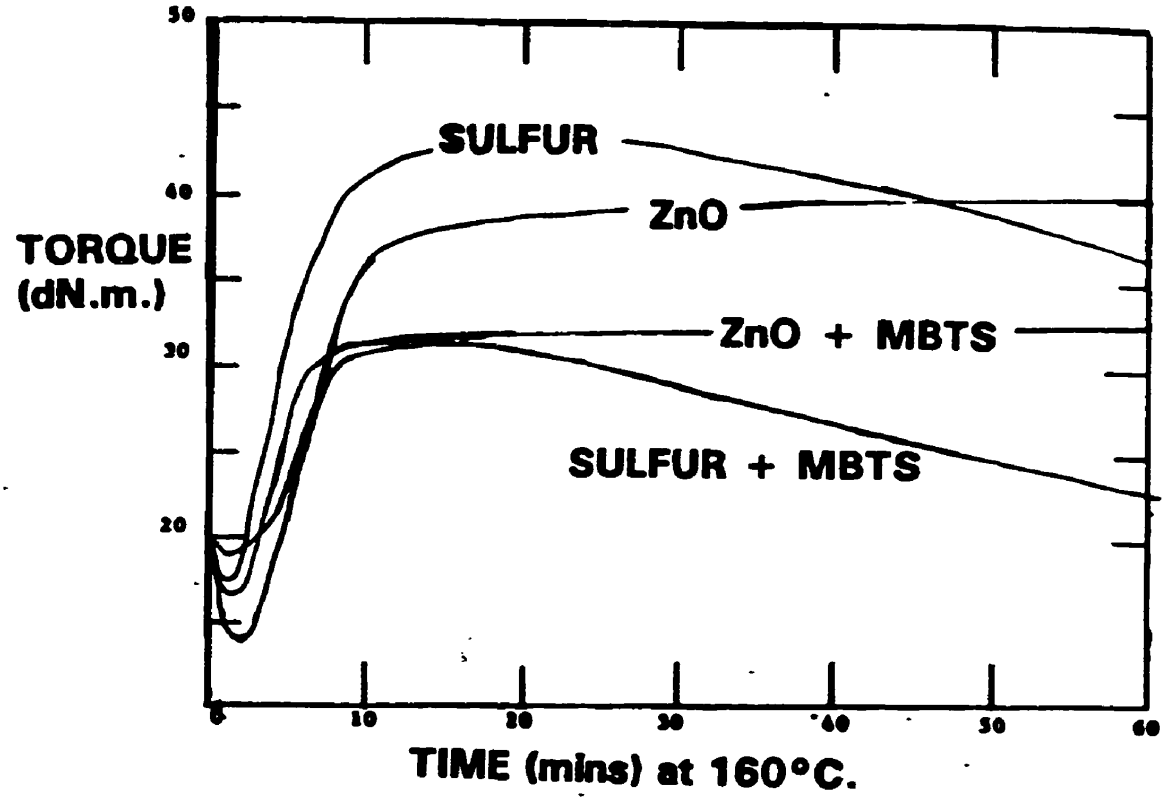


Figure 2.5: Rheometry curves of BIIR for various curative formulations[19]

The ZnO vulcanization of BIIR is relatively inefficient, with only an estimated 20% of the reactive sites producing crosslinks.[1,20] The efficiency can be increased to 50% with the addition of amine antioxidants or to 60% with the incorporation of *bis*-dienophiles such as m-phenylene *bis*-maleimide that form crosslinks with conjugated diene butyl through Diels-Alder type reactions.[1,20]

### 2.3.3 Accelerated Sulphur Cure of Bromobutyl: Sulphur, Zinc Oxide and MBTS

Although it is an effective accelerator in butyl rubber vulcanization, MBTS decreases the crosslink density in the brominated system (Figure 2.5). Nevertheless, it is incorporated into the principal curative recipes because it apparently improves the adhesion of a BIIR inner liner to the outer carcass of a tire. In the case of BIIR, it has been proposed that MBTS grafts directly onto the rubber, forming unreactive rubber-S-Ac pendant groups and MBT.[19] If this reaction occurs in the BIIR system, the resulting reduction in the number of available sites for crosslinking could account for the uncharacteristic reduction in crosslink density of formulations that contain MBTS.

The role of ZnO as a primary curative of BIIR and as an activator for accelerated formulations has been discussed. While Vukov and Wilson[20] have shown that the incorporation of ZnO to a S or S+MBTS curative recipe has a negligible effect on cure efficiency, others have shown that it can significantly increase the crosslink density.[19] Zinc oxide increases the extent of cure by catalyzing the reduction in rank of poly-sulphidic crosslinks to more thermally stable mono- and di-sulphides, and by obstructing the acid catalyzed cleavage of poly-sulphidic crosslinks. Conversely, the elimination of HBr to generate the Lewis acid ($ZnX_2$) reduces the number of available sites for crosslinking, leading to a decrease in sulphur cure efficiency. Therefore, the effect of ZnO on the crosslink density of a S+MBTS cured BIIR vulcanizate is dependent on the cure conditions and the concentration of the formulation components.

## 2.4 Model Compound Approach

### 2.4.1 Introduction and Motivation

The challenges associated with the structural characterization of crosslinked elastomers are formidable since vulcanizates are insoluble, and are therefore not amenable to solution analysis by nuclear magnetic resonance or mass spectroscopy. The structural investigations of vulcanizates using chemical probes,[21] kinetic studies, solid-state spectroscopy, and model compounds have been reviewed.[22] While IIR vulcanizates have been studied by $^{13}$C-NMR, the small amount of unsaturation in IIR and XIIR rubbers prevent the unambiguous characterization of their vulcanizates even using the most sophisticated solid state NMR techniques.[23]

Significant advances in vulcanizate characterization have been made using model compounds that accurately represent the reactive functionality of a polymer. The advantages of this approach include the ability to obtain a reactive functionality at a higher concentration than in a polymer, and to separate and characterize the vulcanization products with standard solution techniques. However, discretion is required when applying the results of model compound studies to vulcanizates because of variation between the model and polymer systems in the areas of network structure (steric hindrance), viscosity (diffusion limited reactions), concentration of reactive functionality, and polarity of the medium.

The cure chemistry of several elastomers including EPDM,[24] polybutadiene, natural rubber (*cis*-polyisoprene) and halogenated butyl rubber have been studied using model compound vulcanization techniques. While many of these studies have focused on

the characterization of model vulcanizates, others have led to an understanding of additional properties including the stability of vulcanizates and crosslink precursors.

The extensive use of the model compound 2-methyl-2-pentene has led to a thorough understanding of the structure and rank of the crosslinks in natural rubber. The vulcanizate structures generated in the accelerated sulphur cure of 2-methyl-2-pentene are presented in Figure 2.6. McSweeney and Morrison determined that the allylic A-type

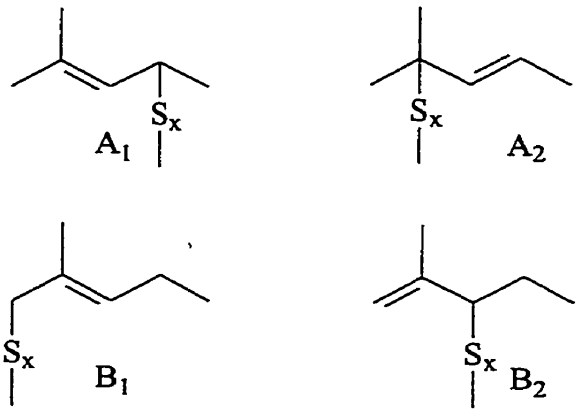


Figure 2.6: Crosslink structures in the accelerated vulcanization of 2-methyl-2-pentene[8]

crosslinks were more thermally stable than their B-type counterparts.[8] Additional work by Morrison and his co-workers investigated the formation, stability, and reactivity of model-$S_x$-Ac crosslink precursors.[7,25,26]

Lautenschlaeger used 2-methyl-2-pentene to determine the effects of reaction time, temperature, curative recipes, and model concentration on the vulcanizate product distribution.[27] This work showed that decreases in sulphur level, increases in accelerator level and extended reaction times promoted the formation of mono-sulphidic crosslinks (Figure 2.7). Zinc oxide was found to increase the cure efficiency and reduce the sulphur rank. Work by Skinner on the dependency of the model and elastomer crosslink rank on

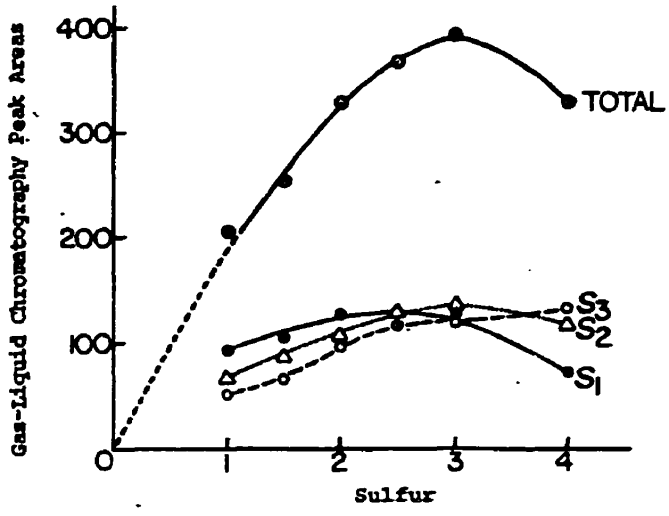


Figure 2.7: Effect of increasing sulphur levels on total sulphidic products and sulphides of different rank[27]

cure time showed direct correlations between the vulcanization of 2-methyl-2-pentene and natural rubber.[28] His work also confirmed that the attachment of sulphur to the model occurs almost exclusively at the allylic position when cured by an accelerated formulation.

The cure chemistry of polybutadiene (PBD) has also been investigated using model compounds. Characterization of the model vulcanizates of cis-hex-3-ene indicated poly-sulphidic crosslinks are formed initially, but undergo desulphuration to the mono- and di-sulphides.[28] In contrast, the accelerated sulphur vulcanization of PBD leads to a complex network with essentially no mono-sulphidic crosslinks. The ineffectiveness of cis-hex-3-ene as a model for PBD was further demonstrated by its inability to form the vicinal crosslinks stemming from adjacent carbons on the elastomer backbone that are known to exist in PBD. Gregg and Katrenick determined the crosslink structural

characteristics of *cis, cis*-1,5-cyclooctadiene, and revealed three membered episulphide rings that may be crosslink intermediates.[29] They further demonstrated agreement between the number of single and vicinal crosslinks in their model, and the theoretical number of effective chemical crosslinks in the vulcanized elastomer. While these model results are consistent with the presumed structure and chemistry of PBD cures, their later work showed that a minimum of three double bonds are necessary to accurately model PBD.[30] This emphasizes the necessity for a model to accurately reflect the functionality of the polymer it represents in order to apply model cure structures and chemistry to the vulcanizate.

### 2.4.2 Brominated 2,2,4,8,8-Pentamethyl-4-nonene: A Model Compound for Bromobutyl Rubber

The model compounds chosen to represent BIIR are the bromination products of 2,2,4,8,8-pentamethyl-4-nonene (**1**), specifically the exomethylene (**5**) and (E,Z)-bromomethyl isomers (**6**). These models represent the random copolymer structure of BIIR in which the brominated isoprene units are distributed uniformly. The model structure is essentially a brominated isoprene unit capped on either end by an isobutylene group.

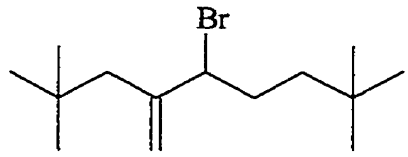


Exomethylene (Exo) (**5**)

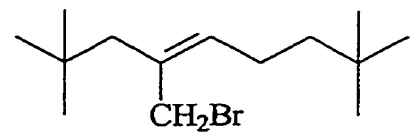


Bromomethyl (BrMe) (**6**)

The synthesis of **1**, originally developed by Steevensz and Clarke[31] and later revised by Chu,[32] is outlined in Figure 2.8. The use of a model requiring such a lengthy

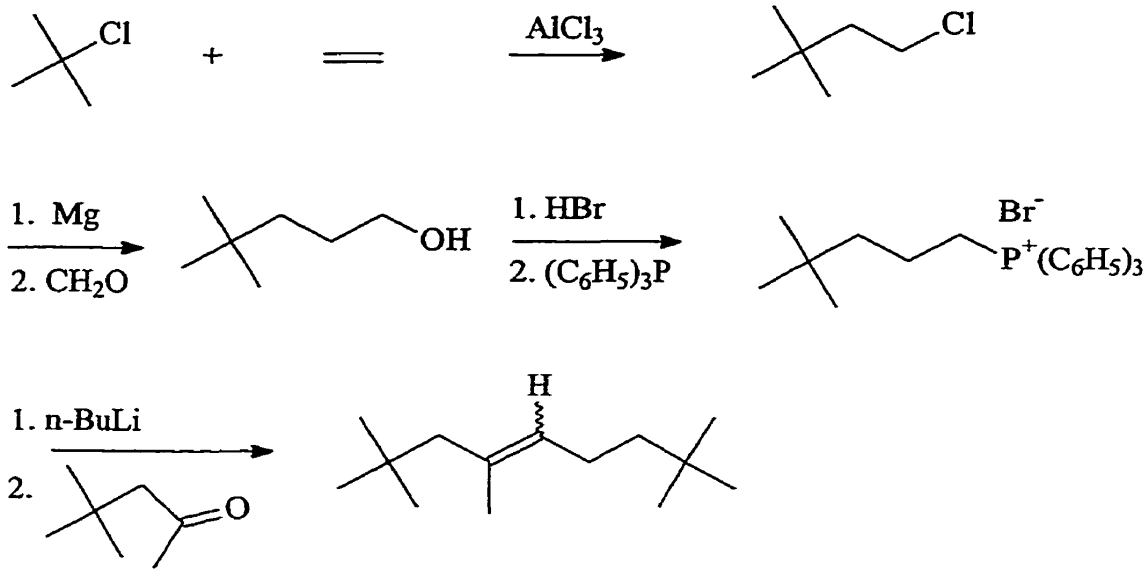


Figure 2.8: Synthesis of 2,2,4,8,8-Pentamethyl-4-nonene (1)

organic synthesis is justified by the inadequacy of simpler tri-substituted alkenes to effectively model the reactivity of IIR towards halogenation, and therefore towards curatives.[6]

While the bromination of the isoprene units in IIR leads exclusively to a mixture of allylic bromide substitution products (**3**,**4**), the bromination of simple tri-substituted alkenes yields only addition products. The halogenation of several alkenes, including 2,2,4,8,8-pentamethyl-4-nonene (**1**) and 4-methyl-4-nonene (**7**), were therefore investigated by Vukov to determine the effects of structure and steric hindrance on the halogenated product distribution.[6]

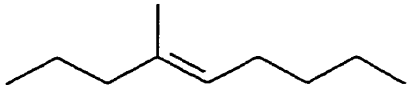

7

The chlorination of **7** resulted in a product distribution of rearranged allylic chloride substitution products (82%), and addition products (18%). In contrast,

chlorination of **1** led exclusively to substitution products. A similar, but more pronounced effect occurred in the bromination of these alkenes. Although bromination of **7** yielded exclusively addition products, bromination of **1** afforded both addition (10-30%) and substitution (70-90%) products, the latter consisting of the exomethylene (**5**) and bromomethyl (**6**) isomers.

The deviations in product distributions between the chlorination and bromination reactions were characteristic of differences in the properties and reaction mechanisms of the halogens. The preferred formation of substitution products in **1** versus **7** was attributed to the structural effects of the sterically bulky t-butyl groups that hinder the approach of the bromide ion ($Br_3^-$) to the intermediate bromonium ion **8**. This was confirmed by brominating **1** using 1,3-dibromo-5,5-dimethylhydantoin (**9**), a source of

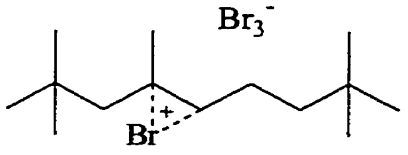


Bromium ion **8**

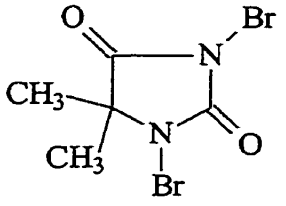


1,3-Dibromo-5,5-dimethylhydantoin **9**

positively charged bromine without a nucleophilic bromide ion, which exclusively led to the formation of the exomethylene and bromomethyl isomers.

By demonstrating halogenation products that are consistent with those found in XIIR, compound **1** is believed to be an effective model. Although allyl bromide and 3-chloro-2-methyl-1-pentene have been used to represent halobutyl rubber, their simple structures have proved incapable of representing the cure chemistry of BIIR and CIIR.[5,18]

In contrast, 2,2,4,8,8-pentamethyl-4-nonene and its brominated and chlorinated derivatives have proven to be effective tools in the investigations of the ZnO cure chemistry and ozonolysis of IIR and XIIR.[6,17,33]

### 2.4.3 Cure Studies of Halogenated 2,2,4,8,8-Pentamethyl-4-nonene and Zinc Oxide

The zinc oxide cure formulation of XIIR was the first to be investigated using the halogenated model compounds.[6,17] Analysis of these model BIIR vulcanizates by mass spectroscopy revealed peaks at *m/e* 194 ($C_{14}H_{26}$: conjugated diene), *m/e* 388 ($C_{28}H_{52}$: model dimer) and a small amount of *m/e* 582 ($C_{42}H_{78}$: model trimer), confirming the formation of C-C crosslinks.

Cationic and free radical mechanisms for the ZnO crosslinking chemistry of XIIR have been proposed.[6] An additional mechanism involving a ZnO catalyzed Diels-Alder mechanism of the conjugated diene was ruled out on the basis of cure reactivity rates, since the disappearance of the conjugated diene in the model cures is slow compared to the rapid cure rate of BIIR.

To determine which model structures are relevant to a ZnO cure, Vukov exposed the halogenated model compounds to typical cure temperatures. While the chlorinated model was stable, the brominated model compound (BrMC), like BIIR, underwent significant rearrangement to the bromomethyl isomer and elimination of HX to form a conjugated diene. The importance of HX elimination to ZnO vulcanization was revealed through studies of methallyl chloride, a simpler allylic halide model that cannot undergo elimination. It was shown that methallyl chloride did not react with ZnO, but did produce an oligomer when exposed to the Lewis acid $ZnCl_2$, which is known to cure

BIIR efficiently. These results led to the ZnO crosslinking mechanism shown in Figure 2.9.

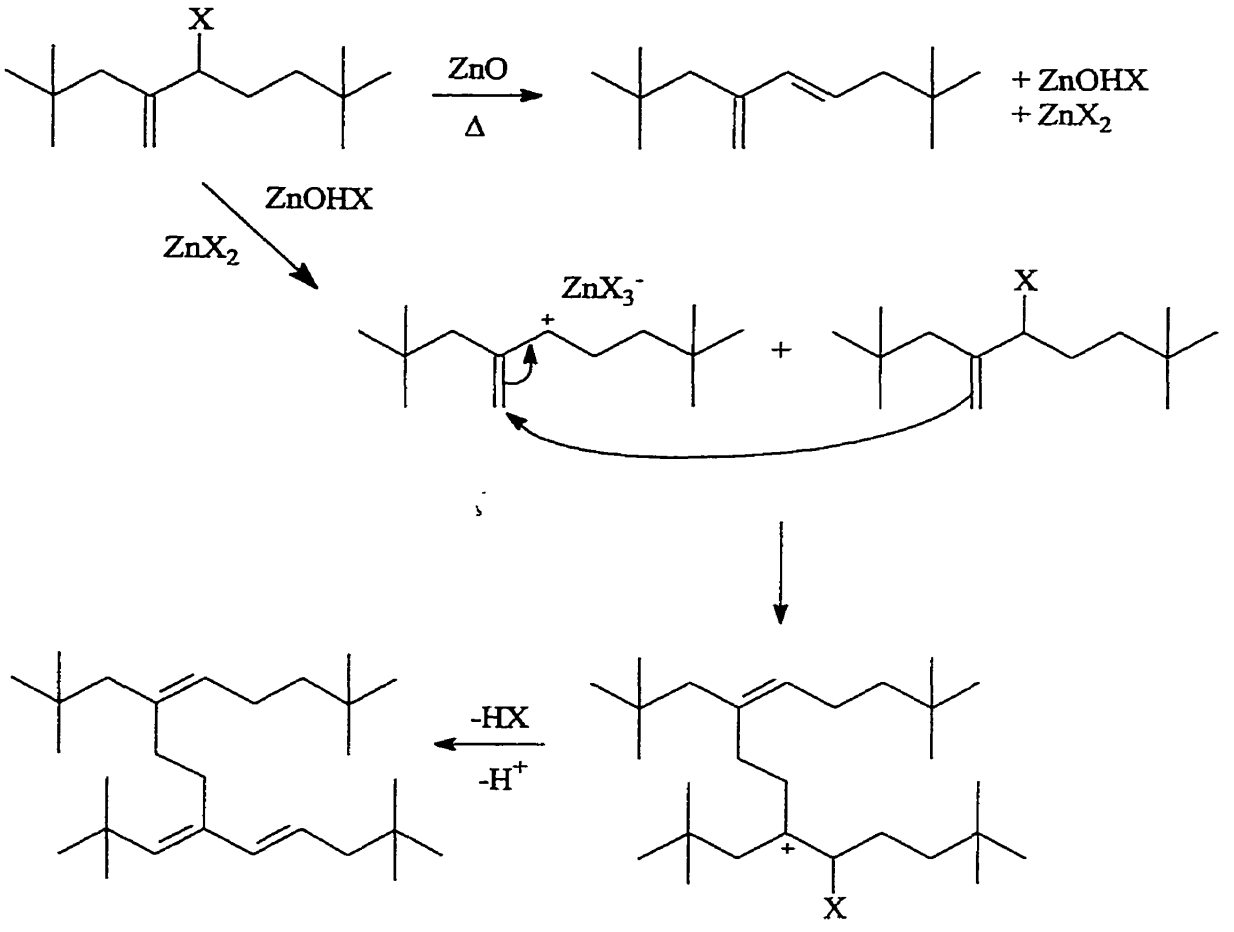


Figure 2.9: Proposed reaction mechanism for the ZnO only cure of BIIR

Prior to the crosslinking reaction, sufficient quantities of the halogenated model must undergo elimination of HX to form a conjugated diene and the Lewis acid. Up to 87% of the halogenated model undergoes elimination, thereby reducing the number of available sites for crosslinking. This is consistent with the relatively low efficiency of the ZnO vulcanization of XIIR (20%).[20] Upon formation of the zinc halide, the Lewis acid

mechanism competes with the elimination reaction to promote oligomerization of the model through a cationic mechanism. The consistency of this reaction scheme with the ZnO vulcanization of BIIR is evidence to support the utility of model investigations into XIIR cure chemistry.

## 2.5 Research Objectives

This thesis is part of a collaborative project between Queen's University and Bayer Inc. investigating BIIR cure chemistry. The research milestones of this project are:

Phase I

- Synthesize significant quantities of 2,2,4,8,8-pentamethyl-4-nonene, a model compound for butyl rubber, for future curing studies

Phase II

- Brominate the model compound and characterize the bromination products
- Determine the thermal stability of the brominated model compound by characterizing isomerization and elimination products
- Determine the relevance of the thermal isomerization and elimination products of the brominated model compound to the vulcanization chemistry of BIIR

Phase III

- React the brominated model compound with sulphur and MBTS
- React the BrMC with binary S+MBTS, S+ZnO, and ZnO+MBTS mixtures as well as a tertiary S+ZnO+MBTS mixture

- Chromatographically separate the complex mixture of cure products and characterize the principal products formed by nuclear magnetic resonance (NMR) and mass spectroscopy (MS)

Phase IV

- Determine the effect of calcium stearate on the S+ZnO+MBTS model vulcanizates
- Analyze the structure of BIIR vulcanizates using solid state NMR spectroscopy

# 3.0 Experimental

## 3.1 General

### 3.1.1 Materials

The following reagents were used as received: 2-chloro-2-methylpropane (99%, Aldrich), ethylene (99.5%, Linde), magnesium metal (FisherScientific), sulphuric acid (95-98%, FisherScientific), sodium bicarbonate (99.5%, BDH), 1,2,3,4-tetrahydronapthalene (97%, Aldrich), bromine (99.8%, Acros), triphenylphosphine (99%, Aldrich), 4,4-dimethyl-2-pentanone (99%, Aldrich), 2,6-di*tert*butyl cresol (99%, Aldrich), sulphur (Bayer Inc.), 2,2'-dithiobisbenzothiazole (Bayer Inc.), and bromobutyl rubber (Bayer Inc.). Paraformaldehyde (95%, Aldrich) and aluminium trichloride (99%, Aldrich) were stored in a dessicator and used as received. Methyl iodide (99%, Aldrich), n-butyl lithium (2.5M in hexanes, Aldrich) and 1,2-epoxydodecane (95%, Aldrich) were stored under refrigeration and used as received. The brominating agent 1,3-dibromo-5,5-dimethyl hydantoin (98%, Aldrich) was recrystallized from hot water then stored under refrigeration prior to use.

Sodium sulphate (99%, BDH) was stored at 110°C and used as received. Activated acidic aluminium oxide (standard grade-150 mesh, 58 Å, Aldrich) and nitrogen (Grade 5 - 99.999%, BOC) were used as received. The following reagent grade solvents were used as received: anhydrous diethyl ether (99%, BDH), hexanes (98.5%, Caledon), methylene chloride (99.5%, Anachemia), anhydrous DMSO (99.8%, Aldrich), anhydrous dodecane (99%, Aldrich), and 1,2,4-trichlorobenzene (99.6%, FisherScientific). Toluene (99.5%, Anachemia) was dried over molecular sieves (type 4Å, BDH).

### 3.1.2 Analytical Techniques

Nuclear magnetic resonance (NMR) spectra were obtained at 200 MHz on a Bruker AC-200 spectrometer, at 300 MHz on a Bruker AM-300 spectrometer, or at 400 MHz on a Bruker AM-400 spectrometer. The NMR solvent used throughout this study was deuterated chloroform ($CDCl_3$, 99.8% d, $^1H$ 7.24 ppm, $^{13}C$ 77.0 ppm, Cambridge Isotope Laboratories), and chemical shifts were recorded in parts per million ($\delta$) relative to the internal standard tetramethylsilane (TMS).

Analytical thin layer chromatography (TLC) was performed on aluminium oxide plates (0.25 mm thickness, Merck), as was preparative TLC (20 x 20 cm, 1.5 mm thickness, Merck). Hexanes (98.5%, Caledon) were used as the eluting solvent.

Normal phase high performance liquid chromatography (HPLC) was performed using a Waters 600 solvent delivery system equipped with ultraviolet (Waters 2487) and refractive index (Waters 2410) peak detectors. The reaction products were loaded onto an analytical Waters Nova-Pak Silica column (60Å, 4 μm, 3.9 x 150 mm) or a semi-preparative Supelco Supelcosil PLC-Si column (12 μm, 21.2 x 250 mm). Hexanes (98.5%, Caledon) and ethyl acetate (99.5%, BDH) were filtered (0.45 μm, Millipore), then used as eluting solvents. The semi-preparative column eluent was fractionated by a Waters Fraction Collector II.

A Fisons VG Quattro triple-quadrupole instrument was used to obtain mass spectra of the semi-preparative HPLC fractions. The samples were introduced into the ionization chamber using a solids probe that was maintained at 25°C for 5 minutes, then ramped to 300°C at 14°C/min. The samples were ionized by chemical ionization (CI) using isobutane.

## 3.2 Preparation of 2,2,4,8,8-Pentamethyl-4-nonene

The preparation of 2,2,4,8,8-pentamethyl-4-nonene was based on the synthesis outlined by Chu that is presented in Figure 2.8.[32]

### 3.2.1 Step 1: Preparation of 1-Chloro-3,3-Dimethylbutane

A dry, 250 ml three-necked, round-bottomed flask, equipped with a mechanical stirrer, was fitted with two gas inlet stopcocks. One stopcock was attached to a nitrogen/vacuum manifold, while the other was attached, via an oil bubbler, to an ethylene cylinder. The reactants were maintained at -20°C for the duration of the reaction by a Neslab external cooler immersed in an ethylene glycol bath. The flask was purged twice with nitrogen, then charged with t-butyl chloride (132 ml, 112 g, 1.209 mol), which was allowed to cool before the further addition of aluminium chloride (1.52 g, 0.0114 mol). The reaction flask was purged twice with ethylene, then a static ethylene atmosphere was maintained over the vigorously stirred reaction mixture for 3 hours.

Upon completion, the reaction mixture was poured into ice water (200 ml). The top organic layer (yellow) was washed with water (4 x 100 ml) and dried over sodium sulphate for 12 hours. The resulting clear liquid was filtered then purified by fractional distillation. The 1-chloro-3,3-dimethylbutane fraction collected at 113-117°C (117 g, 80% yield) was characterized by $^1$H NMR (200 MHz, $CDCl_3$, ppm): δ 0.9 (s, 9H, $-(CH_3)_3$), 1.7 (t, 2H, $-CH_2-$), 3.5 (t, 2H, $ClCH_2-$).

### 3.2.2 Step 2: Preparation of 4,4-Dimethylpentan-1-ol

A dry, 3L three-necked, round-bottomed flask, equipped with a stir bar, was fitted with a glass stopper, a condenser attached to a vacuum/nitrogen manifold, and a pressure

equalizing addition funnel. The flask was charged with freshly ground magnesium turnings (22.15 g, 0.911 mol), then the entire apparatus was purged twice with nitrogen. Anhydrous ether (85 ml) and 1-chloro-3,3-dimethylbutane (16.65 g, 21 ml, 0.138 mol) were combined in the addition funnel, then subsequently added to the vigourously stirred reaction flask along with a few drops of methyl iodide. Using a warm water bath, the reactants were gently refluxed while 1-chloro-3,3-dimethylbutane (83.35g, total 100g , 0.830 mol) in ether (290 ml) was added dropwise through the addition funnel (2-3 hours). After 30 minutes the water bath was removed, and the heat of reaction maintained the reflux. When the addition was complete, the reaction mixture was further refluxed for 30 minutes, and, upon cooling, anhydrous ether (300 ml) was canulated into the reaction flask.

Formaldehyde was generated from a separate dry, 500 ml two-necked, round-bottomed flask charged with paraformaldehyde (45g, 0.5 mol). One neck of this flask was fitted with a narrow bore stopcock attached to a nitrogen manifold, while the other was fitted with a wide gas delivery tube connected to the reaction flask in place of the addition funnel. The hose connecting the condenser to the manifold was replaced by a piece of tubing connecting the condenser to an exit bubbler. The temperature of the paraformaldehyde flask, initially maintained at 160°C using a PID controller acting on a heating mantle, was increased to 200°C at a rate to maintain a slow sweep of formaldehyde through the reaction vessel, indicated by the exit bubbler. When the temperature reached 200°C, a stream of nitrogen was applied in order to maintain the slow sweep rate. When all the paraformaldehyde had been depolymerized, the reactants

had changed from a slightly yellow mixture into a viscous grey liquid, which was stirred overnight.

The entire reaction mixture was then slowly poured into a 3 L Erlenmeyer flask containing an iced 10% sulphuric acid and water solution (750 ml), that was immersed in an ethylene glycol bath at -20°C. The mixture was stirred vigourously for 1 hour, and the yellow ether layer was separated. The remaining aqueous layer was extracted with ether (2 x 200 ml), and all the ether extracts were combined, washed with saturated sodium bicarbonate solution (2 x 100 ml), and dried over anhydrous sodium sulphate. Filtration and concentration by rotary evaporation afforded a clear yellow liquid (75g, 77% yield) that was characterized by $^1$H NMR (200 MHz, $CDCl_3$, ppm): $\delta$ 0.9 (s, 9H, -C($CH_3$)$_3$), 1.2 (m, 2H, -$CH_2$-), 1.5 (m, 2H, -$CH_2$-), 1.8 (s, HO-), 3.6 (t, 2H, -O$CH_2$-).

### 3.2.3 Step 3: Preparation of 1-Bromo-4,4-Dimethylpentane

A 250 ml two necked, round-bottomed flask, equipped with a stir bar, was fitted with a small-bore stopcock and a condenser leading to a base trap (aq. NaOH). The flask was charged with 4,4-dimethylpentan-1-ol (46.4g, 0.40 mol), and maintained at 110°C by a PID controller acting on a heating mantle. Generation of HBr was carried out in a separate 300 ml three-necked, round-bottomed flask equipped with a stir bar and fitted with a small-bore stopcock, delivery tube, and pressure equalizing addition funnel. This flask was charged with tetralin (150 ml), then bromine (50 ml, 0.98 mol) was pipetted into the addition funnel. The stopcock was attached to a nitrogen cylinder, and the delivery tube was connected, via a tetralin bubbler, to the stopcock of the reaction flask. Nitrogen was swept through the system for 10 minutes prior to the reaction. The nitrogen

flow was stopped, and the system was gradually purged with HBr by the dropwise addition of bromine to the tetralin, achieving a HBr atmosphere in the reaction flask. The addition was slow enough to prevent unreacted HBr from venting through the base trap.

When all the bromine had been added, the reaction mixture was cooled to room temperature then the organic layer (top) was separated and washed with concentrated sulphuric acid (2 x 15 ml). Methylene chloride (50 ml) was added to the organic layer (bottom) to facilitate separation prior to further washing with water (2 x 75 ml) and with a saturated sodium bicarbonate solution. The organic layer was dried over anhydrous sodium sulphate, filtered and concentrated by rotary evaporation. The resulting dark red product (54.4 g, 76 % yield) was characterized by $^1$H NMR (200 MHz, $CDCl_3$, ppm): δ 0.9 (s, 9H, $-C(CH_3)_3$), 1.25 (m, 2H, $-CH_2-$), 1.8 (m, 2H, $-CH_2-$), δ3.35 (t, 2H, $BrCH_2-$).

### 3.2.4 Step 4: Preparation of the Phosphonium salt of 1-Bromo-4,4-Dimethylpentane

A dry 500 ml two necked, round-bottomed flask, equipped with a magnetic stirrer, was fitted with a stopper and a condenser connected to a vacuum/nitrogen manifold. The system was purged twice with nitrogen, then subsequently charged with 1-bromo-4,4-dimethylpentane (51 g, 0.280 mol), triphenylphosphine (81 g, 0.309 mol), and dry toluene (200 ml). The reaction mixture was refluxed under a nitrogen atmosphere for 8 hours. The white solid that formed was filtered and washed with hexanes (50 ml). The filtrate was concentrated by rotary evaporator, then the resulting solid was filtered and washed with hot hexanes (50 ml) to remove unreacted triphenylphosphine. The crude solid products were combined, dissolved in the minimum

amount of methylene chloride, and recrystallized by the addition of hexanes. The resulting white powder was filtered and dried in a vacuum oven at 60°C for 24 hours. Drying afforded the phosphonium salt (55 g) in a yield of 46 %. The product was characterized by $^1$H NMR (200 MHz, $CDCl_3$, ppm): δ 0.8 (s, 9H, $-C(CH_3)_3$), 1.5 (m, 4H, $-CH_2-CH_2-$), 3.65 (m, 2H, $-CH_2-$), 7.67 (m, 15H, $-P^+(C_6H_5)_3$).

### 3.2.5 Step 5: Preparation of 2,2,4,8,8-Pentamethyl-4-nonene

A dry 500 ml two necked, round-bottomed flask, equipped with a stirring bar, was fitted with a rubber septum and a gas inlet attached to a nitrogen/vacuum manifold. The flask was purged twice with nitrogen then charged with the phosphonium salt of 1-bromo-4,4-dimethylpentane (40 g, 0.0906 mol). Dry, distilled dimethyl sulfoxide (DMSO, 200 ml) was canulated into the flask, then a solution of n-BuLi (50 ml, 2.5 M in hexanes, 0.125 mol) was added dropwise by syringe. The solution changed from colourless to bright yellow, orange and finally deep red. The reaction mixture was stirred for 30 minutes at room temperature before 4,4-dimethyl-2-pentanone (14.46 g, 0.127 mol) was added dropwise, changing the reaction mixture to an orange-red colour. When the addition was complete, the solution was stirred at room temperature overnight.

The resulting orange-brown mixture was poured into a beaker containing water (800 ml) and allowed to sit for 1 hour. The precipitate was filtered and washed with hexanes (30 ml), and then the filtrate was extracted with hexanes (2 x 100 ml). The combined hexanes fractions were washed with water (2 x 100 ml), and then dried over anhydrous sodium sulphate. The solution was filtered and then concentrated by rotary evaporation, affording a solid-liquid mixture, which was chilled in the refrigerator

overnight. The solid that separated out was filtered off and washed with cold hexanes, and the combined organic fractions were concentrated by rotary evaporation, yielding a clear but slightly yellow liquid.

The crude product was eluted through a column of acid alumina (80 g) with hexanes (150 ml). Concentration by rotary evaporation was followed by a vacuum distillation using a kugelrohr apparatus. The distillation afforded the product (7.76 g, boiling point 70°C, 15 mm Hg) in a yield of 44%. Proton NMR indicated the product was of high purity with a cis:trans ratio of 34:66. $^1$H NMR (200 MHz, $CDCl_3$, ppm): δ 0.9 (m, 18H, 2 x -C($CH_3$)$_3$), 1.2 (m, 2.19H, -$CH_2$-), 1.6 (s, 1.82H, trans –$CH_3$), 1.7 (s,1.03H, cis –$CH_3$), 1.9 (m, 4H, 2 x -$CH_2$-), 5.1 (t, 0.66H, trans -CH), 5.2 (t, 0.33H, cis -CH). NMR Figure 4.1 is attached showing all peak assignments.

### 3.3 Bromination of 2,2,4,8,8-Pentamethyl-4-nonene

Bromination of 2,2,4,8,8-pentamethyl-4-nonene was carried out as outlined by Ho and Guthmann.[33] A 50 ml round-bottomed flask, wrapped in aluminium foil and submerged in an ice water bath, was charged with 2,2,4,8,8-pentamethyl-4-nonene (0.4 g, 2 mmol) and dichloromethane (10 ml). After temperature equilibration, 1,3-dibromo-5,5-dimethylhydantoin (0.32g, 1.12 mmol) and 2,6-di-tert-butylcresol (0.005g, 0.023 mmol) were added to the reaction mixture, which was then stirred vigourously in the dark for 30 minutes. The dichloromethane was removed by rotary evaporation, and then the residue was taken up in hexanes (30 ml) and filtered. The filtrate was concentrated at room temperature, then vacuum distilled using a kugelrohr apparatus. The distillation afforded a clear, yellow liquid (0.349 g, boiling point 70-85°C, 6 mm Hg) in a yield of 64%. The

product, characterized by $^1$H NMR, was a mixture of three isomers of brominated 2,2,4,8,8-pentamethyl-4-nonene: exomethylene (exo) (37%) and (E,Z)-bromomethyl (E,Z-BrMe) (63%).

An alternative procedure to obtain a larger exo:BrMe isomer ratio was carried out at -40°C using a $CO_2$/acetone bath. A 50 mL two necked round bottom flask, fitted with a narrow bore stopcock and a stopper, was wrapped in aluminium foil and lowered into the acetone bath. The flask was charged with 2,2,4,8,8-pentamethyl-4-nonene (0.4 g, 2 mmol) and dichloromethane (10 ml) prior to being evacuated and back filled with nitrogen. After temperature equilibration (-40°C), 1,3-dibromo-5,5-dimethylhydantoin (0.32g, 1.12 mmol) and 2,6-di-*tert*-butylcresol (0.005g, 0.023 mmol) were added to the reaction mixture, which was stirred vigourously in the dark for 90 minutes. The dichloromethane was removed under reduced pressure at -40°C, and then chilled hexanes (40 mL, -30°C) were added to the residue. The stopper was replaced by a chilled glass frit that led to a chilled 100 mL round bottom flask. The entire apparatus was evacuated and backfilled with nitrogen, then inverted such that the 100 mL flask containing the filtered reactants was submerged in the $CO_2$/acetone bath. The hexanes were removed under reduced pressure at -40°C affording a clear yellow liquid. The exo:BrMe isomer ratio, determined by $^1$H NMR, was 90:10.

NMR (400 MHz, $CDCl_3$, ppm): δ 0.8–2.2 (m, 24H, 2 x -$C(CH_3)_3$, 3 x –$CH_2$-), 4.09 (s, 1.631H, Z-BrMe $BrCH_2$-), 4.11 (s, 1.479H, E-BrMe $BrCH_2$-), 4.40 (t, 0.933H, exo -C(HBr)-), 5.02 (s, 1H, exo HC-), 5.39 (s, 1H, exo HC-), 5.41 (t, 0.801H, Z-BrMe HC- ), 5.75 (t, 0.754H, E-BrMe HC-). NMR Figures 4.2 and 4.3 are attached showing all downfield peak assignments.

### 3.4 Thermal Stability Analysis of BIIR in Solution

A 1L round-bottomed flask, equipped with a stir bar and fitted with a condenser, was charged with 1,2,4-trichlorobenzene (91.67g) and maintained at 145°C by a PID controller acting on a heating mantle. With vigourous stirring, a solution containing Polysar BIIR (5.18g) dissolved in 1,2,4-trichlorobenzene (86 g) was added to the reaction flask. Solution aliquots (15 ml) taken at 15, 30, 45, 60, 75, 90, 105 and 120 minutes were precipitated from methanol, filtered, and dried at 40°C overnight in a vacuum oven (11.5 in Hg). The solid polymer samples were dissolved in $CDCl_3$ and characterized by 400 MHz $^1H$ NMR.

### 3.5 Thermal Stability Analysis of BIIR in the Bulk

The thermal stability of Polysar BIIR was investigated with an Atlas Laboratory Mixing Moulder using a rotor speed of 50 RPM. The mixing cup, preheated to 145°C, was charged with a 0.28 g sample of BIIR, and the rotor was lowered onto the polymer for the duration of the experiment. Individual samples were held under these conditions for 15, 30, 45, 60, 80, 100, and 120 minutes. Each sample was extruded, dissolved in $CDCl_3$, and structurally characterized by 400 MHz $^1H$ NMR.

## 3.6 Thermal Stability Analysis of Brominated 2,2,4,8,8-Pentamethyl-4-nonene (BrMC)

### 3.6.1 Design and Control of the Reaction Apparatus

The thermal stability analysis and crosslinking reactions of the BrMC were carried out using Wheaton vials (1 ml) equipped with magnetic stir bars and the heating block shown in Figure A1 (Appendix A). The three 1000 W, 12 inch, ½ inch O.D. Omega cartridge heaters embedded in the aluminium heating block were connected in series and delivered 282 W at 120 V. A thermocouple inserted into a reference vial monitored the reaction temperature, which was maintained by a PID controller tuned using the Ziegler and Nichols method outlined in Seborg et. al.[34] The reactant temperature was maintained within ± 1°C by setting the cycle time to 7 seconds, the proportional gain to 2%, the integral time constant to 12, and the derivative rate to 3.64.

The temperature profiles of the two distinct vial positions in the heating block were determined. In each case, a vial charged with 1,2,4-trichlorobenzene (0.7 ml) was inserted into the heating block which was being maintained at 145°C using a reference vial. The trichlorobenzene within the reaction vials at both positions reached 95% of the set temperature in 90 seconds.

### 3.6.2 Thermal Stability Analysis of Brominated 2,2,4,8,8-Pentamethyl-4-nonene (BrMC)

Experiments investigating the thermal stability of the BrMC were performed under the conditions listed in Table 3.1. Dodecane and 1,2,4-trichlorobenzene were chosen as non-polar solvents for this work on the basis of their $^{1}H$ NMR resonances. The aliphatic resonances of dodecane do not overlap with the aromatic resonances of MBTS,

while the aromatic resonances of 1,2,4-trichlorobenzene do not overlap with the aliphatic resonances of the BrMC.

Each reaction vial was charged with solvent and 1,2-epoxydodecane as required, and inserted into the heating block for at least 15 minutes to allow temperature equilibration. The respective amount of BrMC was then injected into the vial through the PTFE/silicone septum in the lid using a micro-syringe. The total reaction volume of each vial was 0.7 ml. Over the course of each experiment, aliquots (0.1 ml) were taken and transferred into NMR tubes containing chilled $CDCl_3$. The thermal isomerization products were characterized on a 400 MHz NMR spectrometer.

Table 3.1: Experimental conditions for the thermal stability analysis of the BrMC.

| Experiment | Temperature (°C) | Solvent | Concentration of BrMC (mol/L) | Concentration of 1,2-Epoxydodecane (mol/L) |
|---|---|---|---|---|
| 1 | 100 | 1,2,4-trichlorobenzene | 1.77 | 0.00 |
| 2 | 145 | 1,2,4-trichlorobenzene | 1.77 | 0.00 |
| 3 | 145 | 1,2,4-trichlorobenzene | 0.88 | 0.00 |
| 4 | 145 | 1,2,4-trichlorobenzene | 0.78 | 1.87 |
| 5 | 145 | 1,2,4-trichlorobenzene | 0.43 | 1.00 |
| 6 | 140 | dodecane | 0.45 | 1.87 |
| 7 | 140 | dodecane | 0.60 | 1.87 |
| 8 | 140 | dodecane | 0.45 | 1.87 |
| 9 | 145 | compound 1 | 1.02 | 1.52 |

## 3.7 Cure Studies of Brominated 2,2,4,8,8-Pentamethyl-4-nonene (BrMC)

### 3.7.1 Reaction of Brominated 2,2,4,8,8-Pentamethyl-4-nonene (BrMC) with 2,2'-Dithiobisbenzothiazole (MBTS)

Reactions between the brominated model compound and MBTS were carried out in 1 mL Wheaton vials. Each vial was charged with the BrMC (0.15 mL, 0.927 mmol), an equimolar quantity of MBTS (0.3075 g, 0.927 mmol), 1,2-epoxydodecane (0.20 mL, 0.960 mmol), and dodecane (0.3 mL). Using the aluminium heating block described in Section 3.6.1, the vials were maintained at 140°C for 7 minutes.

The crude reaction mixture was separated by TLC using a preparative alumina plate (1.5 mm thickness) with hexanes as the eluting solvent. The resulting four distinct bands with $R_f$ values of 0.00, 0.02-0.14, 0.45-0.50 and 0.54-0.59 were removed from the plate, then filtered and washed with dichloromethane. The filtrate was concentrated by rotary evaporation at room temperature, then analyzed by 400 MHz $^1$H NMR.

### 3.7.2 Reaction of Brominated 2,2,4,8,8-Pentamethyl-4-nonene (BrMC) with Sulphur

Reactions between the brominated model compound and sulphur were carried out in 1 mL Wheaton vials. Each vial was charged with the BrMC (0.15 mL, 0.927 mmol), 1,2-epoxydodecane (0.20 mL, 0.959 mmol), dodecane (0.17 mL) and sulphur ($S_8$)(0.0522g, 0.204 mmol). The quantity of sulphur corresponded to a 2 phr sulphur cure of BIIR that contains approximately 0.22 mol $S_8$ per mol isoprene. Using the aluminium heating block described in Section 3.6.1, the vials were maintained at 140°C for 7 minutes.

The crude reaction mixture was filtered (0.45 μm syringe filter), then separated by semi-preparative HPLC with hexanes as the eluting solvent (7 mL/min). Refractive

index and UV absorbance (254 nm) detectors monitored the column eluent, which was fractionated into collection vials (10 seconds/vial). The contents of the vials containing individual cure products (as identified by peaks in the UV and RI chromatograms) were combined and concentrated by rotary evaporation. The cure products were characterized by 400 MHz $^1$H NMR and mass spectroscopy.

### 3.7.3 Reaction of Brominated 2,2,4,8,8-Pentamethyl-4-nonene (BrMC) with Sulphur and MBTS

Reactions between the brominated model compound sulphur and MBTS (BrMC+S+MBTS) were carried out in 1 mL Wheaton vials. Each vial was charged with the BrMC (0.15 mL, 0.927 mmol), 1,2-epoxydodecane (0.20 mL, 0.959 mmol), dodecane (0.17 mL), sulphur ($S_8$)(0.013g, 0.051 mmol) and MBTS (0.0345g, 0.103 mmol). The quantity of sulphur and MBTS corresponded to a 0.5 phr sulphur/1.3 phr MBTS cure of BIIR that contains approximately 0.055 mol $S_8$ and 0.111 mol MBTS per mol isoprene. Using the aluminium heating block described in Section 3.6.1, the vials were maintained at 140°C for 7 minutes.

The crude reaction mixture was filtered, then separated by preparative TLC with hexanes as the eluting solvent. The resulting five distinct bands with $R_f$ values of 0.00, 0.38-0.47, 0.62-0.68, 0.68-0.72, and 0.72-0.80 were removed from the plate, then filtered and washed with dichloromethane. The filtrate was concentrated by rotary evaporation at room temperature, then analyzed by 400 MHz $^1$H NMR. Characterization of these cure products was by 400 MHz $^1$H NMR and mass spectroscopy.

# 4.0 Results and Discussion

## 4.1 Synthesis of 2,2,4,8,8-Pentamethyl-4-nonene

### 4.1.1 Step 1: Preparation of 1-Chloro-3,3-Dimethylbutane

The procedure of Chu[32] was used (Figure 2.8) with the following modifications: 1) a static ethylene atmosphere was maintained in the reaction flask rather than continuously bubbling the gas through the reaction mixture, and 2) sodium sulphate was used in place of potassium hydroxide as the drying agent in order to prevent substitution reactions with the product. Distillation of the product was required to remove unreacted t-butyl chloride and to obtain a product of sufficient purity for the next step. The product was characterized by $^1$H NMR and the spectrum agreed with that previously reported by Chu: a singlet at 0.9 ppm integrating for the nine protons of the t-butyl group, a triplet at 1.7 ppm integrating for the two -$CH_2$- protons adjacent to the t-butyl group, and a triplet at 3.5 ppm integrating for the two -$CH_2Cl$ protons. The overall yield after distillation was 80% (77% literature yield).

### 4.1.2 Step 2: Preparation of 4,4-dimethylpentan-1-ol.

The procedure of Chu[32] was used with an altered purification procedure; chilling the sulphuric acid solution to 0°C reduced the loss of ether through evaporation and increased product recovery. Distillation was unnecessary, as the concentrated product was of sufficient purity to proceed to the next step. The product was characterized by $^1$H NMR, and the spectrum agreed with that previously reported: a singlet at 0.9 ppm integrating for the nine protons of the t-butyl group, a multiplet at 1.2 ppm integrating for

the two -$CH_2$- protons adjacent to the t-butyl group, a multiplet at 1.5 ppm integrating for the two -$CH_2$- protons adjacent to the -$CH_2O$- protons, a broad singlet at 1.8 ppm for the –OH proton, and a triplet at 3.6 ppm integrating for the two -$CH_2O$- protons. The overall yield after distillation was 77% (85% literature yield).

### 4.1.3 Step 3: Preparation of 1-Bromo-4,4-Dimethylpentane

Two modifications were made to the procedure of Chu.[32] Firstly, the quantity of bromine added was increased, and secondly, a static HBr atmosphere was maintained in the reaction flask instead of sweeping HBr through in a nitrogen stream. The product, which was of sufficient purity to proceed to the next step without distillation, was characterized by proton NMR, and the spectrum agreed with that previously reported: a singlet at 0.9 ppm integrating for the nine protons of the t-butyl group, a multiplet at 1.25 ppm integrating for the two protons of the-$CH_2$- group adjacent to the t-butyl group, a multiplet at 1.8 ppm integrating for the two -$CH_2$- protons adjacent to the -$CH_2Br$ protons, and a triplet at 3.35 ppm integrating for the two -$CH_2Br$ protons. The overall yield was 76% (literature 84%).

### 4.1.4 Step 4: Preparation of the Phosphonium Salt of 1-Bromo-4,4 Dimethylpentane

The phosphonium salt was prepared according to the procedure of Chu.[32] The yield of the salt after recrystallization and drying was 46%, half of what had been previously reported (literature 90%). In an attempt to increase the yield, the reaction time was varied between 5 and 12 hours, and repetitive filtrate concentration and recrystallization sequences were implemented. However, neither technique led to

substantial increases in the overall yield. The $^1$H NMR characterization agreed with that reported previously: a singlet at 0.8 ppm integrating for the nine protons of the t-butyl group, a multiplet at 1.5 ppm integrating for the 4 protons of the $-CH_2-CH_2-$ group adjacent to the t-butyl group, a multiplet at 3.65 ppm integrating for the two protons of the $-CH_2-$ group adjacent to the $-P^+Ph_3$, and a multiplet at 7.67 ppm integrating for the 15 aromatic protons of the $-P^+(C_6H_5)_3$ groups.

### 4.1.5 Step 5: Preparation of 2,2,4,8,8-Pentamethyl-4-nonene (1)

The Wittig reaction was carried out according to the procedure of Chu, with a product yield of 44% (literature 70%).[32] The overall yield in the synthesis of 2,2,4,8,8-pentamethyl-4-nonene was 9.5%, similar to that of Steevensz and Clarke,[31] but one third of that obtained by Chu. Distillation of the crude products was necessary to obtain the compound in high purity for characterization and subsequent bromination. The distilled product was characterized by $^1$H NMR, and the peak assignments, in agreement with those made by Chu, are given in Table 4.1 and shown in Figure 4.1. The resolution of the olefinic protons at 5.10-5.20 ppm enabled the E:Z product ratio to be determined as 66:33; this is consistent with the 67:33 ratio determined previously by GC.

Table 4.1: 400 MHz $^1$H NMR peak assignments of 2,2,4,8,8-pentamethyl-4-nonene in $CDCl_3$

| Chemical Shift (ppm) | Multiplicity[a] | Assignment |
|---|---|---|
| 0.90 | m | t-butyl groups |
| 1.20 | m | $CH_2$ |
| 1.60 | s | $CH_3$, E isomer |
| 1.70 | s | $CH_3$, Z isomer |
| 1.80-2.00 | m | 2 x $CH_2$, E isomer<br>2 x $CH_2$, Z isomer |
| 5.10 | t | olefinic H, E isomer |
| 5.20 | t | olefinic H, Z isomer |

[a] s = singlet, m = multiplet t= triplet

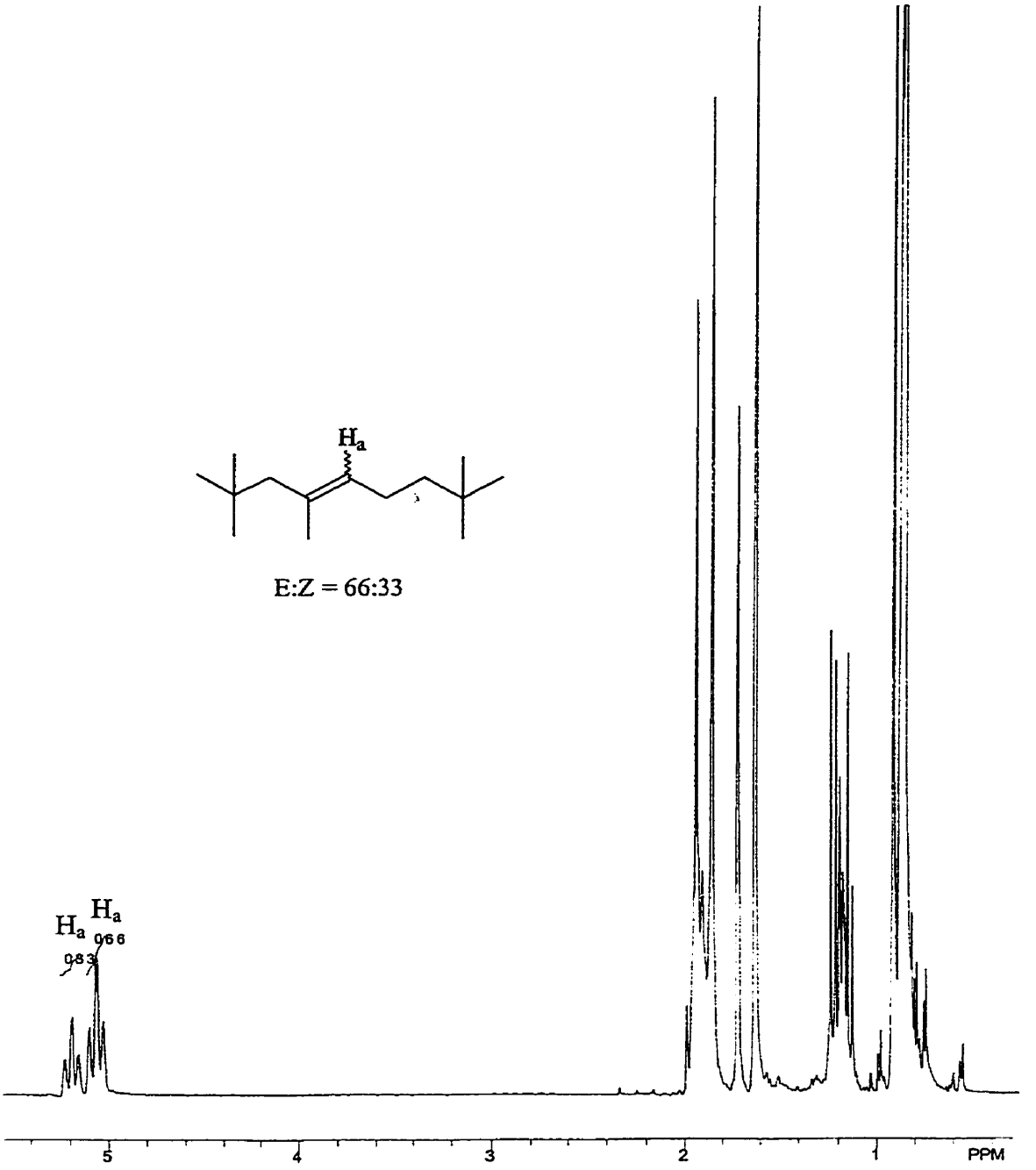


Figure 4.1: 400 MHz $^1$H NMR spectrum of 2,2,4,8,8-pentamethyl-4-nonene in $CDCl_3$

## 4.2 Bromination of 2,2,4,8,8-Pentamethyl-4-nonene (1)

Bromination of the model compound was carried out using 1,3-dibromo-5,5-dimethylhydantoin, which directed the reaction exclusively to substitution products in a yield of 64% after distillation. Characterization by $^1$H NMR indicated that the brominated model compound existed as a mixture of the exomethylene (exo) **5**, E-bromomethyl (E-BrMe) **6a** and Z-bromomethyl (Z-BrMe) **6b** isomers. The spectrum

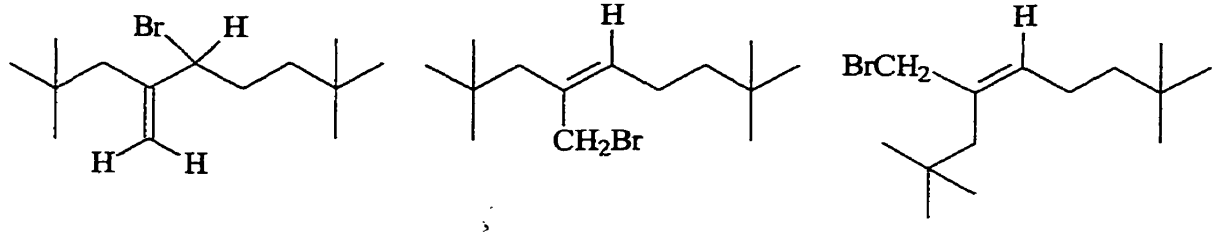


Exo **5** E-BrMe **6a** Z-BrMe **6b**

agreed with that reported by Ho and Guthmann,[33] and the downfield proton peak assignments that were made with the assistance of a COSY correlated NMR experiment are given in Table 4.2 and shown in Figures 4.2 and 4.3.

Table 4.2: Downfield peak assignments in the 400 MHz $^1$H NMR spectrum of Brominated 2,2,4,8,8-pentamethyl-4-nonene

| Chemical Shift (ppm) | Multiplicity[a] | Assignment |
|---|---|---|
| 4.07 | s | $CH_2$, E-BrMe |
| 4.10 | s | $CH_2$, Z-BrMe |
| 4.38 | t | allylic H, Exo |
| 5.03 | s | olefinic H, Exo |
| 5.39 | s | olefinic H, Exo |
| 5.41 | t | olefinic H, E-BrMe |
| 5.76 | t | olefinic H, Z-BrMe |

[a] s = singlet, t= triplet

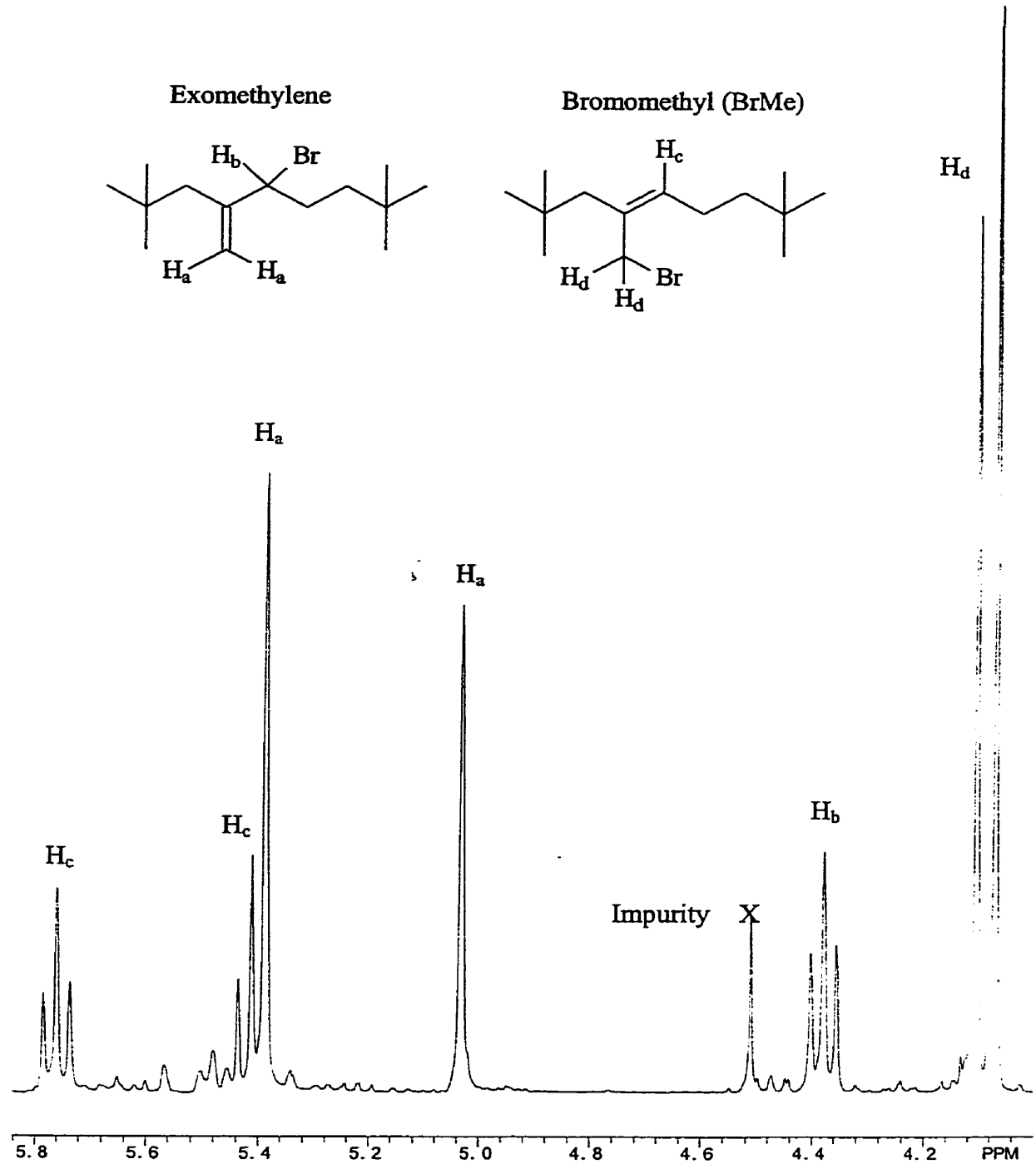


Figure 4.2: Downfield region in the 400 MHz $^1$H NMR spectrum of brominated 2,2,4,8,8-pentamethyl-4-nonene in $CDCl_3$

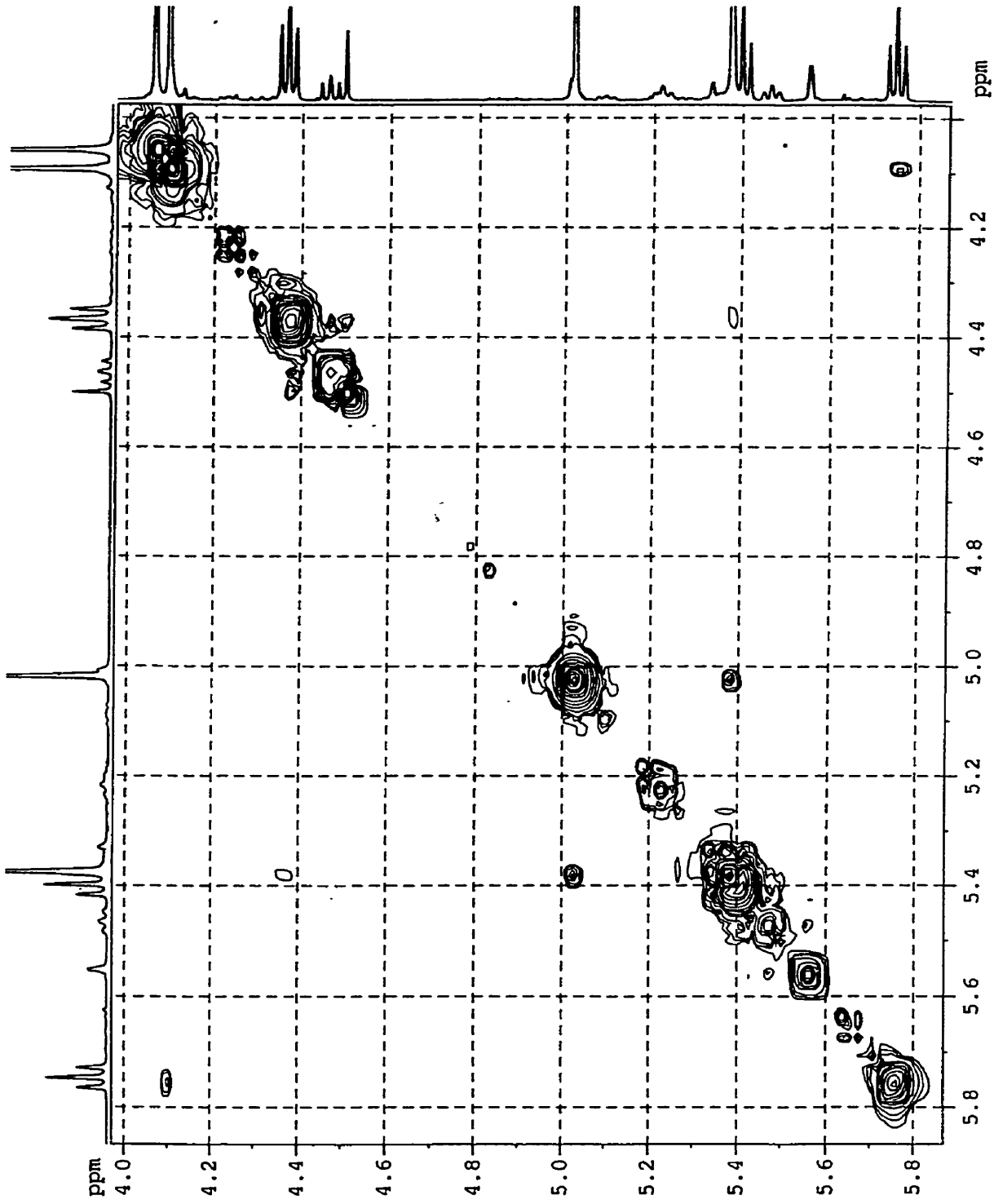


Figure 4.3: Downfield region in the 300 MHz 2D COSY $^1$H NMR spectrum of brominated 2,2,4,8,8-pentamethyl-4-nonene in $CDCl_3$

The bromination of **1** at 0°C followed by isolation and purification at room temperature yielded an exo:BrMe product ratio of 37:63. In contrast, the bromination of IIR almost exclusively yields the exomethylene isomer. Therefore, the effect of reaction and isolation temperatures on the product distribution was investigated in order to obtain the brominated model with a higher exo:BrMe ratio consistent with the structure of BIIR. Bromination and isolation at 0°C improved the exo:BrMe ratio to 54:46, while a reaction and isolation temperature of -40°C produced an exo:BrMe ratio of 90:10. The thermal stability and cure studies were performed using BrMC that had been synthesized at 0°C or -40°C to represent the structure of BIIR more accurately.

## 4.3 Thermal Stability Analysis of Brominated Butyl Rubber

The thermal stability of bromobutyl rubber was investigated to determine which microstructures exist at vulcanization temperatures. These studies were performed in solution (0.03g BIIR/1.0 g 1,2,4-trichlorobenzene) as well as in the bulk.

The structural characterization of BIIR dissolved in $CDCl_3$ was performed by 400 MHz $^1H$ NMR. The spectrum was consistent with that reported previously: two singlets at 4.1 ppm for the two $-CH_2Br$ protons in the E- and Z-BrMe isomer (**4**), a triplet at 4.35 ppm for the –CHBr- proton in the exomethylene isomer (**3**), two singlets at 5.05 and 5.4 ppm for the exomethylene olefinic protons, two multiplets at 5.35 and 5.75 ppm for the olefinic proton in the E- and Z-BrMe isomer, and two multiplets at 5.1 and 4.9 ppm for the residual isoprene (IIR).[16, 35]

### 4.3.1 Thermal Stability of Bromobutyl Rubber in Solution

When dissolved in 1,2,4-trichlorobenzene and heated to 145°C, the elastomer underwent substantial isomerization. After 15 minutes, a significant quantity of the bromomethyl isomer was generated at the expense of the exomethylene isomer. Additional peaks appearing in the spectrum at 30 minutes included doublets at 5.95 and 6.05 ppm, a broad multiplet at 5.7 ppm, and a singlet at 4.8 ppm. These peaks were consistent with the assignments made by Dhaliwal to the exomethylene conjugated diene (**5**) and the endomethylene conjugated diene (**11**), and correlated well with the BrMC peak assignments presented in Table 4.4.[35] After 45 minutes, the polymer existed predominantly as the BrMe and conjugated diene (CDB) structures, with only a small amount of the exomethylene structure remaining. Overlapping peaks and a poor signal to noise ratio in these NMR spectra prevented an accurate estimation of the abundance of these isomerization and elimination products.

After one hour, the apparent loss of molecular weight resulting in a liquid-like product coincided with the appearance of additional peaks in the spectrum. These peaks were attributed to the products of HBr catalyzed β-scission reactions. Given that BIIR cures require 20 minutes or less, these structures were not considered to be important vulcanization products or precursors. The conjugated dienes disappeared after 75 minutes, while the BrMe isomer remained after 2 hours.

### 4.3.2 Thermal Stability Analysis of Bromobutyl Rubber in the Bulk

The thermal stability of BIIR in the bulk was similar to BIIR in solution. Upon heating, generation of the bromomethyl (**4**) isomer was accompanied by a decrease in the exomethylene isomer (**3**), but only minimal elimination to the conjugated diene structures had taken place after 30 minutes. After 60 minutes, significant quantities of the conjugated dienes and the degradation products observed in the BIIR solution study had been formed. The exomethylene isomer disappeared after 80 minutes (45 minutes in solution), but the BrMe isomer was present after two hours.

From these results it was concluded that the exomethylene and bromomethyl isomers are the principle precursors in the formation of crosslinks in brominated butyl rubber under typical curing conditions (150°C, 20 minutes).

Since the HBr concentration is higher in the bulk than in solution, the slower kinetics observed in the bulk study were attributed primarily to restrictions on polymer chain orientation. This introduces a limitation on the brominated model, which is not subject to any structural restrictions. Therefore, the thermal isomerization and elimination kinetics of the brominated model compound were expected to be much faster than in BIIR.

## 4.4 Thermal Stability Analysis of Brominated 2,2,4,8,8-Pentamethyl-4-nonene (BrMC)

Having established that the exomethylene and bromomethyl isomers are the predominant vulcanization precursors in BIIR, the thermal stability of the model structures was investigated using the nine experiments listed in Table 3.1. The complete

results are presented in Appendix B. Three experiments were performed in 1,2,4-trichlorobenzene, while the remaining six experiments were performed in 1,2,4-trichlorobenzene or dodecane and used excess quantities of the neutral acid scavenger 1,2-epoxydodecane. The reaction vials were sampled at various time intervals and their contents were characterized by 400 MHz $^1$H NMR to determine whether the model effectively represented the structure of BIIR under cure conditions.

Without an acid scavenger, the BrMC was not stable at 100°C and 145°C. The elimination of HBr is presumed to have catalyzed β-scission and other destructive reactions that led to a wide range of thermal decomposition products. Proton NMR analysis was performed on the contents of the reaction vials, but no peak assignments were made, with the exception of the exo and BrMe isomers, due to the complexity of the spectra. No effort was made to isolate these reaction products because their $^1$H NMR spectra were inconsistent with those structures that exist within BIIR under similar curing conditions. Changes in the exo to BrMe isomer ratio with time, as determined from the normalized integration ratio between the triplet at 4.35 ppm (1H, allylic H, exo) and the multiplet at 4.07 ppm (2H, -$CH_2$Br, E- and Z-BrMe), is shown in Figure 4.4. The exo:BrMe isomer ratio reached an equilibrium rapidly in all the experiments without the epoxide, indicating that the isomerization of the exo to the BrMe structure is accelerated by HBr. Equilibrium exo:BrMe ratios for the three experiments without the epoxide are given in Table 4.3.

These results demonstrate that the equilibrium between the exo and BrMe isomers is independent of model concentration, and is therefore a thermodynamic quality rather than a kinetic parameter.

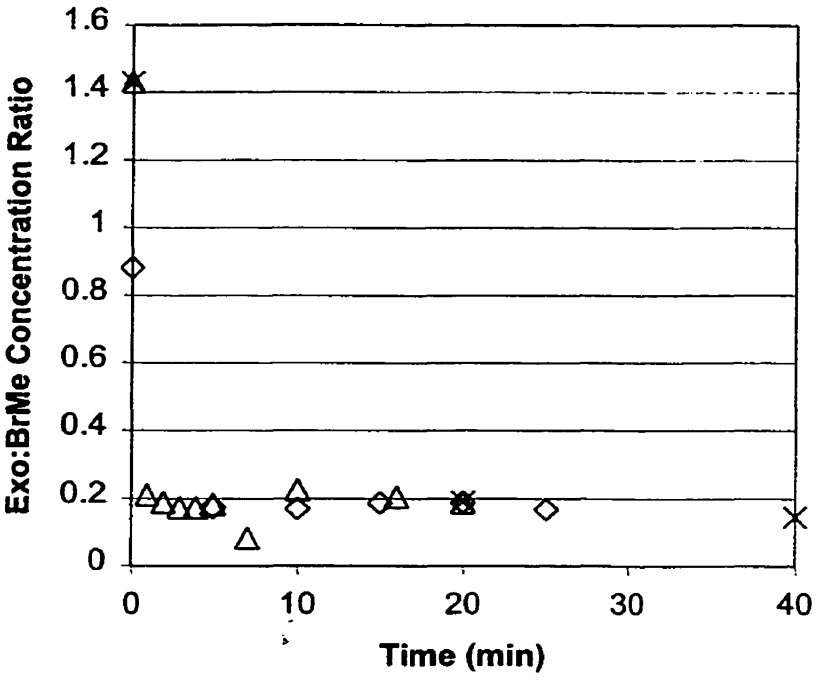


Figure 4.4: Exomethylene to bromomethyl isomer ratio in the absence of 1,2-epoxydodecane in 1,2,4-trichlorobenzene: ◊ (0.88 mol/L, 145°C); × (1.77 mol/L, 100°C); Δ (1.77 mol/L, 145°C).

Table 4.3: Mean exomethylene : bromomethyl isomer ratios in the thermal stability experiments without 1,2-epoxydodecane

| Conditions | Mean Exo:BrMe |
|---|---|
| 100°C, 1.77 mol/L BrMC | 0.1498 |
| 145°C, 1.77 mol/L BrMC | 0.1811 |
| 145°C, 0.88 mol/L BrMC | 0.1768 |
| Overall Average (145°C) | 0.1790 |

The thermal stability experiments that incorporated 1,2-epoxydodecane differed from those conducted in its absence. In this series of experiments, the number of isomerization and elimination products was greatly reduced, and the reaction mixture could be characterized by 400 MHz $^1$H and COSY 2D $^1$H NMR. In addition to the exo and BrMe structures, two elimination products, (E)-2(2,2-dimethylpropyl)-6,6-

dimethylhept-1,3-diene (exomethylene conjugated diene: Exo-CDB) **10**, and (3Z,5E)-2,2,4,8,8-pentamethylnon-3,5-diene (endomethylene conjugated diene: Endo-CDB) **11**, were generated. Their olefinic NMR peak assignments are given in Table 4.4, and shown in Figures 4.5 and 4.6.

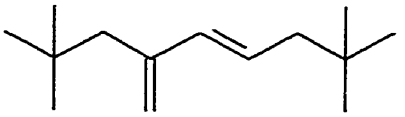

Exo Conjugated Diene (Exo-CDB) **10**

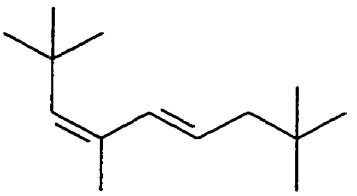

Endo Conjugated Diene (Endo-CDB) **11**

Table 4.4: Olefinic $^1$H NMR peak assignments of the exo-CDB and endo-CDB elimination products. Conditions: 145°C for 40 minutes in 1,3,5-trichlorobenzene. NMR solvent: $CDCl_3$

| Chemical Shift (ppm) | Multiplicity[a] | Assignment |
|---|---|---|
| 4.78 | d | exo olefinic H, Exo-CDB |
| 5.05 | d | exo olefinic H, Exo-CDB |
| 5.43 | s | isolated olefinic H, Endo-CDB |
| 5.60 | d of t | olefinic H, Endo-CDB |
| 5.75 | d of t | olefinic H, Exo-CDB |
| 5.98 | d | olefinic H, Endo-CDB |
| 6.05 | d | olefinic H, Exo-CDB |

[a] s = singlet, d = doublet, d of t= doublet of triplets

The assignments of the exo-CDB peaks are in agreement with those reported previously, and were made on the basis of the unique NMR signature of the exomethylene type protons at 4.78 and 5.05 ppm.[35] The two remaining olefinic protons in this structure appeared as a doublet at 6.05 ppm, and a doublet of triplets at 5.98 ppm, split by the adjacent olefinic proton and $-CH_2-$ group. The exo-CDB product existed as a single isomer, and molecular modelling indicated that the E-isomer was energetically favoured.[36]

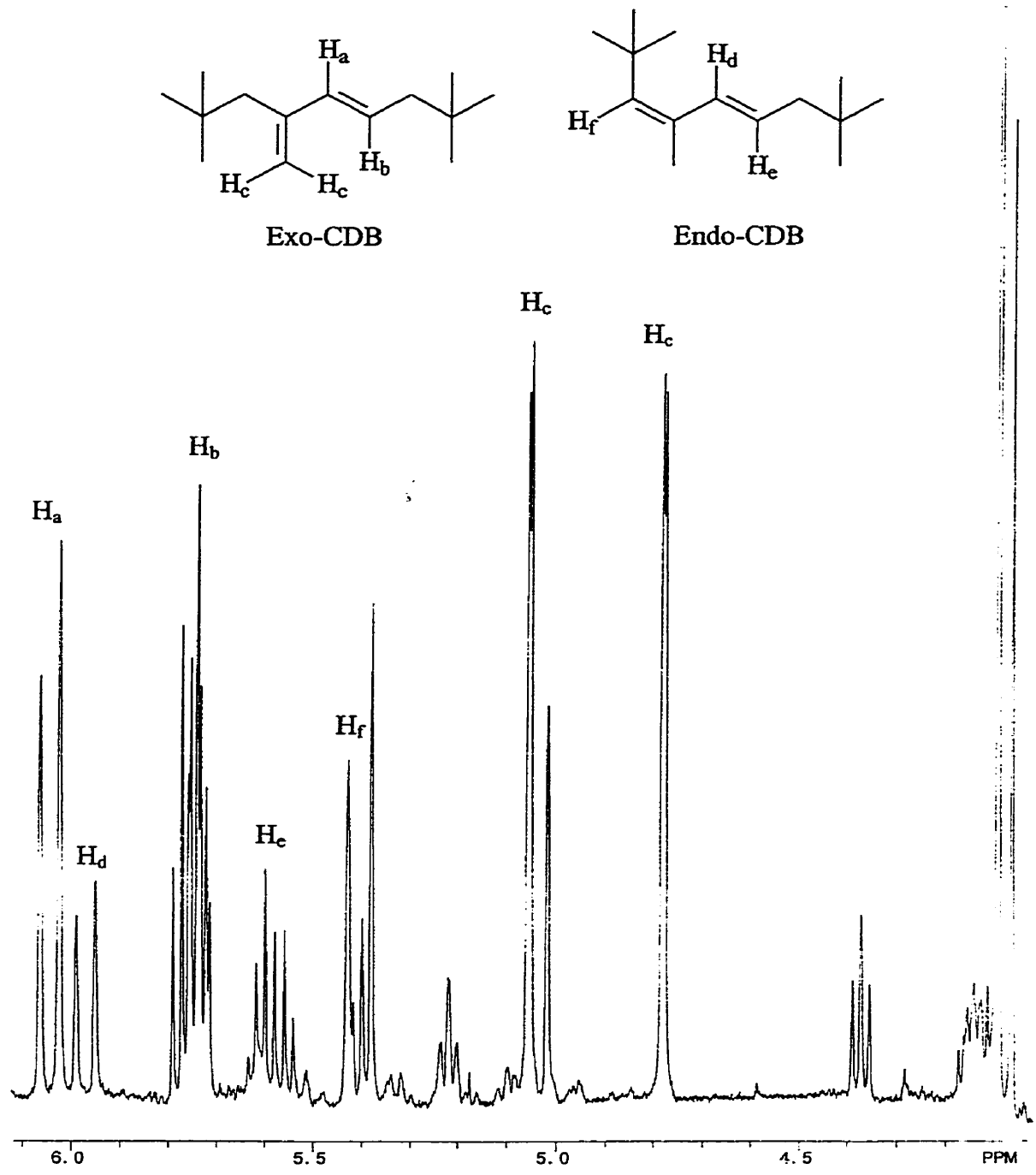


Figure 4.5: Downfield region in the 400 MHz $^1$H NMR spectrum of brominated 2,2,4,8,8-pentamethyl-4-nonene in $CDCl_3$. Conditions: 40 minutes at 145°C in 1,2,4-trichlorobenzene with excess 1,2-epoxydodecane

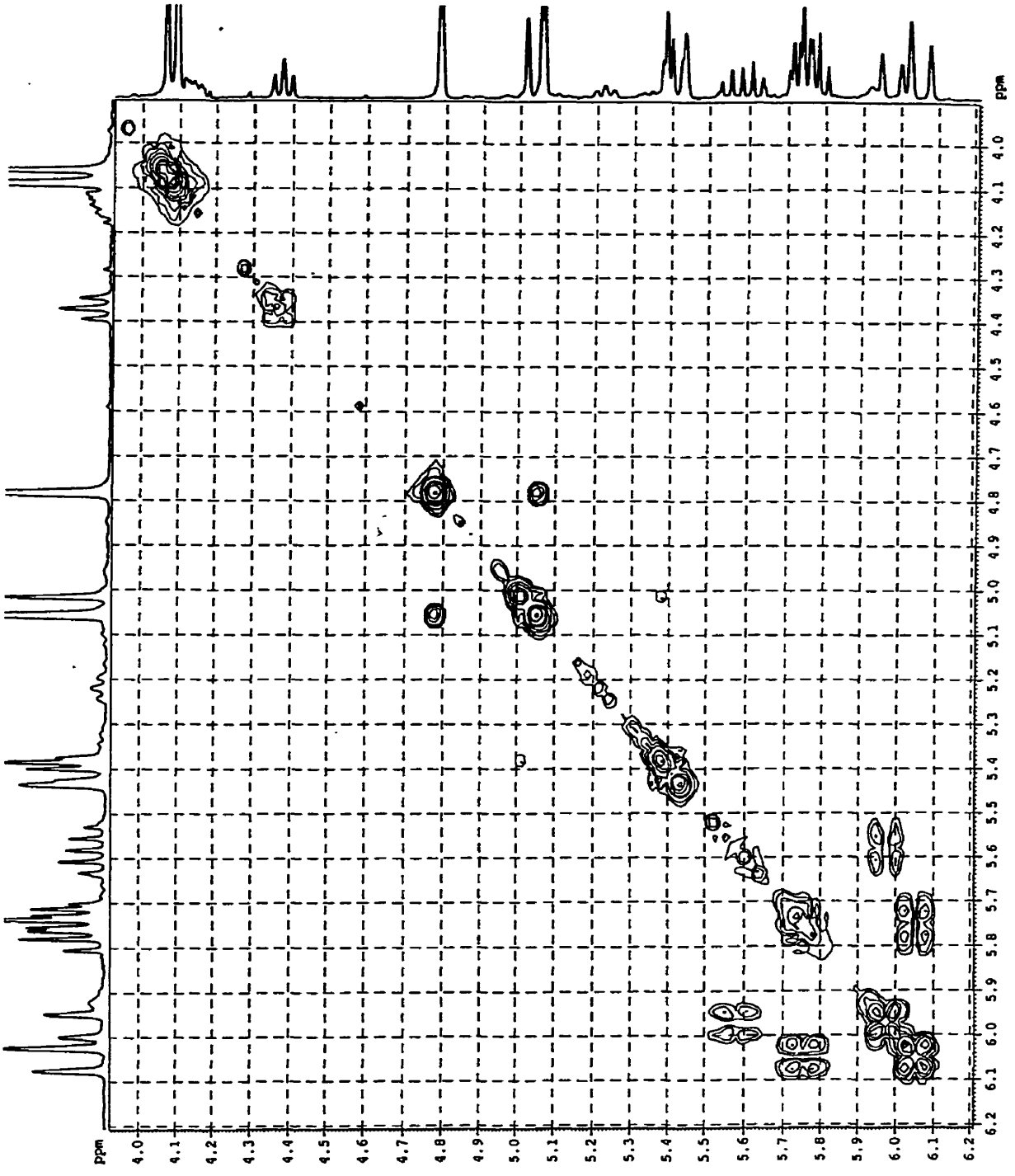


Figure 4.6: Downfield region in the 400 MHz 2D COSY $^1$H NMR spectrum of brominated 2,2,4,8,8-pentamethyl-4-nonene in $CDCl_3$. Conditions: 40 minutes at 145°C in 1,2,4-trichlorobenzene with excess 1,2-epoxydodecane

The three remaining olefinic peaks in the spectrum were assigned to the Endo-CDB isomer with the following justification. Two dimensional COSY $^{1}H$ NMR coupling of the doublet at 5.98 ppm to the doublet of triplets at 5.6 indicated that this structure contained two olefinic protons similar in orientation to those in the exo-CDB (Figure 4.6). In addition, the singlet at 5.43 ppm represents a third olefinic proton that is isolated with no adjacent neighbours. Based on this unique NMR coupling pattern, the endo-CDB peak assignments were confirmed, and molecular modelling suggested that the Z-E isomer was energetically favoured.[36]

The addition of 1,2-epoxydodecane to BrMC solutions reduced the rate of decomposition and elimination reactions. Therefore, the component concentrations could be determined over the course of these experiments from the normalized 400 MHz $^{1}H$ NMR integration of the following peaks: the doublet at 4.1 ppm (2H, E and Z-BrMe), the triplet at 4.4 ppm (1H, exo), the doublet at 5.98 ppm (1H, endo-CDB), and the doublet at 6.05 ppm (1H, exo-CDB).

Figure 4.7 illustrates the observed thermal stability of the BrMC at 145°C in 1,2,4-trichlorobenzene, as characterized by this experimental method. A rapid decline in the exomethylene isomer concentration was accompanied by the generation of the endo-CDB and exo-CDB structures. The decreasing rate of formation of the endo-CDB, and the concentration inversion of the endo-CDB and exo-CDB isomers at 18 minutes suggests that the endo-CDB is the kinetically favoured elimination product, while the exo-CDB is thermodynamically more stable.

When heated to 140°C in dodecane, the BrMe structure was again identified as the more stable isomer. The thermal stability of the BrMC in dodecane is shown in

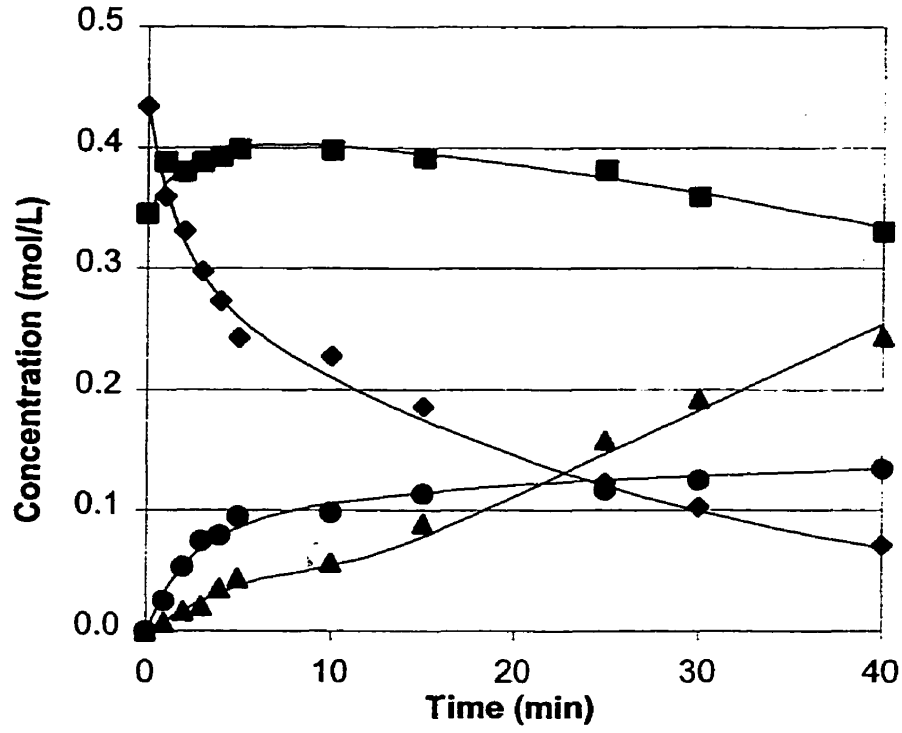


Figure 4.7: Thermal stability of 0.78 mol/L BrMC and 1.77 mol/L 1,2-epoxydodecane in 1,2,4-trichlorobenzene at 145°C: ◆ (exomethylene); ■ (bromomethyl); ▲ (exo-CDB); ● (endo-CDB).

Figure 4.8 with model predictions (model development is presented in Appendix B). With an initial exo:BrMe ratio similar to that of BIIR, the BrMC isomerized rapidly from the exo to the BrMe isomer, but formation of the conjugated dienes was suppressed by the large excess in 1,2-epoxydodecane concentration.

The mechanisms proposed for the isomerization and elimination reactions of the BrMC are presented in Figure 4.9. Under acidic conditions, a rapid equilibrium is established between the exo and BrMe isomers, and HBr appears to catalyze β-

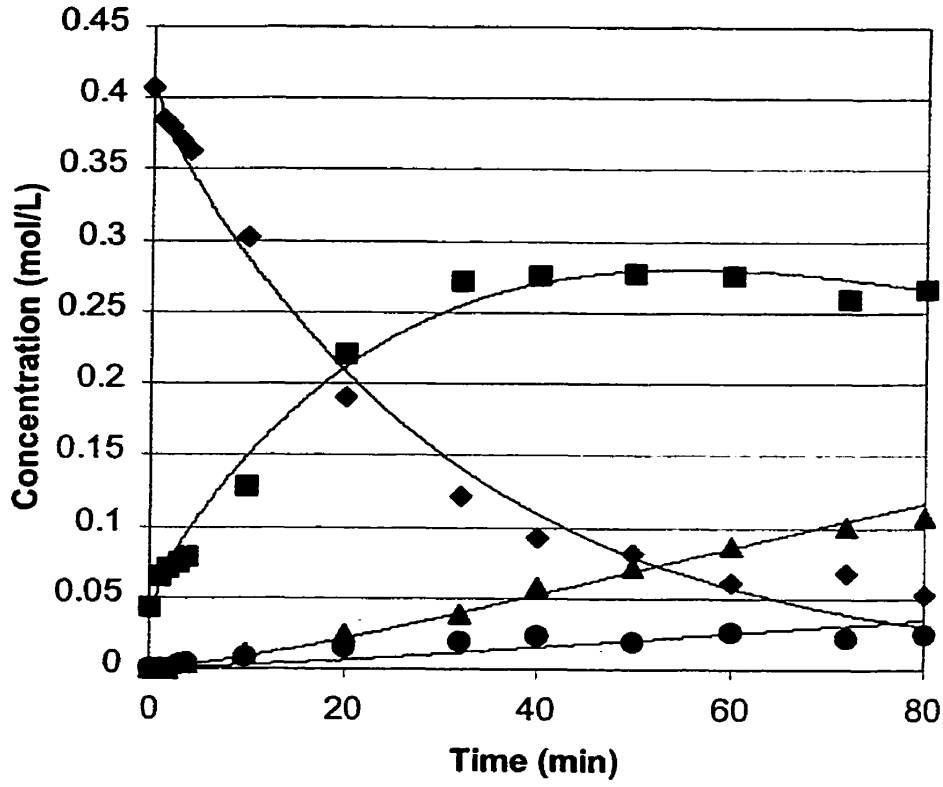


Figure 4.8 Thermal stability of 0.45 mol/L BrMC and 1.87 mol/L 1,2-epoxydodecane in dodecane at 140°C with optimized model predictions: ◆(exomethylene); ■ (bromomethyl); ▲ (exo-CDB); ●(endo-CDB)

scission reactions that lead to decomposition products. Conversely, when epoxydodecane is incorporated, the conversion between the exo and bromomethyl isomers is slow and proceeds through the proposed ionic mechanism. The endo-CDB kinetic product is then formed from these ionic intermediates by proton abstraction before reversion and subsequent generation of the thermodynamically favoured exo-CDB product.

These thermal stability studies have demonstrated that the BrMC does not accurately represent the functionality of BIIR at vulcanization temperatures unless an acid scavenger is present. This is due to the large concentration of eliminated HBr in the model experiments, which catalyzes the formation of decomposition products not

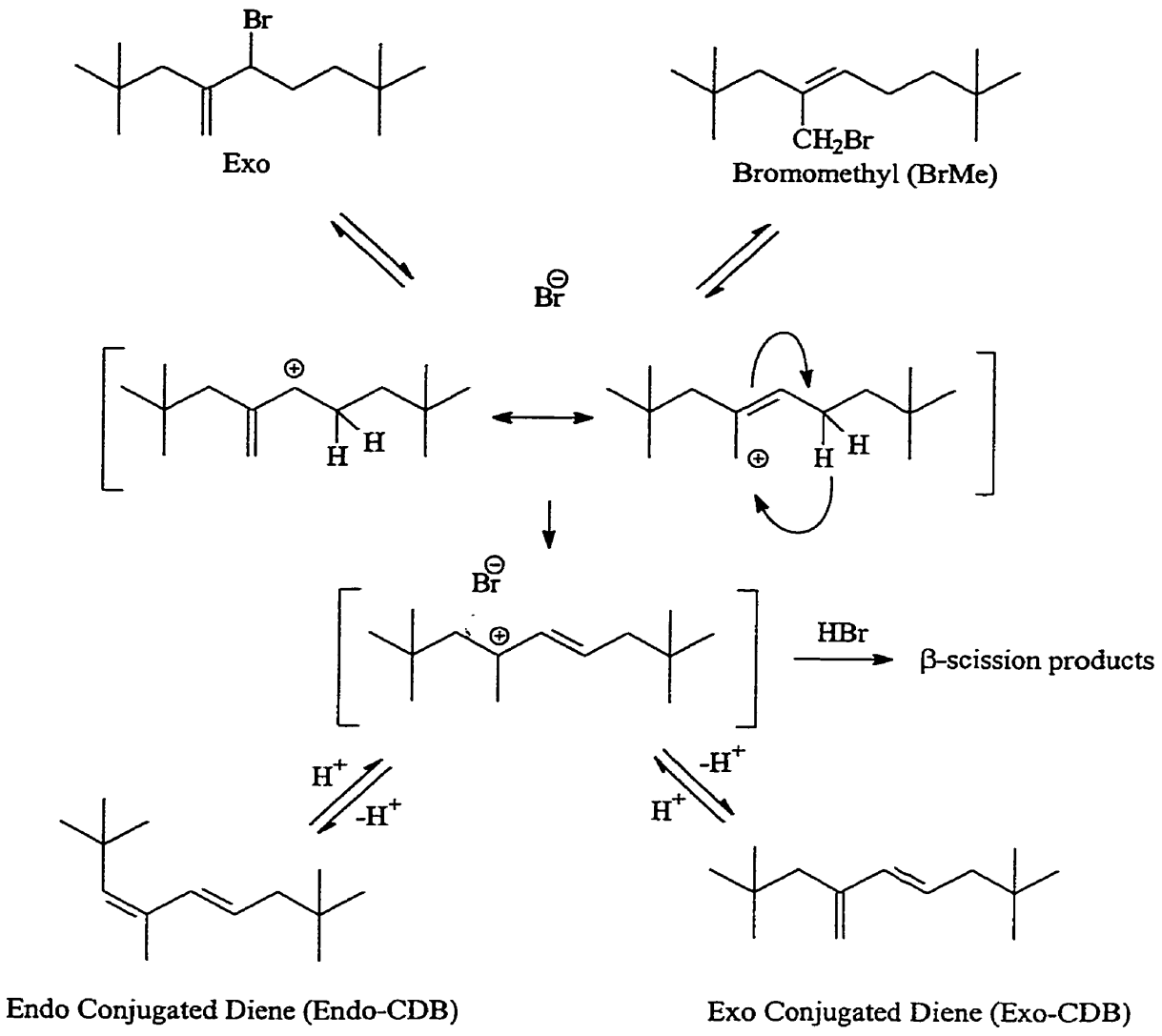


Figure 4.9: Proposed mechanism for the isomerization and elimination reactions of brominated 2,2,4,8,8-pentamethyl-4-nonene

observed in BIIR under similar conditions. Therefore, 1,2-epoxydodecane must be incorporated into model curative formulations in order for the BrMC to accurately reflect the reactivity of BIIR towards curatives.

## 4.5 Cure Studies of Brominated 2,2,4,8,8-Pentamethyl-4-nonene (BrMC)

### 4.5.1 Reaction Conditions

In order to accurately represent the reactivity of BIIR under curing conditions, the model vulcanization experiments were carried out in the presence of 1,2-epoxydodecane for 7 minutes. The incorporation of the acid scavenger minimized degradation, reversion, and elimination reactions, while a reaction time of 7 minutes ensured the isolated cure products were derived predominantly from the exomethylene and bromomethyl isomers of the brominated model. Dodecane was used as the solvent because it is non-polar and has a NMR resonances that do not overlap with olefinic and aromatic signals of interest.

### 4.5.2 Reaction of Brominated 2,2,4,8,8-Pentamethyl-4-nonene (BrMC) with 2,2'-Dithiobisbenzothiazole (MBTS)

The products of the BrMC (exo:BrMe = 60:40) and MBTS reaction were separated by preparative thin layer chromatography into four distinct bands with $R_f$ values of 0.00, 0.02-0.14, 0.45-0.50 and 0.54-0.59. These were subsequently analyzed by mass spectroscopy and 400 MHz $^1$H NMR.

Based on previous peak assignments, the top band ($R_f$ 0.54-0.59) was characterized as unreacted BrMC and conjugated diene structures. The absence of aromatic proton resonances in the spectrum ruled out the presence of MBTS derived compounds.

The principle component eluting in the second TLC band ($R_f$ 0.45-0.50) was identified by mass spectroscopy and characterized by NMR as an adduct of 2-mercaptobenzothiazole (MBT) with the model (**12**). The mass spectrum of this band,

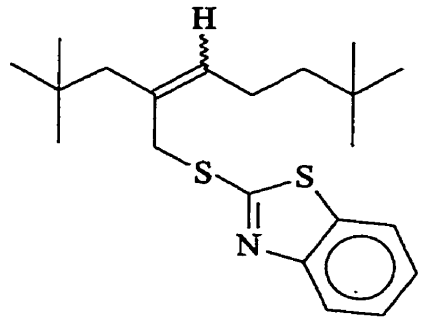

**12**

presented in Figure 4.10, contains the molecular ion peak at *m/e* 362 ($C_{21}H_{31}NS_2 + H^+$: MC-MBT + $H^+$) in addition to major fragments at *m/e* 168 ($C_7H_6NS_2$: MBT+$H^+$) and *m/e* 167 ($C_7H_6NS_2$: $MBT^+$). The NMR peak assignments of **12**, which were made with the assistance of COSY ($^1H$: $^1H$) and HMQC ($^1H$:$^{13}C$) correlated NMR experiments, are presented in Table 4.5 and shown in Figure 4.11. NMR peak integration indicated a 1:1 mole ratio of aromatic to olefinic protons, and an E:Z isomer ratio of 60:40.

Table 4.5: Downfield $^1H$ NMR peak assignments of the BrMC and MBTS reaction product **12** Conditions: 145°C for 7 minutes in dodecane. NMR sovent: $CDCl_3$.

| Chemical Shift (ppm) | Multiplicity[a] | Assignment |
|---|---|---|
| 4.06 | s | $CH_2$, Z isomer |
| 4.14 | s | $CH_2$, E isomer |
| 5.41 | t | olefinic H, E isomer |
| 5.67 | t | olefinic H, Z isomer |
| 7.30 | t | aromatic H |
| 7.42 | t | aromatic H |
| 7.77 | d | aromatic H |
| 7.84 | d | aromatic H |

[a] s = singlet, d = doublet, t= triplet

The chemical shift and multiplicity of the peaks in Table 4.5 are very similar to those of the bromomethyl isomer **6** described previously (Table 4.2). However, significant differences arise in the two-dimensional COSY and HMQC correlation NMR

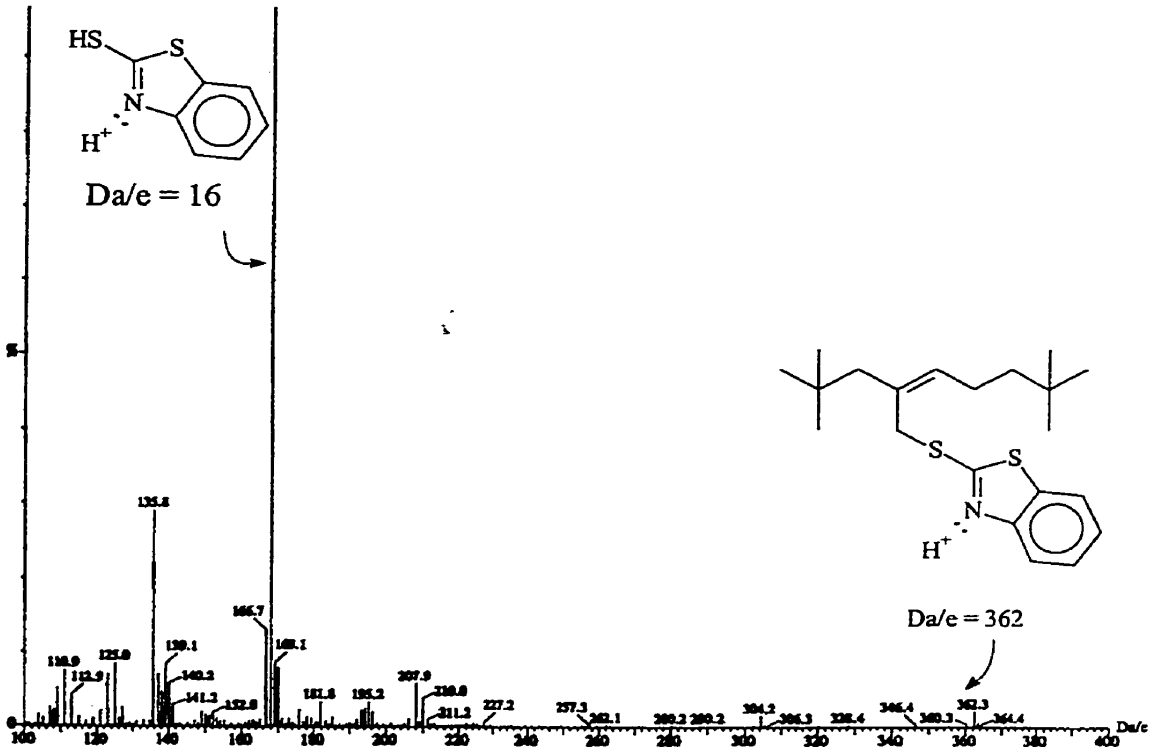


Figure 4.10: Mass spectrum of the MBT graft product **12**

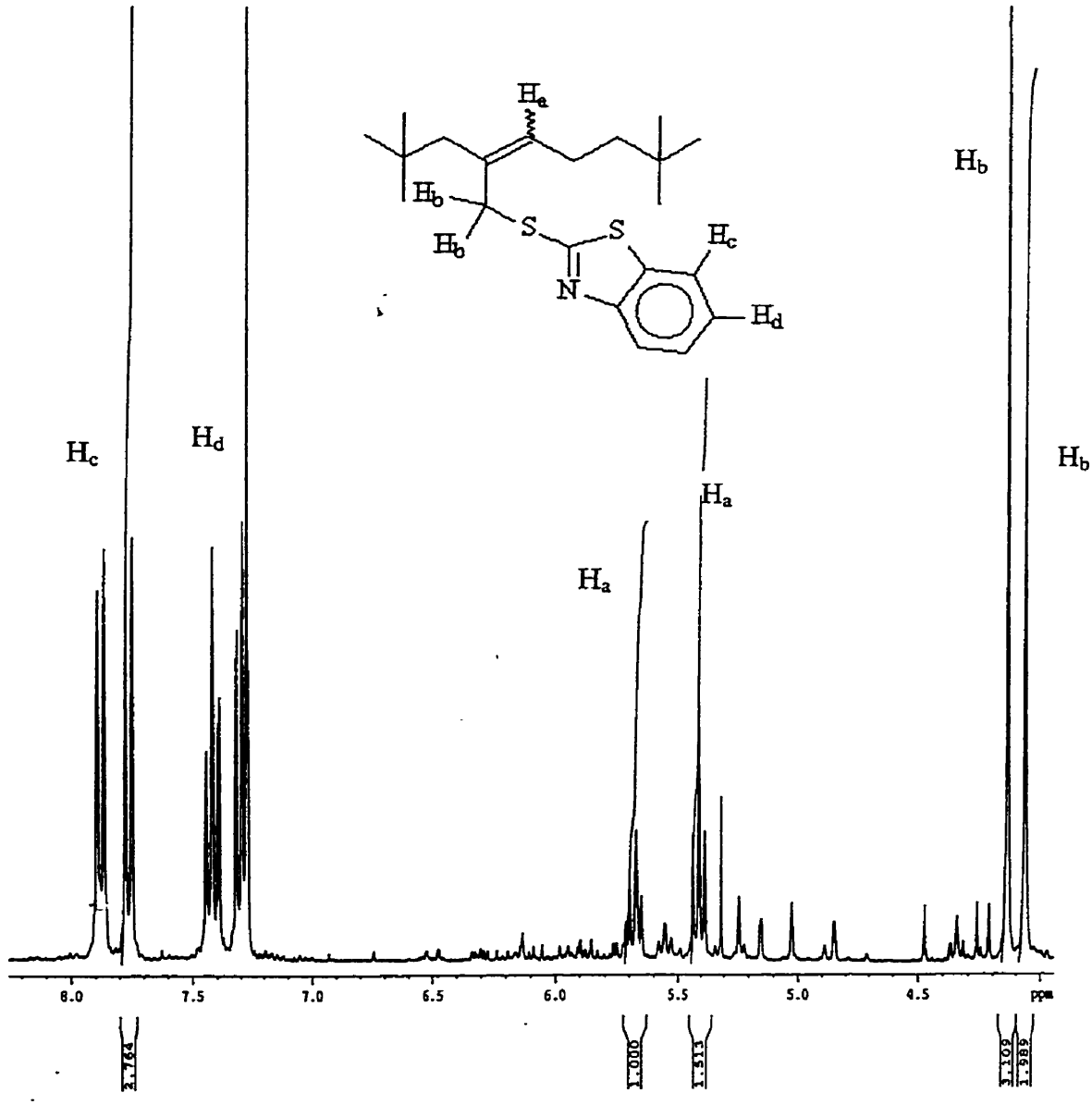


Figure 4.11: Downfield region in the 400 MHz $^1$H NMR spectrum of 12 in $CDCl_3$

spectra of these compounds. These differences, summarized in Table 4.6 and shown in Figures 4.12 and 4.13, differentiate the MBT grafted product from the BrMe isomer.

Table 4.6: COSY and HMQC correlations of the BrMC and the MBT grafted product.

| Brominated Model Compound: Bromomethyl Isomer **6a, 6b** | | |
|---|---|---|
| Chemical Shift[a] (ppm) | Assignment | Coupling |
| 4.07 (s) | $CH_2$, E-BrMe | HMQC: 33.0 ppm |
| 4.10 (s) | $CH_2$, Z-BrMe | COSY (long range): 5.76 (t)<br>HMQC: 42.5 ppm |
| 5.41 (t) | olefinic H, E isomer | HMQC: 137.0 ppm |
| 5.76 (t) | olefinic H, Z isomer | COSY (long range): 4.10 (s)<br>HMQC: 136.5 ppm |
| MBT Grafted Product (**12**) | | |
| Chemical Shift[a] (ppm) | Assignment | Coupling |
| 4.06 (s) | $CH_2$, Z isomer | COSY (long range): 5.68 (t)<br>HMQC: 43.5 ppm |
| 4.14 (s) | $CH_2$, E isomer | COSY (long range): 5.41 (t)<br>HMQC: 35.7ppm |
| 5.41 (t) | olefinic H, E isomer | COSY (long range): 4.14 (s)<br>HMQC: 137.0 ppm |
| 5.68 (t) | olefinic H, Z isomer | COSY (long range): 4.06 (s)<br>HMQC: 136.5 ppm |

[a] s = singlet, t = triplet

COSY experiments revealed long range coupling in the BrMe isomer between the olefinic triplet furthest downfield at 5.76 ppm (Z-BrMe) and the allylic $CH_2$ singlet furthest downfield at 4.10 ppm. In contrast, the olefinic triplet in the Z-isomer of **12** is a triplet at 5.68 ppm that demonstrates long range coupling to the allylic $CH_2$ singlet furthest upfield at 4.06 ppm, rather than the singlet furthest downfield as was the case in the Z-BrMe isomer. Therefore, the allylic $CH_2$ singlet furthest downfield is assigned to the Z-isomer in the BrMe structure, but to the E-isomer in the MBT adduct. Further NMR differentiation between the BrMe isomer and **12** is seen in the HMQC experiment (Figure 4.13), where the $^1H$ singlet at 4.06 ppm is coupled to the $^{13}C$ peak at 33 ppm in the BrMe

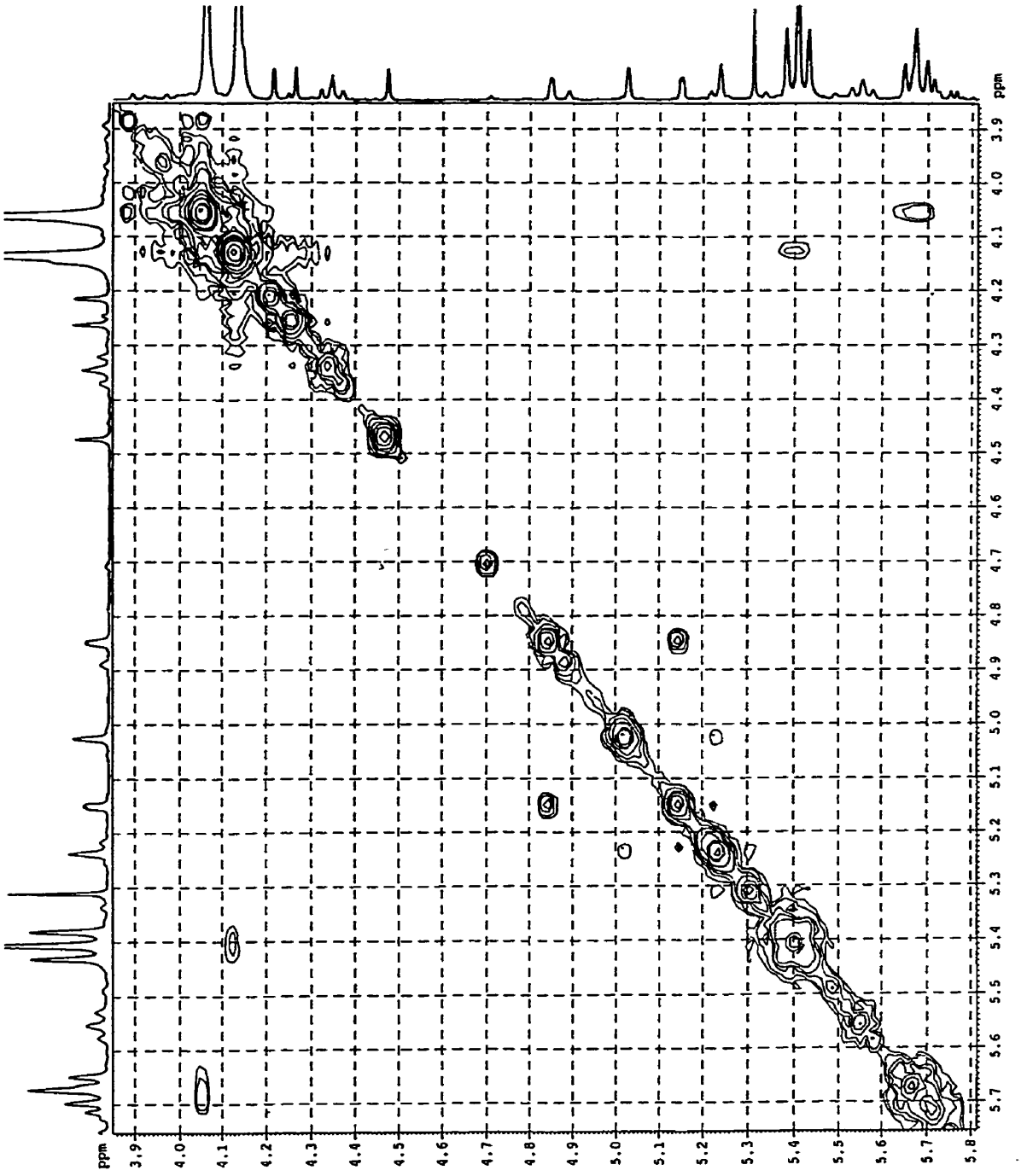


Figure 4.12: Downfield region in the 400 MHz 2D COSY $^1$H NMR spectrum of **12** in $CDCl_3$

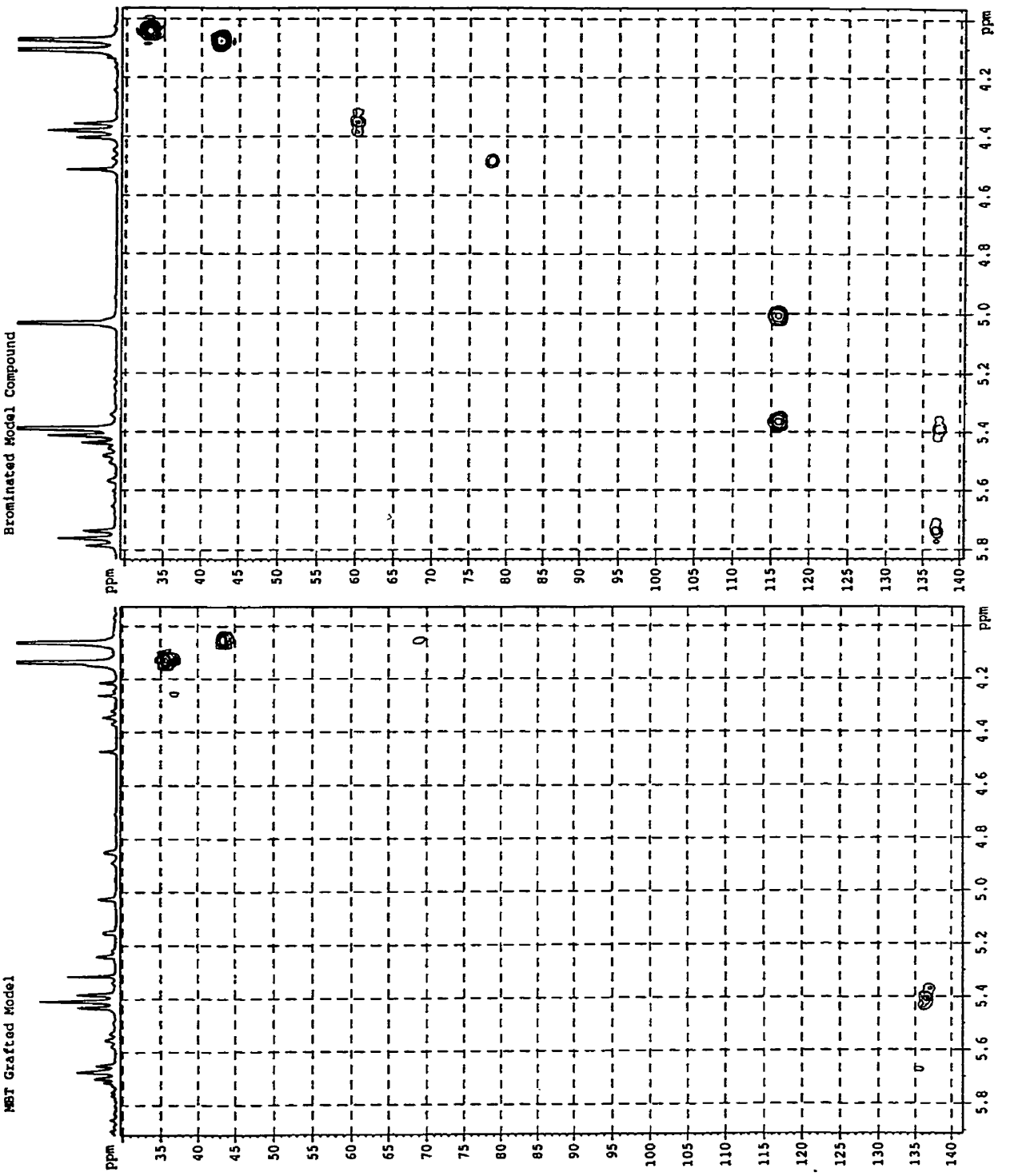


Figure 4.13: Downfield region in the 400 MHz 2D HMQC $^{1}H$:$^{13}C$ NMR spectrum of **12** and the BrMC in $CDCl_3$

isomer, but to the $^{13}C$ peak at 43.5 ppm in the MBT adduct. Therefore, long range coupling and $^{1}H/^{13}C$ correlation spectroscopy have confirmed the characterization of the MBT grafted product (**12**) and differentiated it from the BrMe isomer.

Figure 4.14 illustrates the proposed mechanism for the reaction of the BrMC with MBTS to form **12**. The exomethylene isomer likely reacts through an $S_N2'$ mechanism, while the BrMe isomer may react via an $S_N1$ or $S_N2$ mechanism.

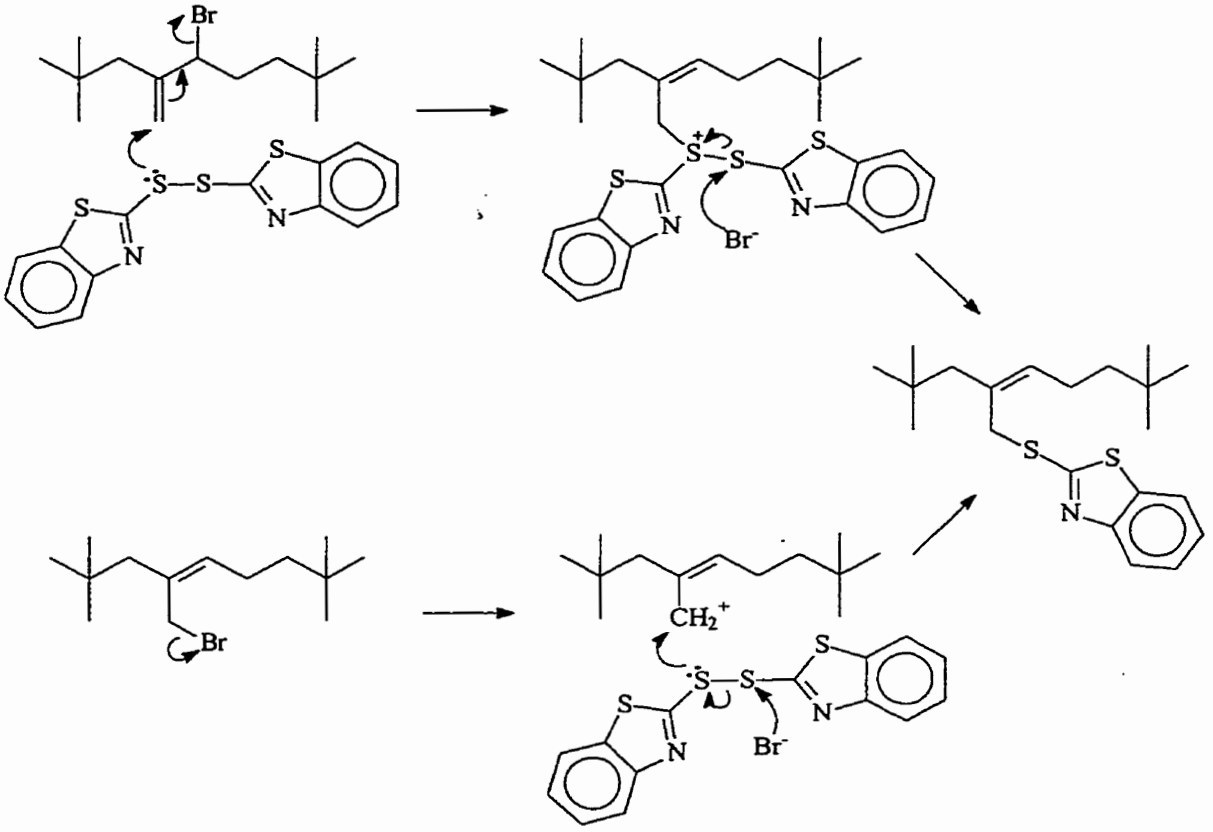


Figure 4.14: Proposed mechanism for the formation of the MBT adduct **12**

The third TLC band ($R_f$ of 0.02-0.14) was found to contain predominantly 1,2-epoxydodecane and its bromohydrin, while the NMR spectrum of the bottom and last TLC band contained unreacted MBTS and potentially MBT.

In contrast to other elastomers, the incorporation of the accelerator MBTS into BIIR curative formulations decreases the crosslink density. This uncharacteristic behavior can be explained by the MBT adduct generated in the reaction of the BrMC with MBTS. If produced in BIIR, **12** would reduce the number of sites available for crosslinking, and could result in the observed decrease in cure efficiency.

### 4.5.3 Reaction of Brominated 2,2,4,8,8-Pentamethyl-4-nonene (BrMC) with Sulphur

The crude S+BrMC (exo:BrMe 54:46) products of reaction were separated by normal phase preparative HPLC using a silica column with hexanes elution. Although reverse phase HPLC has previously been used to separate other model vulcanizates, the immiscibility and instability of the $C_{14}$ brominated model in polar solvent systems prevented separation using a C-18 column. The isolated HPLC fractions presented in Table 4.7 correspond to the refractive index (RI) chromatogram of the BrMC+S product separation shown in Figure 4.15. These fractions do not include epoxydodecane or the bromohydrin, which were eluted after Fraction D when the solvent composition was changed to 90% hexanes and 10% ethyl acetate.

Table 4.7: Isolated fractions in the HPLC separation of the BrMC+S cure products

| Fraction | Collection Time (min) | Peak Area (% of total) |
|---|---|---|
| A | 9.42-10.25 | 50.6 |
| B | 10.25-10.92 | 8.9 |
| C | 10.92-11.42 | 26.5 |
| D | 11.42-12.25 | 14.0 |

Fraction A, which did not have a corresponding peak in the UV-VIS chromatogram, was characterized as dodecane. $^1$H NMR analysis of Fraction B (Figure 4.16) revealed primarily of 2,2,4,8,8-pentamethyl-4-nonene (**1**) as well as the

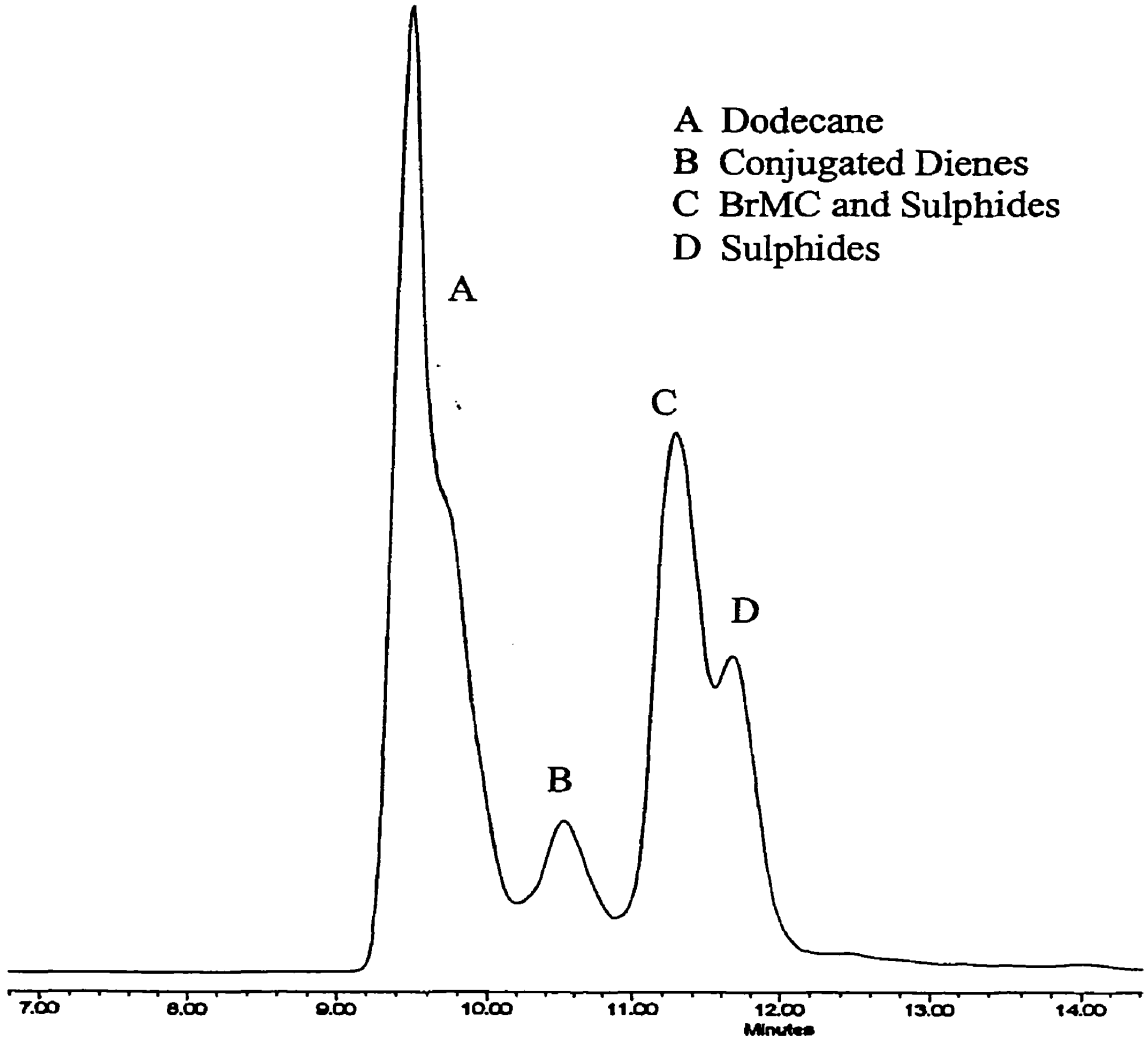


Figure 4.15: RI chromatogram of the BrMC+S product separation. Conditions: Supelco PLC-Si column, 7 ml/min hexane

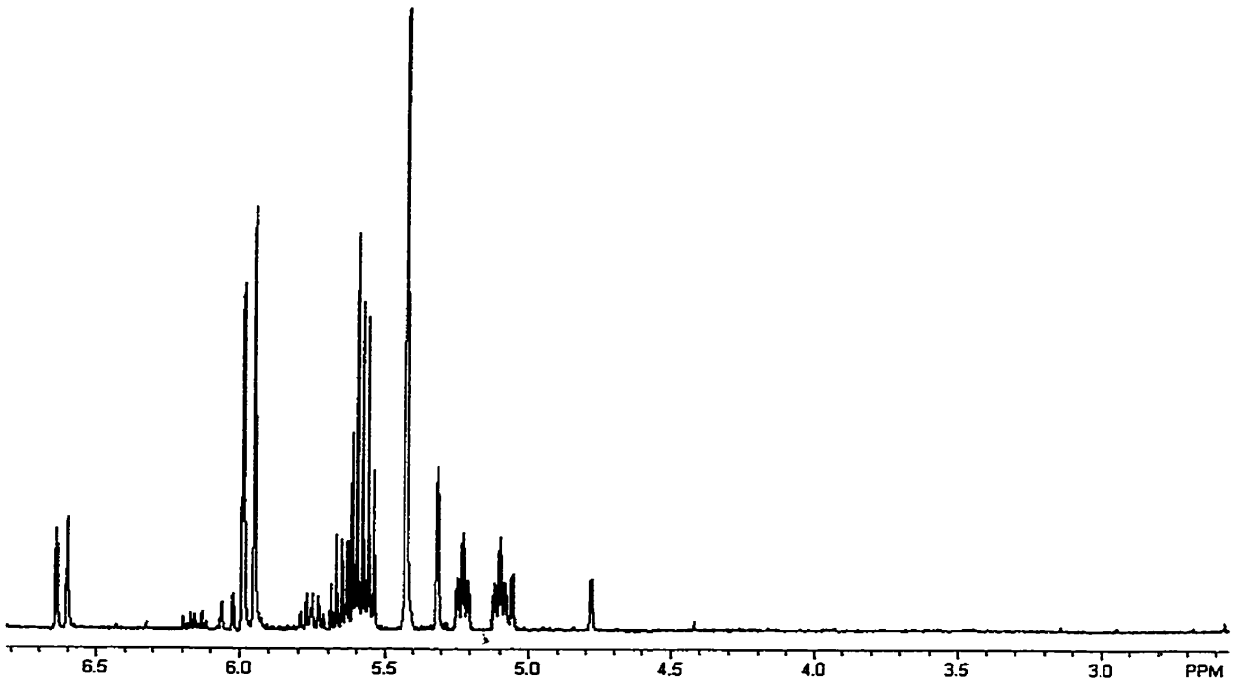


Figure 4.16: 400 MHz $^1$H NMR spectrum of Fraction B in the S+BrMC product separation.

exomethylene and backbone conjugated dienes (**10, 11**). An additional component contained in this fraction was represented by the following peaks: a doublet at 6.62 ppm coupled to a multiplet at 5.65 ppm, and a singlet at 5.31 ppm. While this coupling pattern is identical to that of the endo-CDB, the significant downfield shift of the doublet indicates this component is not simply a diastereomer of the conjugated diene. A sulphur appended endo-CDB structure consistent with the *m/e* 257 ($C_{14}H_{26}S_2^+$) peak in the mass spectrum (not shown) has been proposed to account for this downfield shift, but the absence of peaks in the allylic heteroatom region has prevented the unambiguous characterization of this compound at this time.

Mass spectroscopy of Fraction C identified a mixture of BrMC+S reaction products. The peak assignments shown in Table 4.8 and Figure 4.17 were consistent with

Table 4.8: Mass spectroscopy peak assignments for Fraction C of the HPLC S+BrMC product separation

| Mass *m/e* | Peak Assignments Fraction C |
|---|---|
| 111 | $C_8H_{15}^+$ |
| 125 | $C_9H_{17}^+$ |
| 139 | $C_{10}H_{19}^+$ |
| 195 | $C_{14}H_{27}^+$ |
| 225 | $C_{14}H_{25}S^+$: thiophene + $H^+$ |
| 227 | $C_{14}H_{27}S^+$: MC-$S^+$ |
| 259 | $C_{14}H_{27}S_2^+$: MC-S-$S^+$ |
| 291 | $C_{14}H_{27}S_3^+$: MC-S-S-$S^+$ |
| 422 | $C_{28}H_{55}S_1^+$: MC-S-MC + $H^+$ |
| 454 | $C_{28}H_{55}S_2^+$: MC-S-S-MC + $H^+$ |
| 486 | $C_{28}H_{55}S_3^+$: MC-S-S-S-MC + $H^+$ |

the calculated M ($^{12}C$, $^{32}S$), M+1 ($^{13}C$, $^{32}S$) and M+2 ($^{12}C$, $^{34}S$) peak intensities.[37] Lower intensity peaks at *m/e* 422, 454, and 486 indicated that mono-, di- and tri-sulphide bridged $C_{14}H_{27}$ dimers were generated by the cure reaction. Fragmentation of these sulphides resulted in the base peak at *m/e* 227 in addition to the peaks at *m/e* 259 and *m/e* 291.

Structural characterization of the S+BrMC reaction products contained in Fraction C was accomplished using 400 MHz $^1H$ NMR. The chemical shift and multiplicity of the peaks in Figure 4.18 identified the bromomethyl analogue **13** as the principal sulphidic dimer. Peak assignments of **13**, presented in Table 4.9, are consistent with those made

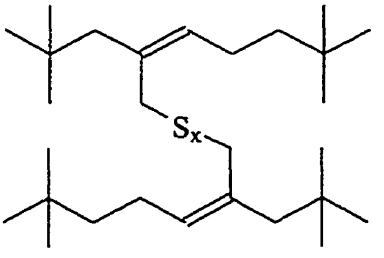


**13** (E,Z isomers)

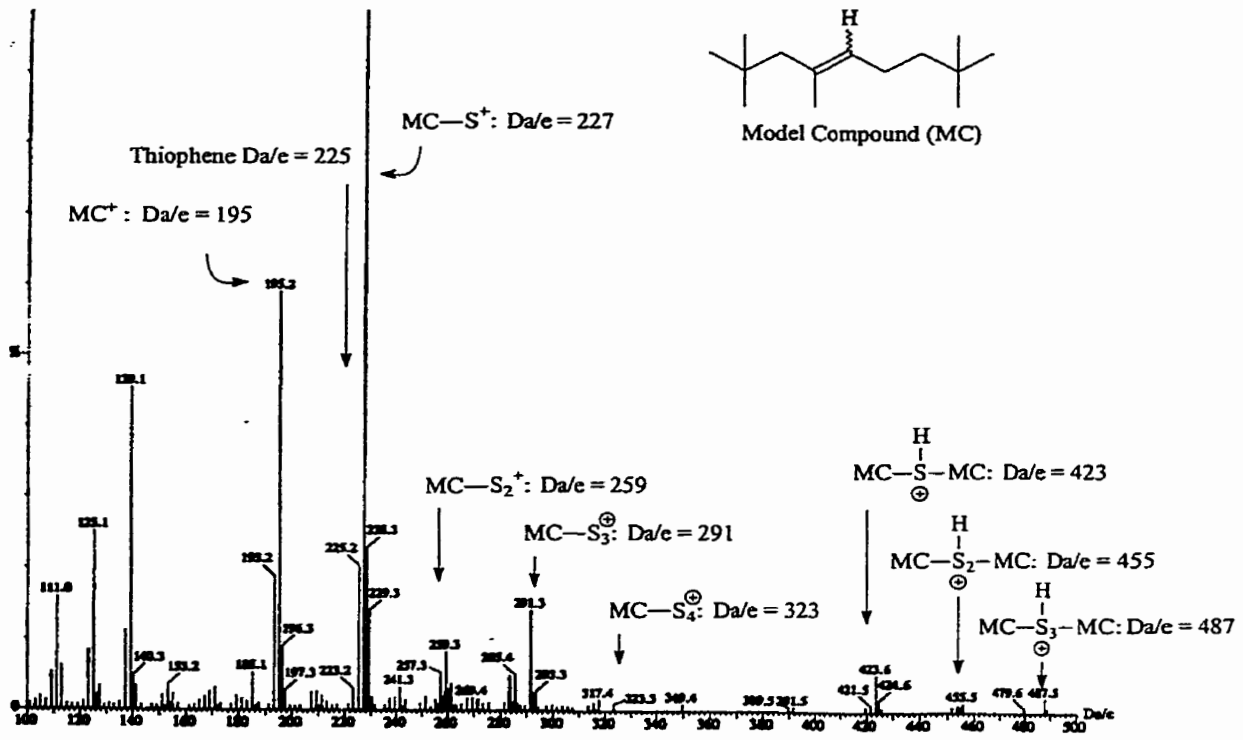


Figure 4.17: Mass spectrum of Fraction C in the S+BrMC product separation

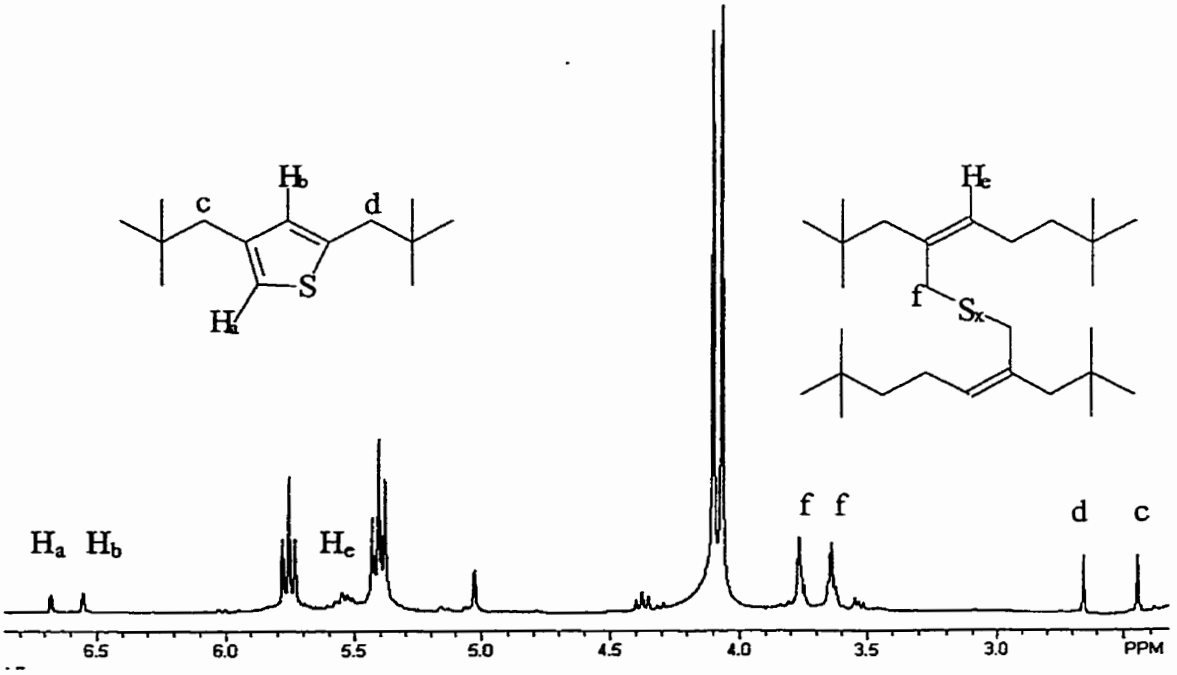


Figure 4.18: Downfield region in the 400 MHz $^1$H NMR spectrum of Fraction C in the S+BrMC product separation

Table 4.9: Downfield 400 MHz $^1$H NMR peak assignments for Fraction C of the HPLC S+BrMC product separation

| Chemical Shift (ppm) | Multiplicity[a] | Assignment | Coupling |
|---|---|---|---|
| 2.45 | s | allylic H, **14** | 6.67 (s) |
| 2.65 | s | allylic H, **14** | 6.55 (s) |
| 3.60 | s | $CH_2$, E-**13** | |
| 3.75 | s | $CH_2$, Z-**13** | |
| 5.50 | m | olefinic H, **13** | |
| 6.55 | s | aromatic H, **14** | 6.67 (s), 2.65 (s) |
| 6.67 | s | aromatic H, **14** | 6.55 (s), 2.45 (s) |

[a] s = singlet, m = multiplet

by Hahn et al. in their study of the model 2,3-dimethylbut-2-ene.[38] The poor resolution of the multiplet at 5.5 ppm and the singlets at 3.65 ppm and 3.75 ppm was attributed to the overlap between Fractions C and D. The sulphide dimer **13** was expected to have the following three distinct -$CH_2$-$S_x$-$CH_2$- isomers: (E,E), (Z,Z), and (E,Z). The fact that there are only two allylic $CH_2$ singlets suggests that their chemical shift is not highly dependent upon their isomer compliment, or that one major thermodynamic isomer is formed (E,Z).

Additional peaks in the NMR spectrum of Fraction C included those of the BrMC and the singlets at 6.67, 6.55, 2.65, and 2.45 ppm that were assigned to the thiophene **14**.

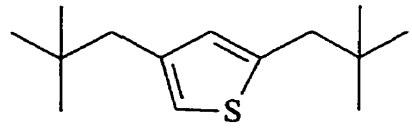


**14** Thiophene

Thiophenes have been identified as reversion products in studies of other models.[38] This cure reversion product was identified in the mass spectrum (*m/e* = 225), and the NMR

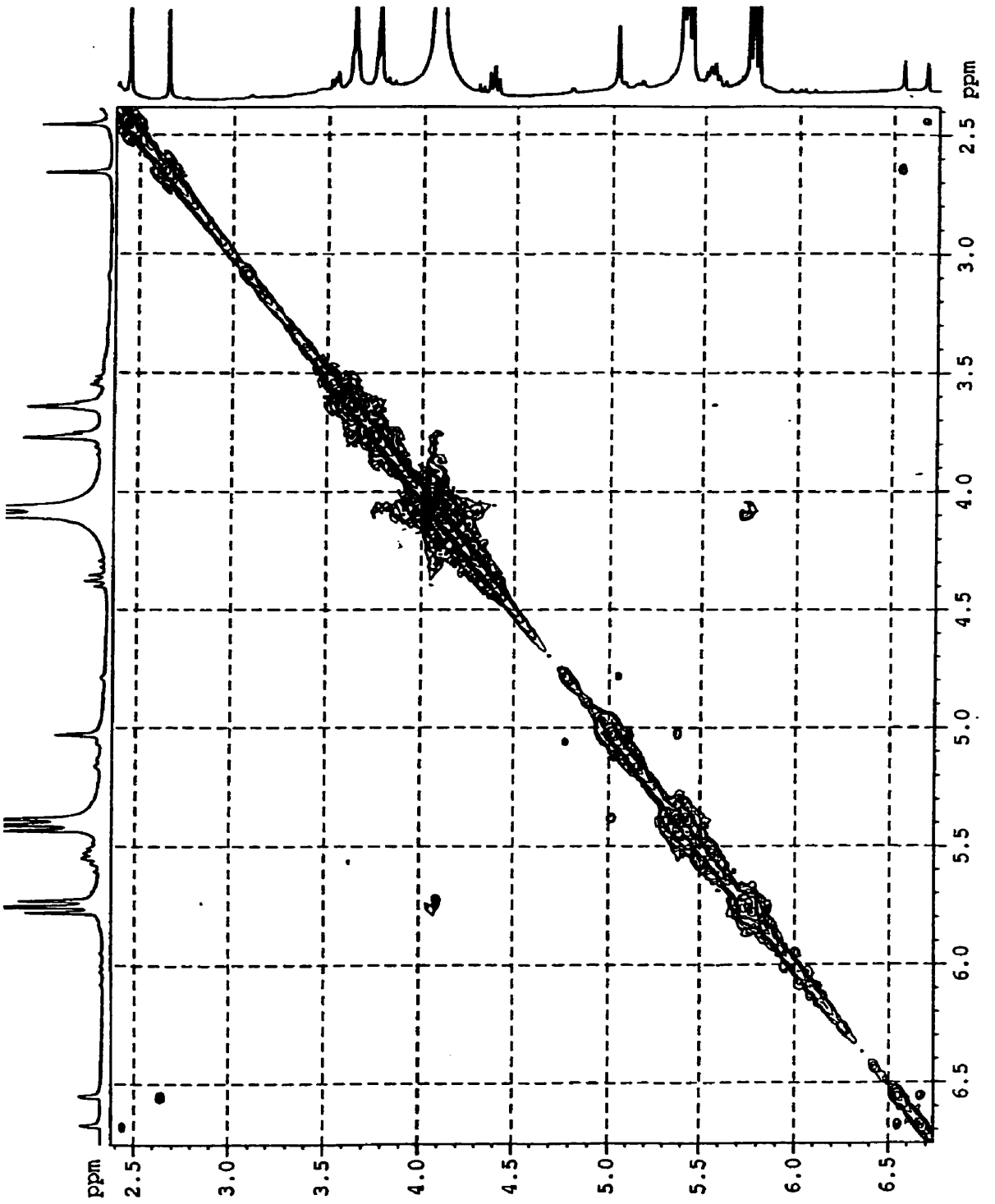


Figure 4.19: Downfield region in the 400 MHz COSY spectrum of Fraction C in the S+BrMC product separation

peak assignments (Table 4.9, Figure 4.18) were confirmed by the unique long range coupling in the COSY spectrum shown in Figure 4.19.

An overall scheme depicting the formation of **14** is presented in Figure 4.20. Exomethylene sulphide dimers (to be discussed in Section 4.5.4) are not able to support thiophene production. The second product formed in this reversion reaction is 2,2,4,8,8-pentamethyl-4-nonene, which was identified in Fraction B. The formation of the thiophene from allylic sulphide crosslinks could account for the significant reversion observed in sulphur cured BIIR vulcanizates.

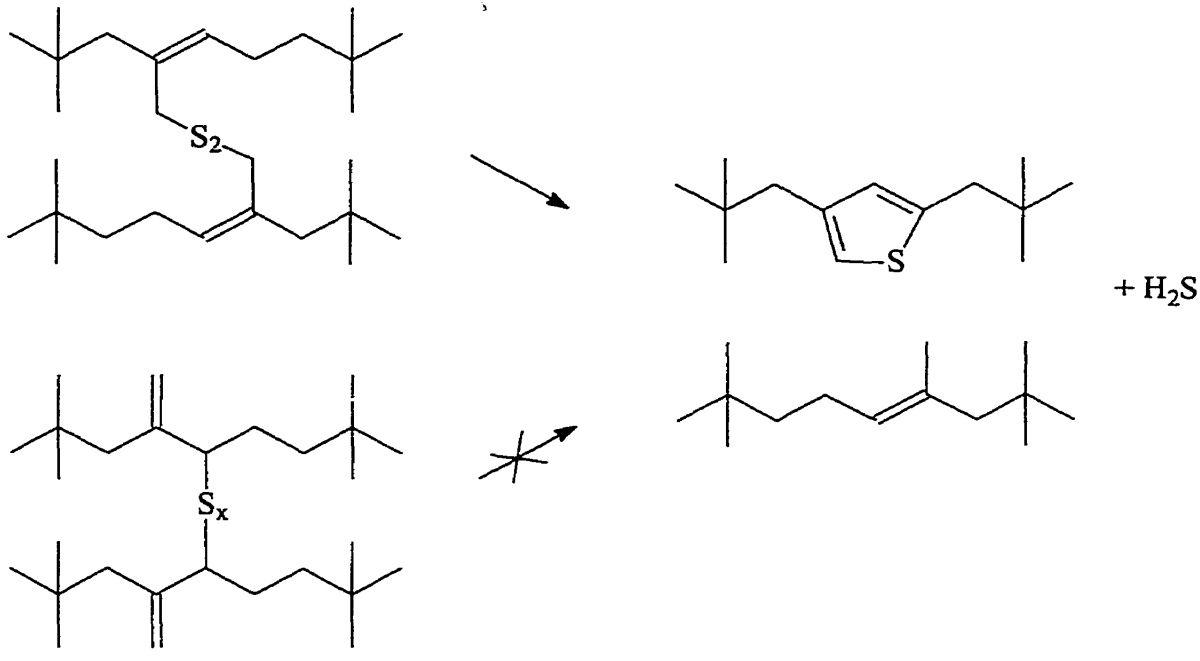


Figure 4.20: Overall scheme for the formation of the thiophene reversion product

The mass spectrum of Fraction D identified many of the same BrMC+S reaction products seen in Fraction C. However, the NMR spectrum of this fraction, shown in Figure 4.21, was considerably more complex (Peak assignments are presented in Table 4.10). The peaks in region f represent the allylic R–$CH_2$-$S_x$- protons in sulphidic dimers (structure **13**) of various sulphur rank. Previous work has established a chemical shift dependence on sulphur rank, with higher rank generating a greater downfield chemical shift.[38,39] This would suggest that Fraction D contained a mixture of sulphidic dimers of lower rank, while Fraction C contained one principal sulphidic dimer of high rank.

There was no indication in the NMR spectra of Fractions A-D that exomethylene type sulphidic dimers were generated.

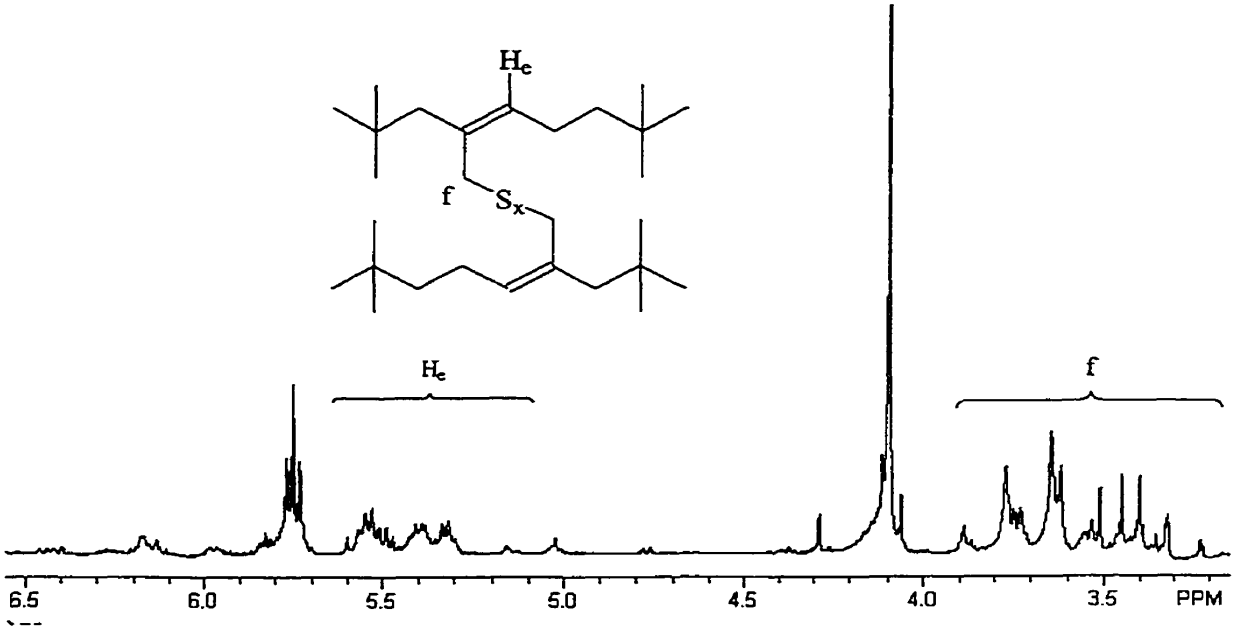


Figure 4.21: Downfield region in the 400 MHz $^1$H NMR spectrum of Fraction D in the BrMC+S product separation

Table 4.10: Downfield $^1$H NMR peak assignments for Fraction D in the S+BrMC product separation (**13**)

| Chemical Shift (ppm) | Multiplicity[a] | Assignment |
|---|---|---|
| 3.30-4.20 | s | allylic $CH_2$-$S_x$-, E,Z isomer **13** (x = 1-8) |
| 5.50-5.56 | t,m | olefinic H, **13** |

[a] s = singlet, m = multiplet, t= triplet

### 4.5.4 Reaction of Brominated 2,2,4,8,8-Pentamethyl-4-nonene with 2,2'-Dithiobisbenzothiazole (MBTS) and Sulphur

The brominated model compound used in the reactions with S+MBTS had an exo:BrMe isomer ratio of 90:10 that represented the structure of BIIR more closely than the material used in the previous cure studies (54:46). This difference gave rise to several reaction products that were not observed in the sulphur and MBTS reactions. The curative recipe chosen for these experiments corresponded to a standard 0.5 phr S, 1.3 phr MBTS BIIR formulation. Preparative TLC was used to separate the crude BrMC+MBTS+S reaction mixture into 5 bands ($R_f$ 0.00, 0.38-0.47, 0.62-0.68, 0.68-0.72, 0.72-0.80) that were characterized by mass spectroscopy and 400 MHz $^1$H NMR.

NMR analysis of the top band ($R_f$= 0.72-0.80) identified the exomethylene and endomethylene conjugated dienes, 2,2,4,8,8-pentamethyl-4-nonene, and the uncharacterized product previously described in Section 4.5.3 (Fraction B). In addition to conjugated dienes, the second band ($R_f$ = 0.68-0.72) also contained unreacted BrMC (BrMe isomer only).

Sulphur crosslinked dimers of the BrMC were isolated in the third TLC band ($R_f$ = 0.62-0.68). The mass spectrum of this band, containing peaks at *m/e* 227 (MC-$S^+$) and *m/e* 257 ($C_{14}H_{25}$-$S_2^+$), is shown in Figure 4.22. Further examination of this band by proton NMR (Figure 4.23) identified the bromomethyl analogue sulphide dimers (**13**)

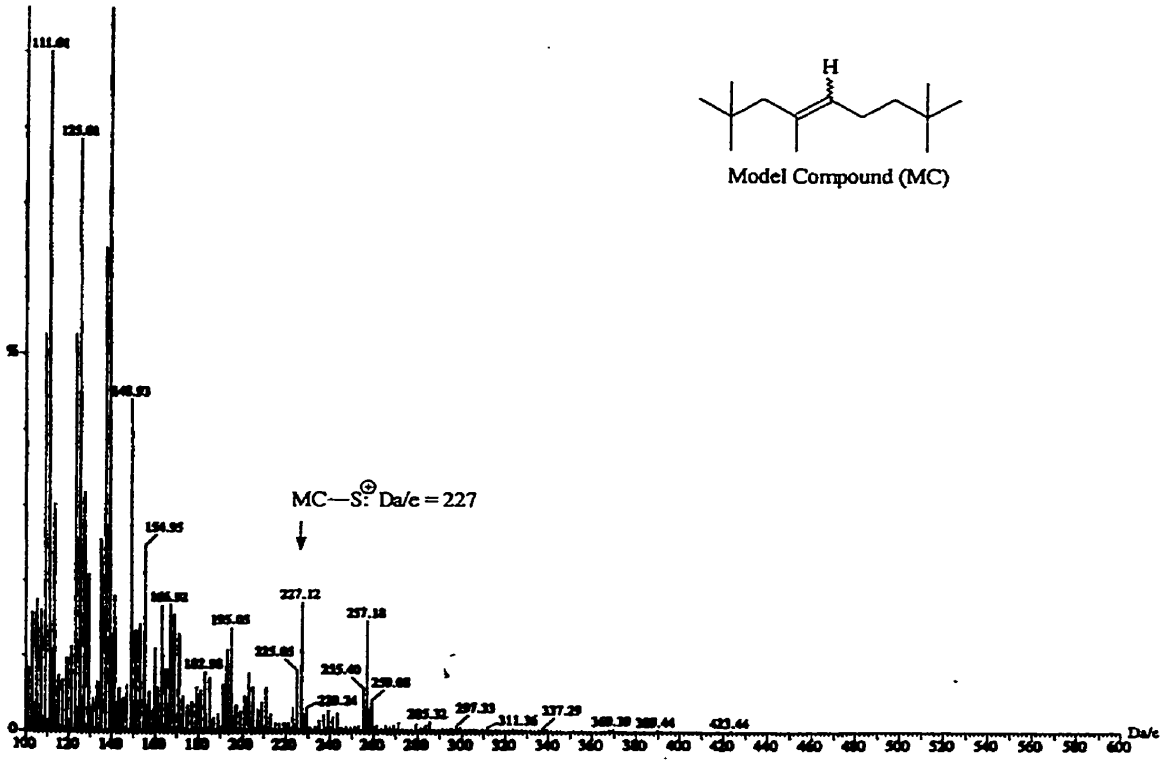


Figure 4.22: Mass spectrum of the third TLC band of the BrMC+MBTS+S product separation

observed in the BrMC+S cure, as well as several exomethylene sulphide dimers (**15**). The complexity of regions f and $H_e$ was attributed to the distribution in sulphur rank of structures **13** and **15**, and the probable formation of the hybrid dimer **16**. The peak assignments of **13** are consistent with those made previously, while the peak assignments

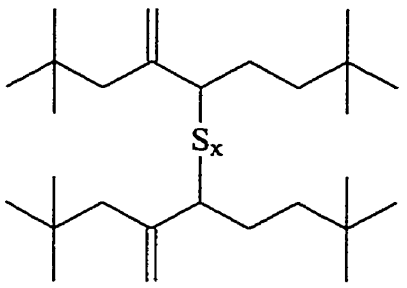


**15**

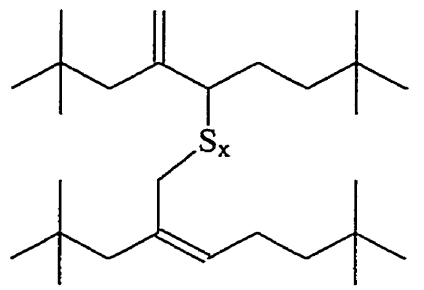


**16**

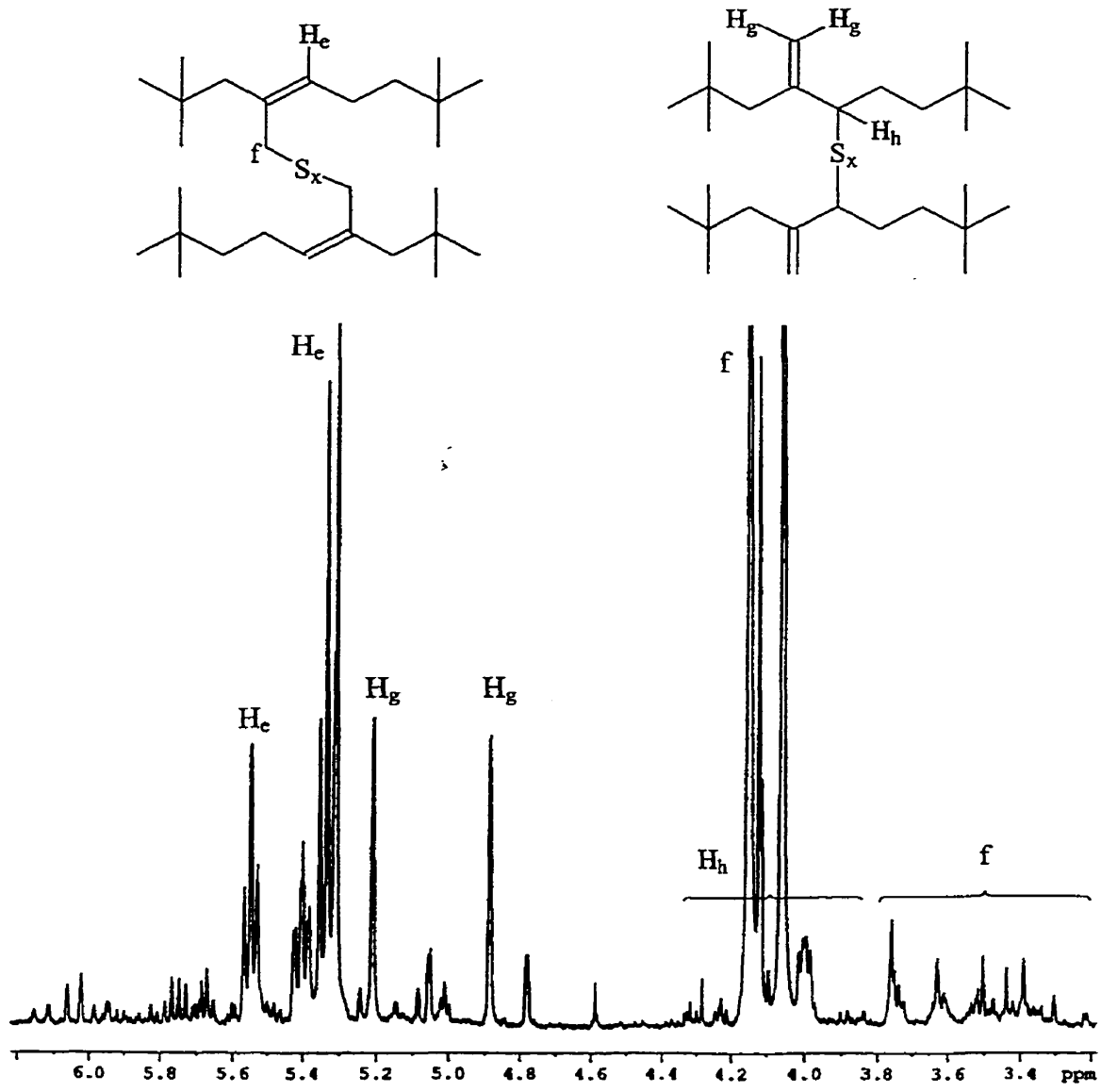


Figure 4.23: Downfield region in the 400 MHz $^{1}$H NMR spectrum of the third TLC band in the BrMC+S+MBTS reaction product separation

of **15**, presented in Table 4.11, were based on the unique vicinal (H-C-H) coupling of the exomethylene protons. These exomethylene sulphide dimers were not observed in the BrMC+S cure, presumably due to the lower exo:BrMe isomer ratio of the BrMC used in those reactions.

Table 4.11: Downfield $^1$H NMR peak assignments for the third TLC band of the S+MBTS+BrMC product separation (**13, 15**)

| Chemical Shift (ppm) | Multiplicity[a] | Assignment |
|---|---|---|
| 3.30-4.20 | s | allylic $CH_2$-$S_x$-, E,Z isomer **13** (x = 1-8) |
| 3.90-4.50 | t,m | allylic H-C-$S_x$-, **15** (x = 1-8) |
| 4.90 | s | olefinic H, **15** |
| 5.20 | s | olefinic H, **15** |
| 5.35 | t | olefinic H, **13** |
| 5.55 | t | olefinic H, **13** |

[a] s = singlet, m = multiplet, t= triplet

The fourth TLC band had an $R_f$ value of 0.38-0.47, and was therefore unlikely to contain any of the allylic sulphide dimers described previously (**13, 15, 16**). Figure 4.24 shows the mass spectrum of this band, which contains a parent ion peak at *m/e* 362 (MC-MBT + $H^+$) but no evidence of di- or poly-sulphidic MBT adducts.

The NMR spectrum of this band, shown in Figure 4.25, confirmed the presence of the MBT adduct **12** (see Figure 4.11, Table 4.5). Triplets at 5.55 ppm and 5.30 ppm, as well as the additional singlets around 4.10 ppm, may arise from a polysulphidic thiomethyl MBT adduct, but there is no supporting evidence in the mass spectrum.

Unique exomethylene type peaks in the NMR spectrum indicate that an exo-MBT adduct (**17**) was generated. Multiple sets of exomethylene protons suggest this product may have a distribution in sulphide rank. Peak assignments of **17** are given in Table 4.12 and shown in Figure 4.25.

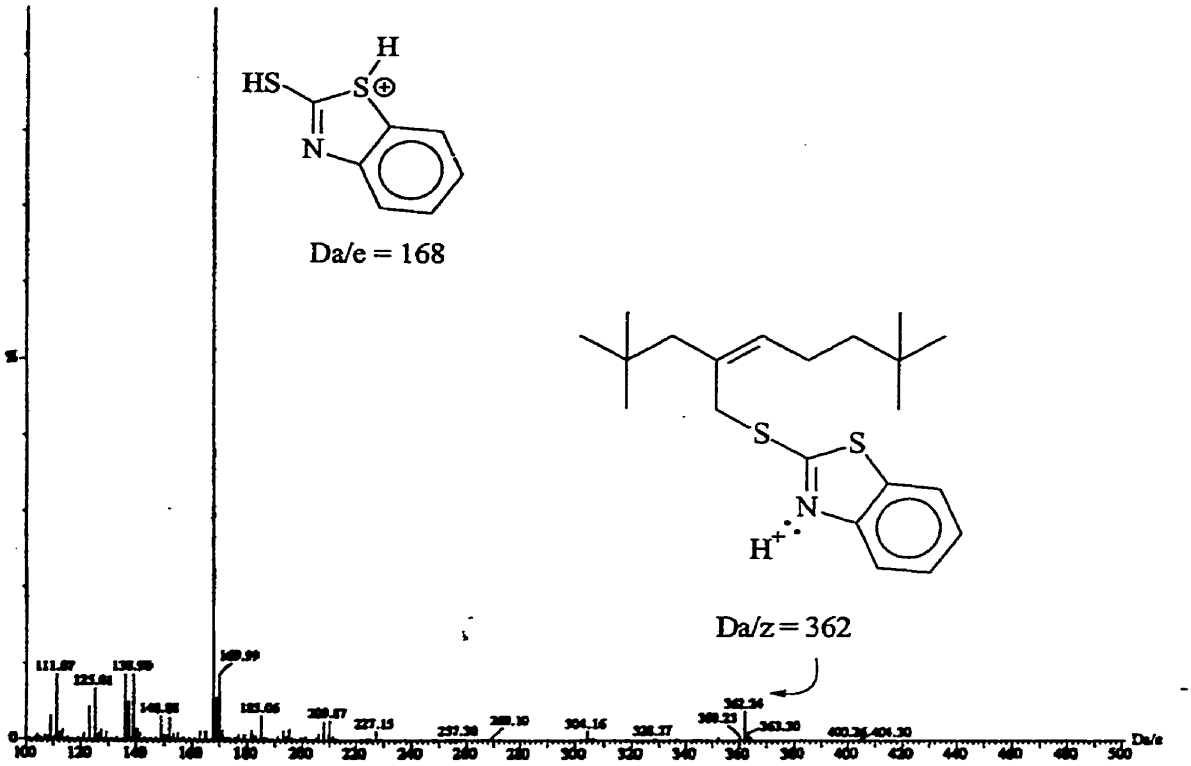


Figure 4.24: Mass spectrum of the fourth TLC band in the BrMC+S+MBTS product separation

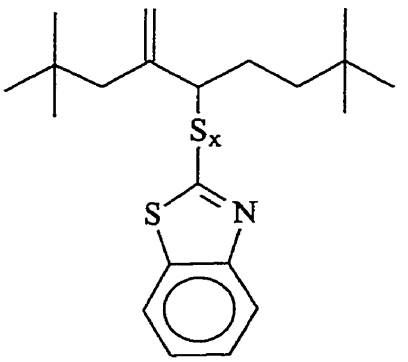


17

The bottom TLC fraction contained unreacted MBTS or MBT. There was no indication in any of the isolated fractions that the thiophene (14) had been produced. This was attributed to the larger concentration of exomethylene type products, which cannot react to form cyclic reversion products.

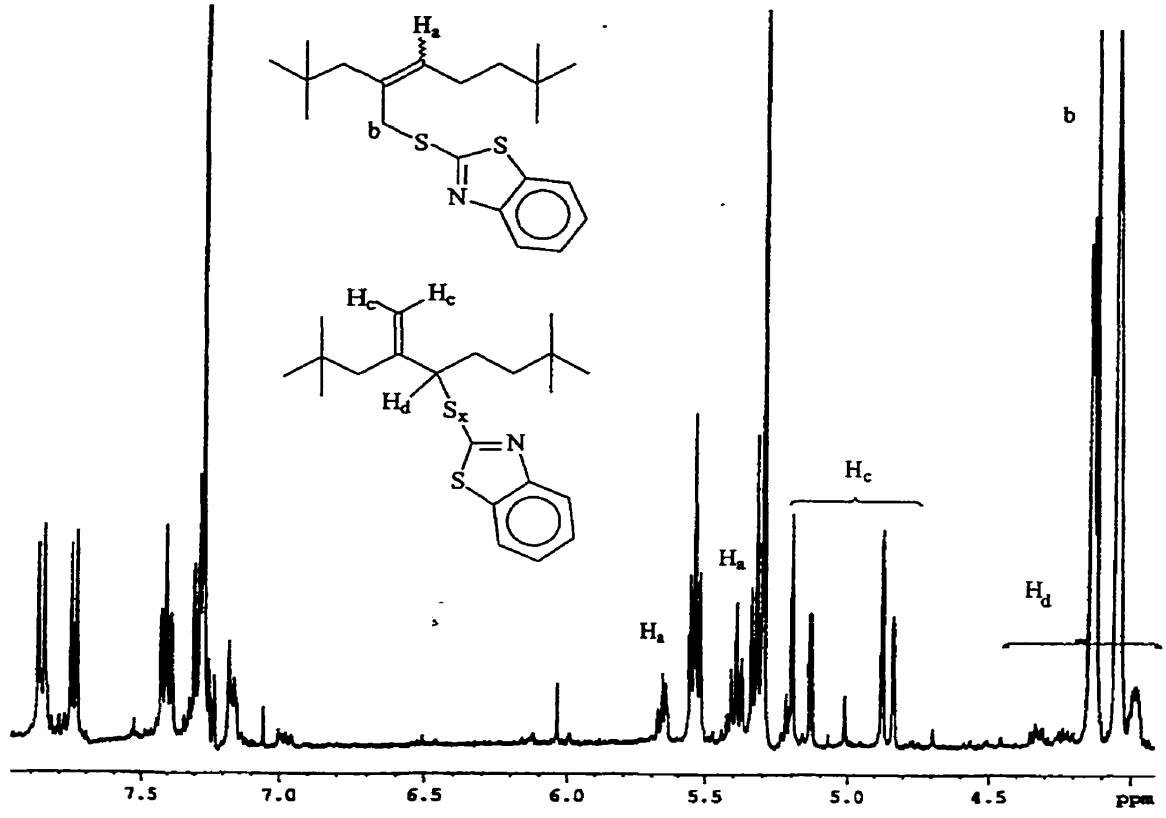


Figure 4.25: Downfield region of the 400 MHz $^1$H NMR spectrum of the fourth band in the BrMC+S+MBTS reaction product separation

Table 4.12: Downfield $^1$H NMR peak assignments of the proposed BrMC and MBTS reaction product **17**.

| Chemical Shift (ppm) | Multiplicity[a] | Assignment |
|---|---|---|
| 3.90-4.4 | t,m | allylic H, **17** |
| 4.80- 5.20 | s | exomethylene H, **17** |
| 7.30 | t | aromatic H, **17** |
| 7.42 | t | aromatic H, **17** |
| 7.77 | d | aromatic H, **17** |
| 7.84 | d | aromatic H, **17** |

[a] s = singlet, d = doublet, t = triplet, m = multiplet

# 5.0 Conclusions and Future Work

## 5.1 Conclusions

1) The compound 2,2,4,8,8-pentametyl-4-nonene (**1**) was synthesized in an overall yield of 9.5% with an E:Z ratio of 66:33. Bromination of **1** using 1,3-dibromo-5,5-dimethylhydantoin produced only the exomethylene (**5**) and bromomethyl (**6**) substitution products that are found in BIIR. Brominations carried out at 0°C produced an exo:BrMe isomer ratio of 54:46, while those at -40°C generated a ratio of 90:10 that more closely represented the structure of BIIR.
2) Analysis of the structures of BIIR at vulcanization temperatures confirmed that the exomethylene and bromomethyl isomers are the principal crosslink precursors. Significant isomerization of the exomethylene structure to the more stable bromomethyl structure occurred over a 30 minute period. At longer times, elimination of HBr to generate the exomethylene and endomethylene conjugated dienes was accompanied by the formation of decomposition products.
3) When the brominated model compound (BrMC) was heated above 100°C, a rapid equilibrium was established between the exomethylene and bromomethyl isomers. However, the BrMC also generated a range of decomposition products at vulcanization temperatures that were not consistent with the structure of BIIR. Incorporation of the neutral acid scavenger 1,2-epoxydodecane inhibited these decomposition reactions, and preserved the exo/BrMe isomers and their elimination products (exomethylene and endomethylene conjugated dienes, Figure 5.1). The epoxide was therefore required in the thermal stability and cure studies that followed in order for the BrMC to accurately represent the structure of BIIR.

4) Reaction of the BrMC (exo:BrMe 54:46) with MBTS produced the MBT adduct **12**, which is not believed to be a crosslink precursor (Figure 5.1). If formed in BIIR, **12** would reduce the number of sites available for crosslinking, and would reduce the ultimate state of cure in BIIR curative formulations containing MBTS.

5) The bromomethyl analogue sulphide dimer **13** was the principal cure product formed in the reaction of sulphur with the BrMC (exo:BrMe 54:46). A distribution in the sulphur rank of the crosslinks was identified by mass spectroscopy. Decomposition of this model vulcanizate yielded a thiophene (**14**), which could account for the significant reversion observed in sulphur cured BIIR vulcanizates.

6) A mixture of MBTS, sulphur and BrMC containing a large exo:BrMe isomer ratio (90:10) afforded two products in addition to **12** and **13** (Figure 5.1). The exomethylene sulphide dimer **15**, as well as the exo-MBT adduct **17** were produced. There was no evidence of thiophene formation, which is consistent with the inability of exomethylene type sulphides to form cyclic reversion products.

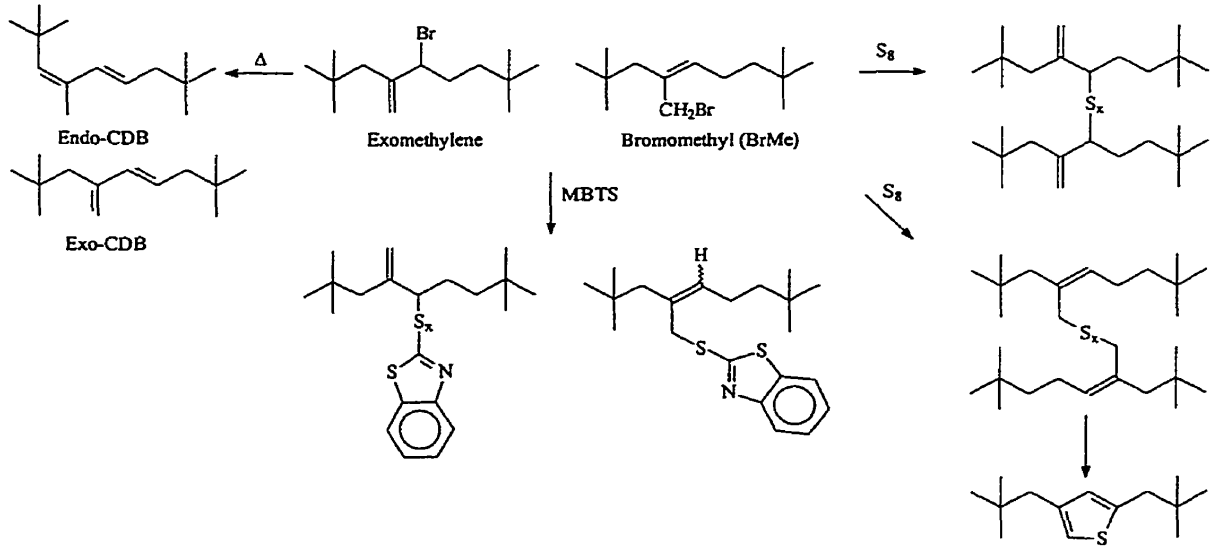


Figure 5.1: Summary of the thermal elimination and cure reactions of the BrMC

## 5.2 Future Work

1) The products generated by reaction of the BrMC with S+MBTS should be clarified.
2) In order to complete our knowledge of the vulcanization chemistry of BIIR, the principal crosslink structures formed in the binary ZnO+S and ZnO+MBTS curative recipes as well as the tertiary ZnO+S+MBTS formulation should be identified using the brominated model compound.
3) The effect of calcium stearate on BrMC+S+ZnO+MBTS model vulcanizates should be determined.

# 6.0 References


1 Edwards, D.C.; **Progress in Butyl/Halobutyl Vulcanization Chemistry**, Bayer Inc. internal report (1988).

2 Chu, C.Y., and R. Vukov; **Determination of the Structure of Butyl Rubber by NMR Spectroscopy**, *Macromolecules*, **18**, 1423-1430 (1985).

3 Wilson, G. J.; **Polysar's World of Technology: Butyl and Halobutyl Elastomers**, Bayer Inc., internal report (1989).

4 Coran, A. Y. in "*Science and Technology of Rubber, Second Edition*"(J. E. Mark, Ed.), Academic Press Inc., San Diego, pp. 341, 345 (1994).

5 Robinson, K. J., G. Feniak, and J. Walker; **The Curing of Bromobutyl Rubber**, Presented to the International Rubber Conference, Prague, Czechoslovakia (17-20/08/1973).

6 Vukov, R.; **Halogenation of Butyl Rubber and the Zinc Oxide Cross-Linking Chemistry of Halogenated Derivatives**, Presented to the ACS Rubber Division, Houston, Texas (25/09/1983).

7 Morrison, N. J., and M. Porter; **Temperature Effects on the Stability of Intermediates and Crosslinks in Sulfur Vulcanization**, *Rubber Chem. Technol.*, **57**, 63-84 (1984).

8 McSweeney, G. P. and N. J. Morrison, **The Thermal Stability of Monosulfidic Crosslinks in Natural Rubber**, *Rubber Chem. Technol.*, **56**, 337-343 (1983).

9 Campbell, R. H. and R. W. Wise; **Vulcanization. Part I. Fate of Curing System During the Sulfur Vulcanization of Natural Rubber Accelerated by Benzothiazole Derivatives**, *Rubber Chem. Technol.*, **37**, 635-649 (1964).

10 Campbell, R. H. and R. W. Wise; **Vulcanization. Part II. Fate of Curing System During Sulfur Curing of NR Accelerated by MBT Derivatives and Activated by Zinc Stearate**, *Rubber Chem. Technol.*, **37**, 650-667 (1964).

11 Coran, A. Y.; **Vulcanization. Part VII. Kinetics of Sulfur Vulcanization of Natural Rubber in Presence of Delayed-Action Accelerators**, *Rubber Chem. Technol.*, **38**, 1-13 (1965).

12 Skinner, T. D. and A. A. Watson; **EV Systems for NR. I. The Purpose of Efficient Vulcanization and Development of Curing System**, *Rubber Chem. Technol.*, **42**, 404-417 (1969).

13 Wolfe, J. R., T. L. Pugh and A. S. Killian; **The Chemistry of Sulfur Curing. III. Effects of Zinc Oxide on the Mechanism of the Reaction of Cyclohexene with Sulfur,** *Rubber Chem. Technol.,* **41**, 1329-1338 (1968).

14 Coran, A. Y.; **Vulcanization. Part V. The Formation of Crosslinks in the System: Natural Rubber-Sulfur-MBT-Zinc Ion,** *Rubber Chem. Technol.,* **37**, 679-688 (1964).

15 Milligan, B.; **Vulcanization Accelerator and Activator Complexes. 2. Chemistry of Amine and Zinc Carboxylate Complexes of Zinc and Cadmium Benzothiazolyl Mercaptides,** *Rubber Chem. Technol.,* **39**, 1115-1125 (1966).

16 Chu, C. Y., K. N. Watson and R. Vukov; **Determination of the Structure of Chlorobutyl and Bromobutyl Rubber by NMR Spectroscopy,** *Rubber Chem. Technol.,* **60**, 636-646 (1987).

17 Vukov, R.; **Zinc Oxide Crosslinking Chemistry of Halobutyl Elastomers – A Model Compound Approach,** *Rubber Chem. Technol.,* **57**, 284-290 (1984).

18 Kuntz, I., R. L. Zapp and R. J. Pancirov; **The Chemistry of the Zinc Oxide Cure of Halobutyl,** *Rubber Chem. Technol.,* **57**, 813-825 (1984).

19 Hopkins, W. and W. Von Hellens; **Vulcanization Chemistry of Bromobutyl with Sulfur, Zinc Oxide, M.B.T.S.,** Bayer Technical Report, unpublished data.

20 Vukov, R. and G. J. Wilson; **Crosslinking Efficiency of Some Halobutyl Curing Reactions,** Presented at a meeting of the ACS Rubber Division, Denver, Colorado (23-26/10/1984).

21 Cunneen, J. I. and R. M. Russell; **Occurrence and Prevention of Changes in the Chemical Structure of Natural Rubber Tire Tread Vulcanizates During Service,** *Rubber Chem. Technol.,* **43**, 1215-1224 (1970).

22 Krejsa, M. R. and J. L. Koenig; **A Review of Sulfur Crosslinking Fundamentals for Accelerated and Unaccelerated Vulcanization,** *Rubber Chem. Technol.,* **66**, 376-410 (1992).

23 Krejsa, M. R. and J. L. Koenig; **Solid-State Carbon-13 Studies of Vulcanized Elastomers. VIII. Accelerated Sulfur-Vulcanized Butyl Rubber at 75.5 MHz,** *Rubber Chem. Technol.,* **64**, 40-55 (1990).

24 van den Berg, J. H., J. W. Beulen and E. Duynstee; **Model Vulcanization of EPDM Compounds – Structure Determination of Vulcanization Products from Ethylene Norborane,** *Rubber Chem. Technol., 57, 265-274 (1984).*

25 Morrison, N. J.; **The Reactions of Crosslink Precursors in Natural Rubber,** *Rubber Chem. Technol.,* **57**, 86-96 (1984).

26 Morrison, N. J.; **The Formation of Crosslink Precursors in the Sulfur Vulcanization of Natural Rubber**, *Rubber Chem. Technol.*, **57**, 97-103 (1984).

27 Lautenschlaeger, F. K.; **Model Compound Vulcanization – Part I. Basic Studies**, *Rubber Chem. Technol.*, **52**, 213-231 (1979).

28 Skinner, T. D.; **The CBS-Accelerated Sulfuration of Natural Rubber and *cis*-1,4-Polybutadiene**, *Rubber Chem. Technol.*, **45**, 182-192 (1972).

29 Gregg, E. C. and S. E. Katrenick; **Chemical Structures in *cis*-1,4-Polybutadiene Vulcanizates. Model Compound Approach**, *Rubber Chem. Technol.*, **43**, 549-571 (1970).

30 Gregg, E. C. and R. P. Lattimer; **Polybutadiene Vulcanization. Chemical Structures From Sulfur-Donor Vulcanization of an Accurate Model**, *Rubber Chem. Technol.*, **57**, 10561096 (1984).

31 Steevensz, R. and I. Clarke; **Synthesis (Revised) of Butyl Rubber Model Compound 2,2,4,8,8-Pentamethyl-4-nonene,** Bayer Technical Report TR.630.86 (1986).

32 Chu, C.Y.; **A Further Revision of the Total Synthesis of 2,2,4,8,8-Pentamethyl-4-nonene – The Model compound for Butyl Rubber,** Bayer Technical Report CR200.01.87 No. 02 (1987).

33 Ho, K.W., J.E. Guthmann; **Ozonolysis of Butyl Elastomers**, *Journal of Polymer Science: Part A: Polymer Chemistry*, **27**, 2435-2455 (1989).

34 Seborg, D.E., T.F. Edgar and D.A. Mellichamp; **Process Dynamics and Control**, John Wiley & Sons, Toronto, pp. 296-297 (1989).

35 Dhaliwal, G.K. **Procedure for the Measurement of Unsaturation in Butyls by 500 MHz $^{1}$H NMR Spectroscopy**, Bayer Memorandum November 19, 1993.

36 R. A. Whitney, personal communication, unpublished data.

37 Sheffield ChemPuter Isotope Pattern Calculation; http://www.chem.shef.ac.uk/WebElements.cgi$isot

38 Hahn, J., P. Palloch and N. Thelen; **Reversion Stable Networks with Polysulfide Polymers at Vulcanization Agents**, Presented at a meeting of the Rubber Division, American Chemical Society, Chicago, Illinois (13-16/04/1999).

39 Hulst, R., R. Seyger, J. van duynhoven, L. van der Does, J. Noordermeer and A. Bantjes; **Vulcanization of Butadiene Rubber by Means of cyclic Disulfides. 3. A 2D Solid State HRMAS NMR Study on Accelerated Sulfur Vulcanizates of BR Rubber**, *Macromolecules*, **32**, 7521-7529 (1999).

# APPENDIX A

## Heating Block for Thermal Stability and Cure Studies of the Brominated Model Compound

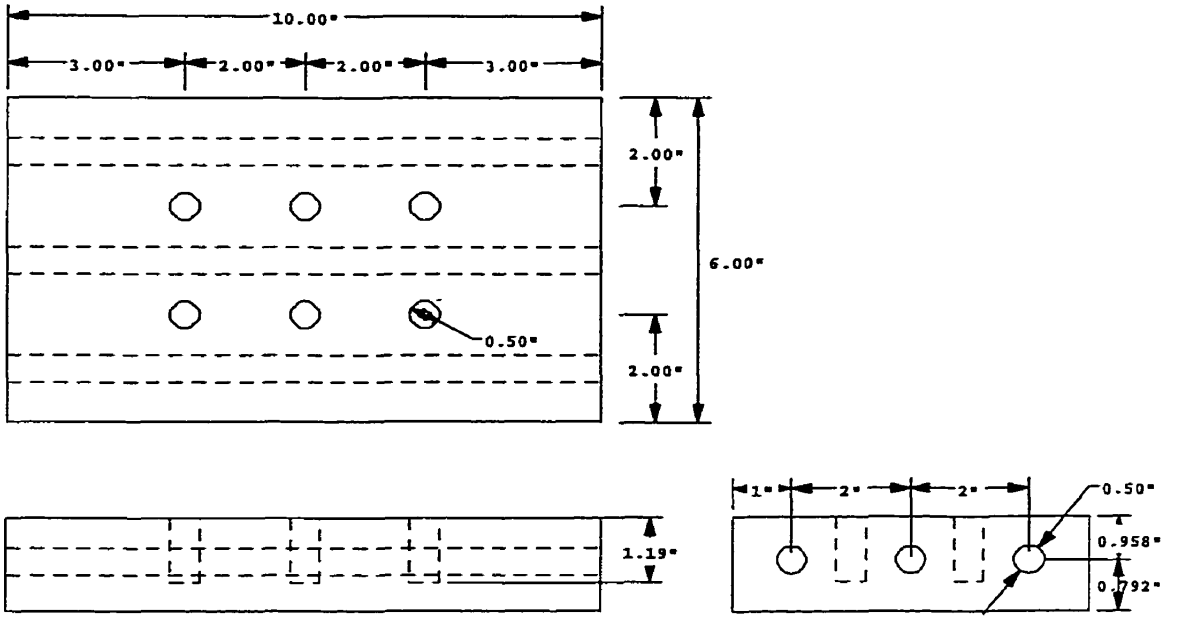


Figure A1: Heating block for the thermal stability and cure studies of the brominated model compound

## APPENDIX B

### Thermal Stability of the Brominated Model Compound

The complete results of the thermal stability studies of the brominated model compound with and without the neutral acid scavenger 1,2-epoxydodecane are presented in Tables B1 through B7.

Table B1: Thermal Stability experiments of the BrMC in the absence of 1,2-epoxydodecane

| Time (min) | 1.77 mol/L BrMC 100°C [Exo]/[BrMe] | 1.77 mol/L BrMC 145°C [Exo]/[BrMe] | 0.88 mol/L BrMC 145°C [Exo]/[BrMe] |
|---|---|---|---|
| 0 | 1.43 | 1.43 | 0.88 |
| 1 | | 0.21 | |
| 2 | | 0.19 | |
| 3 | | 0.17 | |
| 4 | | 0.17 | |
| 5 | | 0.18 | 0.17 |
| 7 | | 0.18 | |
| 10 | | 0.23 | 0.17 |
| 15 | | 0.20 | 0.19 |
| 20 | 0.19 | 0.19 | 0.19 |
| 25 | | | 0.17 |
| 40 | 0.15 | | |
| 60 | 0.15 | | |
| 80 | 0.15 | | |
| 100 | 0.15 | | |
| 120 | 0.16 | | |
| 140 | 0.14 | | |
| 160 | 0.15 | | |
| 180 | 0.16 | | |
| 205 | 0.15 | | |
| 220 | 0.14 | | |
| 240 | 0.19 | | |
| 255 | 0.17 | | |

Table B2: Thermal stability of 0.78 mol/L BrMC and 1.77 mol/L 1,2-epoxydodecane in 1,2,4-trichlorobenzene at 145°C

| Time | Concentration (mol/L) | | | |
|---|---|---|---|---|
| (min) | Exo | BrMe | Exo-CDB | Endo-CDB |
| 0 | 0.43 | 0.35 | 0.00 | 0.00 |
| 1 | 0.36 | 0.39 | 0.01 | 0.03 |
| 2 | 0.33 | 0.38 | 0.02 | 0.05 |
| 3 | 0.30 | 0.39 | 0.02 | 0.07 |
| 4 | 0.27 | 0.39 | 0.04 | 0.08 |
| 5 | 0.24 | 0.40 | 0.04 | 0.09 |
| 10 | 0.23 | 0.40 | 0.06 | 0.10 |
| 15 | 0.19 | 0.39 | 0.09 | 0.11 |
| 25 | 0.12 | 0.38 | 0.16 | 0.12 |
| 30 | 0.10 | 0.36 | 0.19 | 0.13 |
| 40 | 0.07 | 0.33 | 0.24 | 0.13 |

Table B3: Thermal stability of 0.43 mol/L BrMC and 1.00 mol/L 1,2-epoxydodecane in 1,2,4-trichlorobenzene at 145°C

| Time | Concentration (mol/L) | | | |
|---|---|---|---|---|
| (min) | Exo | BrMe | Exo-CDB | Endo-CDB |
| 0 | 0.20 | 0.23 | 0.00 | 0.00 |
| 5 | 0.13 | 0.30 | 0.02 | 0.05 |
| 10 | 0.10 | 0.23 | 0.05 | 0.06 |
| 15 | 0.08 | 0.22 | 0.07 | 0.07 |
| 20 | 0.06 | 0.21 | 0.10 | 0.07 |
| 25 | 0.06 | 0.21 | 0.09 | 0.07 |
| 30 | 0.05 | 0.20 | 0.11 | 0.07 |
| 35 | 0.04 | 0.19 | 0.13 | 0.07 |

Table B4: Thermal stability of 0.45 mol/L BrMC and 1.87 mol/L 1,2-epoxydodecane in dodecane at 140°C

| Time (min) | Concentration (mol/L) | | | |
|---|---|---|---|---|
| | Exo | BrMe | Exo-CDB | Endo-CDB |
| 0 | 0.07 | 0.38 | 0.00 | 0.00 |
| 5 | 0.07 | 0.33 | 0.02 | 0.03 |
| 10 | 0.04 | 0.34 | 0.02 | 0.04 |
| 15 | 0.04 | 0.30 | 0.05 | 0.06 |
| 20 | 0.05 | 0.27 | 0.07 | 0.07 |
| 25 | 0.05 | 0.23 | 0.10 | 0.07 |
| 30 | 0.04 | 0.23 | 0.10 | 0.07 |
| 35 | 0.04 | 0.23 | 0.11 | 0.07 |

Table B5: Thermal stability of 0.60 mol/L BrMC and 1.87 mol/L 1,2-epoxydodecane in dodecane at 140°C

| Time (min) | Concentration (mol/L) | | | |
|---|---|---|---|---|
| | Exo | BrMe | Exo-CDB | Endo-CDB |
| 0 | 0.23 | 0.37 | 0.00 | 0.00 |
| 5 | 0.17 | 0.36 | 0.03 | 0.04 |
| 10 | 0.14 | 0.33 | 0.06 | 0.07 |
| 15 | 0.11 | 0.30 | 0.12 | 0.07 |
| 20 | 0.08 | 0.26 | 0.16 | 0.09 |
| 25 | 0.06 | 0.24 | 0.20 | 0.10 |
| 30 | 0.05 | 0.22 | 0.23 | 0.10 |
| 35 | 0.04 | 0.20 | 0.28 | 0.08 |
| 95 | 0.02 | 0.16 | 0.32 | 0.10 |

Table B6: Thermal stability of 0.45 mol/L BrMC and 1.87 mol/L 1,2-epoxydodecane in dodecane at 140°C

| Time (min) | Concentration (mol/L) | | | |
|---|---|---|---|---|
| | Exo | BrMe | Exo-CDB | Endo-CDB |
| 0 | 0.41 | 0.04 | 0.00 | 0.00 |
| 1 | 0.39 | 0.06 | 0.00 | 0.00 |
| 2 | 0.38 | 0.07 | 0.00 | 0.00 |
| 3 | 0.37 | 0.07 | 0.01 | 0.00 |
| 4 | 0.36 | 0.08 | 0.01 | 0.00 |
| 10 | 0.30 | 0.13 | 0.01 | 0.01 |
| 20 | 0.19 | 0.22 | 0.02 | 0.01 |
| 32 | 0.12 | 0.27 | 0.04 | 0.02 |
| 40 | 0.09 | 0.28 | 0.06 | 0.02 |
| 50 | 0.08 | 0.28 | 0.07 | 0.02 |
| 60 | 0.06 | 0.28 | 0.09 | 0.03 |
| 72 | 0.07 | 0.26 | 0.10 | 0.02 |
| 80 | 0.05 | 0.27 | 0.11 | 0.02 |

Table B7: Thermal stability of 0.45 mol/L BrMC and 1.87 mol/L 1,2-epoxydodecane in dodecane at 140°C

| Time (min) | Concentration (mol/L) | | | |
|---|---|---|---|---|
| | Exo | BrMe | Exo-CDB | Endo-CDB |
| 0 | 0.99 | 0.09 | 0.00 | 0.00 |
| 11 | 0.27 | 0.64 | 0.06 | 0.04 |
| 20 | 0.14 | 0.66 | 0.15 | 0.06 |
| 30 | 0.10 | 0.60 | 0.25 | 0.07 |
| 40 | 0.07 | 0.56 | 0.31 | 0.07 |
| 55 | 0.06 | 0.45 | 0.43 | 0.08 |
| 70 | 0.03 | 0.40 | 0.51 | 0.08 |
| 85 | 0.02 | 0.33 | 0.58 | 0.09 |

The experimental data presented in Table B6 was modeled according to the simplified mechanism presented in Figure B1, where the ionic intermediates have been lumped together.

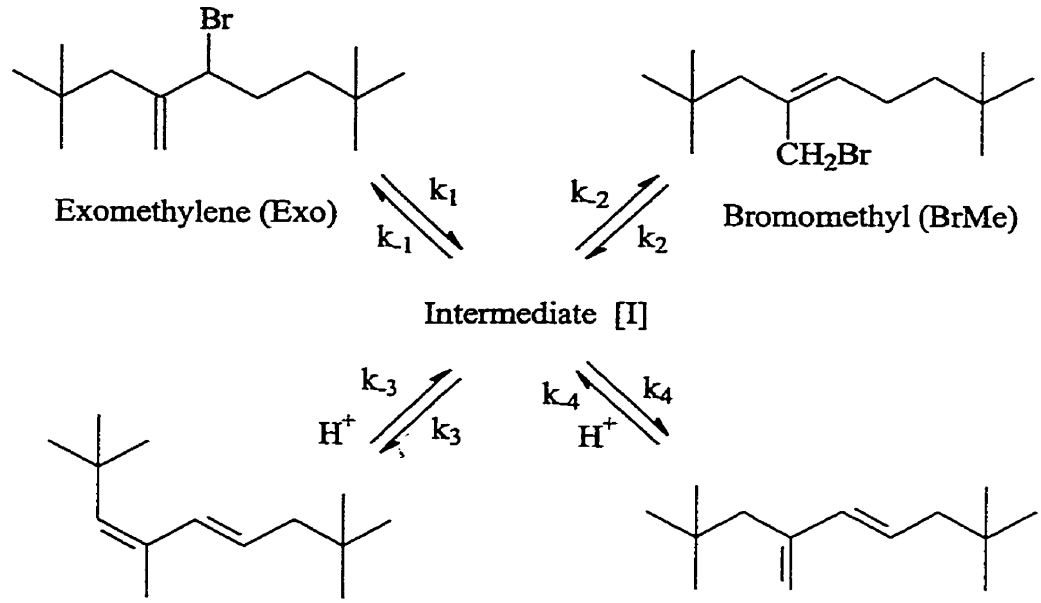


Figure B1: Simplified reaction mechanism for modelling of the experimental data

Based on this scheme, the following four dependent differential equations can be written to describe the changes in concentration of the exomethylene and bromomethyl isomers as well as the exomethylene and endomethylene conjugated dienes:

$$\frac{d[Exo]}{dt} = -k_1[Exo] + k_{-1}[I] \qquad (1)$$

$$\frac{d[BrMe]}{dt} = -k_2[BrMe] + k_{-2}[I] \qquad (2)$$

$$\frac{d[Endo-CDB]}{dt} = -k_{-3}[Endo-CDB][HBr]_f + k_3[I] \qquad (3)$$

$$\frac{d[Exo-CDB]}{dt} = -k_{-4}[Exo-CDB][HBr]_f + k_4[I] \quad (4)$$

The concentration of the intermediate [I] was determined from the overall mass balance (total BrMC concentration = 0.45 mol/L):

$$[I] = 0.45 \text{ mol/L} - [Exo] - [BrMe] - [Exo\text{-}CDB] - [Endo\text{-}CDB] \quad (5)$$

$[HBr]_f$ is the concentration of free HBr that is able to react with the conjugated dienes or the epoxydodecane. If the epoxide [edod] is in equilibrium with its bromohydrin [BH], an equilibrium constant can be determined as follows:

$$[edod] + [HBr]_f \rightleftharpoons [BH]$$

$$\frac{[BH]}{[edod][HBr]_f} = K_e \quad \therefore [BH] = K_e[edod][HBr]_f \quad (6)$$

The free HBr in this system is the total quantity generated in the elimination reactions minus the quantity bound in the bromohydrin:

$$[HBr]_f = [exo\text{-}CDB] + [endo\text{-}CDB] - [BH] \quad (7)$$

This equation could not be accurately balanced because HBr was lost through the vial septum when taking aliquots for characterization. Therefore, the following development was used to obtain an estimate of free HBr concentration. Substituting **(6)** into **(7)**,and solving for $[HBr]_f$ yields:

$$[HBr]_f = \frac{[exo-CDB]+[endo-CDB]}{1+K_e[edod]} \quad (8)$$

The large excess in epoxydodecane concentration enabled equation **(8)** to be simplified by inserting an average [edod] concentration. Equation **(8)** was inserted into equations **(3)** and **(4)** as an estimate of $[HBr]_f$.

The rapid equilibrium observed between the exo and bromomethyl isomers in the absence of epoxydodecane places the additional thermodynamic constraint on $k_1$ identified in the following development:

$$[\text{Exo}] \underset{k_{-1}}{\overset{k_1}{\rightleftharpoons}} [\text{I}] \underset{k_{-2}}{\overset{k_2}{\rightleftharpoons}} [\text{BrMe}]$$

$$\frac{[\text{Exo}]}{[\text{I}]} = \frac{k_{-1}}{k_1}$$

$$\frac{[\text{I}]}{[\text{BrMe}]} = \frac{k_2}{k_{-2}}$$

$$\frac{[Exo]/[I]}{[I]/[BrMe]} = \frac{[Exo]}{[BrMe]} = \frac{k_{-1}/k_1}{k_2/k_{-2}} = \frac{k_{-1}k_{-2}}{k_1k_2} = 0.1790$$

$$k_1 = \frac{k_{-1}k_{-2}}{0.1790k_2} \qquad \textbf{(9)}$$

Using the Implicit Euler's Method with a step size of 0.1 minutes, the differential equations **(1)** through **(4)** were solved simultaneously subject to the constraint **(9)** on $k_1$. These calculations, performed using the solver routine in MS-Excel, minimized the squared error between the experimental data and the model prediction by optimizing the estimates of each of the eight rate constants. The optimized rate constants for the experiment using 0.45 mol/L BrMC and 1.87 mol/L epoxydodecane in dodecane at

140°C (Table B6) are given in Table B8. The model predictions are plotted with experimental data in Figure 4.8.

Table B8: Optimized rate constants for the proposed isomerization and elimination reaction mechanism. Conditions: 0.45 mol/L BrMC and 1.87 mol/L epoxide in dodecane at 140°C.

| Parameter | Rate Constant |
|---|---|
| $k_1$ | 0.03 $s^{-1}$ |
| $k_{-1}$ | 0.001 $s^{-1}$ |
| $k_2$ | 0.18 $s^{-1}$ |
| $k_{-2}$ | 18.49 $s^{-1}$ |
| $k_3$ | 0.18 $s^{-1}$ |
| $k_{-3}$ | 0.00 L $mol^{-1}$ $s^{-1}$ |
| $k_4$ | 0.60 $s^{-1}$ |
| $k_{-4}$ | 0.00 L $mol^{-1}$ $s^{-1}$ |